Society of Vertebrate Paleontology Memoir 8
Journal of Vertebrate Paleontology
Volume 27, Supplement to Number 2: 127–162, June 2007

THE POSTCRANIAL AXIAL SKELETON OF *MAJUNGASAURUS CRENATISSIMUS* (THEROPODA: ABELISAURIDAE) FROM THE LATE CRETACEOUS OF MADAGASCAR

PATRICK M. O'CONNOR
Department of Biomedical Sciences, 228 Irvine Hall, Ohio University College of Osteopathic Medicine, Athens, OH 45701; oconnorp@ohiou.edu

ABSTRACT—Recent fieldwork in Upper Cretaceous terrestrial deposits in northwestern Madagascar has yielded a remarkable diversity of vertebrates, including several specimens of the abelisaurid theropod *Majungasaurus crenatissimus* (Depéret, 1896) Lavocat, 1955. Featured among the discoveries is an exquisite specimen (UA 8678) that preserves a virtually complete precaudal vertebral column, numerous costal elements, and portions of the skull and appendicular skeleton. This contribution represents the first description highlighting the postcranial axial skeleton of *Majungasaurus*. Owing to the completeness and quality of preservation, this specimen allows an examination of the serial transformation of features along the length of the axial skeleton, including a detailed analysis of postcranial pneumaticity in a nontetanuran theropod. Notable features of *Majungasaurus* include pneumatic cervical ribs with caudally bifurcate shafts and extensive pneumaticity of all postatlantal, precaudal vertebrae. Several postcranial features exhibited by *Majungasaurus*—including a well-developed cervical epipophysis, laterally expanded dorsal parapophysis, and sub-divided infradiapophyseal fossa in middle dorsal series—support previous phylogenetic studies placing it within Abelisauroidea and Abelisauridae. *Majungasaurus* (and abelisaurids generally) exhibit a robust cervical skeleton that features tightly interlocking cervical ribs, hyperossification of cervical rib shafts, and hypertrophied muscle attachment sites relative to other basal theropods. These features together highlight an axial core constructed to withstand high stresses, likely reflecting feeding adaptations for predation on large-bodied prey.

MALAGASY ABSTRACT (FAMINTINANA)—Ireo fikarohana natao tamina faritra misy tany iangonan'ireo taolambalon-javamananaina tamin'ny vanim-potoanan'ny Cretacées Ambony tany amin'ny faritra avaratra andrefan'i Madagasikara iny dia nahafahana nanampongatra karazana sisan-dinaozora misy karazany marobe, ahitana sisana abelisaurid theropod *Majungasaurus crenatissimus* misimisy (Depéret, 1896) Lavocat, 1955. Isan'ireo voka-pikarohana misongadina amin'izany ny sisan-javamananaina (UA 8678) iray izay mbola feno ny taolan-katoka mitondra mitohy amin'ny hazondamosiny rehetra, ny taolan-tratrany maromaro, ny ampahany amin'ny karan-dohany ary ny taolan-drambony. Maneho ny fanoritsoritana voalohany ny taolan-damosina ao am-para-hatoky ny *Majungasaurus* io vokam-pikarohana io. Satria mbola voatahiry tsara sy mbola eo daholo ny singan-javatra rehetra momba azy, dia ahafahana mandinika ireo dingampivoaran'ny endriky ny taolan-damosiny ity sisan-javamananaina ity, ka tafiditra ao anatin'izany ny fandinihana lalina kokoa ny fiangonan'ny rivotra ao am-para-hatoka-na 'nontetanuran' theropod. Isan'ny ireo zavatra mampiavaka ny *Majungasaurus* ny fananany taolan-katoka madinika iangonan-drivotra izay manana tandrony mizara roa ary mahafoka rivotra be tokoa amin'ny taolan-damosiny rehetra. Maro amin'ireo toetoetran'ny farahatokin'ny *Majungasaurus,* ohatra ny fivontosana be eo amin'ny vohitra 'épipophyse'-ny hatoka, ny fivelaran'ny vohitra 'parapophyses'aoriana amin'ny lafiny havia sy havanana, ny fizarazaran'ny lavaka eo ambanin'ny 'diapophyse' dia manamafy ireo fandinihina 'phylogenetic' nametraka azy ao amin'ny fianakavian'ny Abelisauroidea sy Abelisauridae. *Majungasaurus* (sy abelisaurids amin'ny ankapobeny) dia mampiseho taolan-katoka matanjaka narafitra mafy manodidina sy mifehy ny fihetsehin'ny taolan-katoka, sy ny fivontosan'ny vantan-taolana ary ny fihenana be dia be ny hozatra mifandray aminy raha ampitahaina amin'ireo faritra amin'ny vatana ambany eo amin'ny theropods. Ny fananany ireo toetra ireo mitambatra dia mampisongadina ny fisihan'ny andry voarafitra ahazakany fisehoan-javatra sarotra sy manahirana, toy ny fahazarana amin'ny fihinanana haza vaventy vatana.

INTRODUCTION

Charles Depéret first reported theropod dinosaur remains from the Late Cretaceous of Madagascar in 1896. He described two teeth, an ungual phalanx, a partial sacrum, and a single caudal vertebral centrum, and assigned these materials to *Megalosaurus crenatissimus*. Subsequent reports of theropod fossils from Madagascar during the first three quarters of the 20th century documented similarly sparse, usually isolated skeletal elements (e.g., Lavocat, 1955). Although over a century of taxonomic ambiguity surrounds this medium-sized theropod, the materials described herein are referred to *Majungasaurus crenatissimus* (see Krause et al., [this volume] for a historical taxonomic overview of *Megalosaurus crenatissimus*, *Majungatholus atopus*, and *Majungasaurus crenatissimus*).

Since 1993 joint Stony Brook University–Université d'Antananarivo expeditions have recovered numerous theropods from the Upper Cretaceous (Maastrichtian) Maevarano Formation, Mahajanga Basin, northwestern Madagascar. Among these finds are represented multiple avian and at least two nonavian theropods. Taxa described thus far include the birds *Rahonavis ostromi* and *Vorona berivotrensis*, and two members of the abelisauroid clade, *Majungasaurus crenatissimus* and *Masiakasaurus knopfleri* (Forster et al., 1996, 1998; Sampson et al., 1998, 2001; Carrano et al., 2002). Additionally, at least three other undescribed avian taxa have been recovered from the formation (Forster and O'Connor, 2000).

In contrast to isolated skeletal elements recovered on earlier expeditions, the 1996 field season yielded substantially more complete and associated nonavian theropod specimens. Notable among these is the exquisitely preserved, nearly complete skull and associated tail of *Majungasaurus crenatissimus* (FMNH PR 2100; Sampson et al., 1998; Sampson and Witmer, this volume). During the same field season, a second specimen of *Majungasaurus* (UA 8678) was discovered that preserves a semiarticulated, near-complete precaudal vertebral column in addition to

cranial and pelvic elements (O'Connor and Sampson, 1998). Finally, numerous isolated elements collected over eight field seasons complement the collection of axial skeletal specimens referable to *Majungasaurus*; see Figure 1 for a skeletal reconstruction of recovered postcranial axial elements preserved for *Majungasaurus.* This paper details the postcranial axial skeleton of *Majungasaurus crenatissimus.* All specimens described here were recovered from the Anembalemba Member of the Upper Cretaceous (Maastrichtian) Maevarano Formation (Rogers et al., 2000, this volume).

A preliminary examination of both cranial and postcranial features has allied *Majungasaurus* with members of the Abelisauridae (O'Connor and Sampson, 1998; Sampson et al., 1998; Carrano et al., 2002; Coria et al., 2002; Wilson et al., 2003; Novas et al., 2004; Sereno et al., 2004; Tykoski and Rowe, 2004). Certain features (e.g., external maxillary sculpturing, enlarged cervical epipophyses) indicate a close phylogenetic relationship with abelisaurid taxa such as *Ilokelesia aguadagrandensis*, *Aucasaurus garridoi*, and *Carnotaurus sastrei* from Late Cretaceous deposits in Argentina, *Rajasaurus narmadensis* from the Maastrichtian of India, and *Rugops primus* from the Albian-Cenomanian of Niger (Sampson et al., 1998; Carrano et al., 2002; Coria et al., 2002; Wilson et al., 2003; Sereno et al., 2004). Preliminary biogeographic interpretations suggest that abelisaurids represent a Cretaceous radiation of large-bodied theropod dinosaurs predominantly limited to Gondwanan landmasses (Bonaparte and Novas, 1985; Coria and Salgado, 1998; Sampson et al., 1998; 2001; Carrano et al., 2002; Coria et al., 2002; Lamanna et al., 2002; Novas et al., 2004; Sereno et al., 2004; Krause et al., 2006, this volume); also see (Buffetaut et al., 1988; Accarie et al., 1995).

Institutional Abbreviations—**BMNH**, Natural History Museum, London, United Kingdom; **CMN**, Canadian Museum of Nature, Ottawa, Canada; **FMNH**, Field Museum of Natural History, Chicago, IL; **GSI**, Geological Survey of India, Kolkata, India; **ISI**, Indian Statistical Institute, Kolkata, India; **IVPP**, Institute of Vertebrate Palaeontology and Palaeoanthropology, Beijing, China; **MACN-CH**, Museo Argentino de Ciencias Naturales, Colección Chubut, Buenos Aires, Argentina; **MB**, Museum für Naturkunde der Humboldt-Universität, Berlin, Germany; **MCF-PVPH**, Museo Municipal Carmen Funes, Paleontología de Vertebrados, Plaza Huincul, Argentina**; MNHN**, Muséum National de l'Histoire Naturelle, Paris; **MNN**, Musée National du Niger, Niamey, Niger; **MOR**, Museum of the Rockies, Bozeman, MT; **PVL**, Fundación-Instituto Miguel Lillo, Tucumán, Argentina; **SMU**, Southern Methodist University, Dallas, TX; **UA**, Université d'Antananarivo, Antananarivo, Madagascar; **UCMP**, University of California Museum of Paleontology, Berkeley, CA; **USNM**, National Museum of Natural History, Washington D. C.; **UUVP**, University of Utah, Vertebrate Paleontology Collection, Salt Lake City, UT.

Comparative Taxa and Specimens—Figure 2 illustrates the primary comparative taxa used in this study, which include most basal theropods and non-coelurosaurian neotheropods, and their proposed relationships with one another (based on Coria and Salgado, 1998; Sereno, 1999; Carrano et al., 2002; Coria et al., 2002; and Sereno et al., 2004). Museum numbers of specimens based on a single specimen used for comparative statements will be provided during the first usage only, with subsequent comparisons utilizing only citation and, when necessary, figure notation. For comparisons utilizing multi-specimen species, individual specimen numbers will be used for all comparative statements unless only a single specimen was examined for the purposes of the study.

Anatomical Note—When referencing position within the precaudal vertebral column, cranial and caudal are used as descriptors rather than anterior and posterior in compliance with standardized terms in both Nomina Anatomica Avium and Nomina Anatomica Veterinaria. Proximal and distal are used to describe relative position of caudal vertebrae and chevrons within the tail. Nomenclature for vertebral laminae follows that of Wilson (1999). The only proposed change to this system is the replacement of cranial for anterior and caudal for posterior (e.g., cranial centrodiapophyseal lamina rather than anterior centrodiapophyseal lamina) as relational descriptors.

SYSTEMATIC PALEONTOLOGY

DINOSAURIA Owen, 1842
SAURISCHIA Seeley, 1888
THEROPODA Marsh, 1881
CERATOSAURIA Marsh, 1884
ABELISAUROIDEA (Bonaparte and Novas, 1985)
ABELISAURIDAE Bonaparte and Novas, 1985
MAJUNGASAURUS Lavocat, 1955
MAJUNGSAURUS CRENATISSIMUS (Depéret, 1896) Lavocat, 1955

Type Specimen—MNHN MAJ.1, nearly complete right dentary of subadult individual (Lavocat, 1955).

Referred Specimens—See complete listing in Krause et al. (this volume).

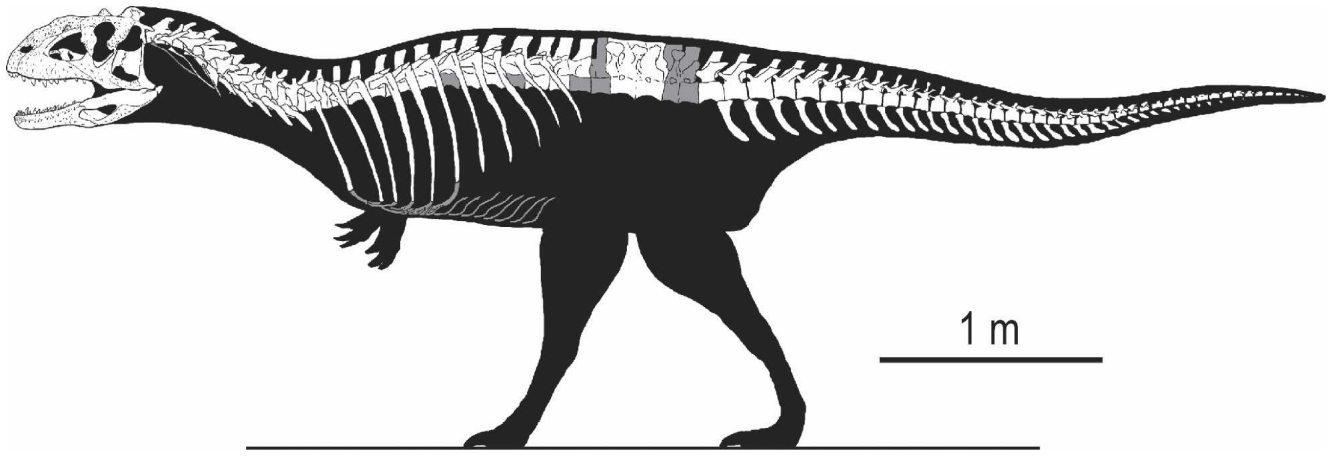

FIGURE 1. Composite axial skeletal reconstruction of *Majungasaurus crenatissimus* in left lateral view, based on UA 8678 (postcranial axial skeleton through the fifth caudal vertebra) and FMNH PR 2100 (skull and tail). Shaded elements represent the only missing components of the UA 8678 postcranial axial skeleton.

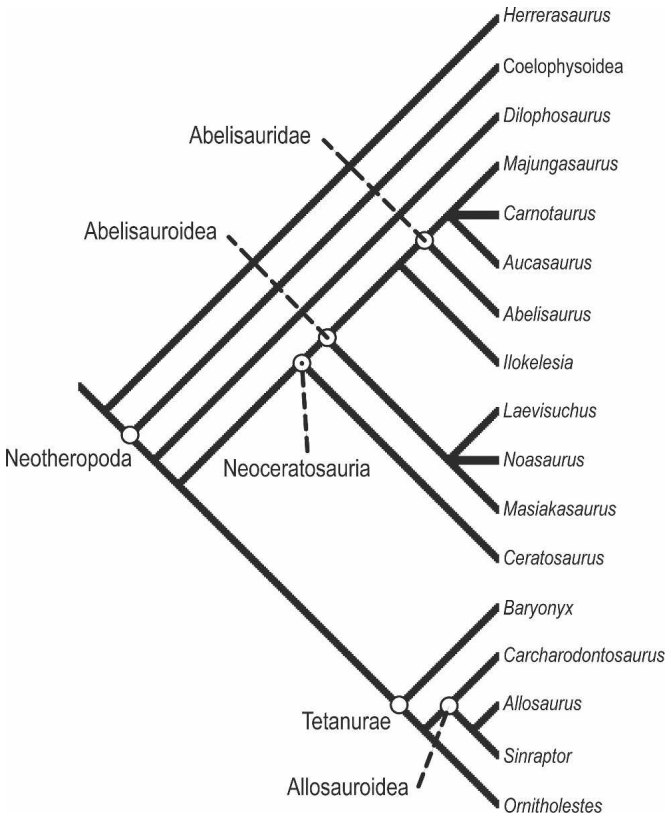

FIGURE 2. Cladogram depicting hypothesized relationships and major named clades of the primary theropod taxa used for comparative purposes in this study (based on Sereno, 1999; Coria and Salgado, 2000; Carrano et al., 2002; Coria et al., 2002; Sereno et al., 2004).

Revised Diagnosis—See Krause et al. (this volume).

Age and Distribution—All specimens assigned to *Majungasaurus crenatissimus* were recovered from deposits exposed near the village of Berivotra, Mahajanga Basin, northwestern Madagascar. Specimens were concentrated in the uppermost white sandstone unit (Anembalemba Member) of the Maevarano Formation, which has been dated as Maastrichtian. For an overview of the stratigraphy, see Rogers et al. (2000, this volume), and for a complete listing of localities see Krause et al. (this volume).

Described Material—The following description is based primarily on a partially articulated, subadult theropod specimen (UA 8678) from locality MAD 96-21. Discovered in 1996, the specimen consists of 23 presacral vertebrae, a partial sacrum, six (five proximal and one middle) caudal vertebrae, and the first haemal arch. Although the presacral vertebral column is mostly complete, the atlas consists solely of the left neurapophysis, and the seventh, tenth, and thirteenth dorsal vertebrae are represented only by neural arches. Also recovered were 13 cervical and 14 dorsal ribs, many of which are incomplete distally. A second, larger bodied specimen recovered from locality MAD 96-01 (FMNH PR 2100) includes 26 caudal vertebrae and 18 haemal arches (as well as an extremely well-preserved skull and jaws; see Sampson and Witmer, this volume), and provides the primary basis for description of the tail skeleton. Four proximal caudal vertebrae (UA 9089) were collected near locality MAD96-01 in 1989 (Ravoavy, 1991; Krause et al., this volume); however their association with FMNH PR 2100 remains questionable.

Specimen UA 8678 is here considered a subadult based on incomplete fusion of numerous vertebral neural arches and centra, whereas specimen FMNH PR 2100 represents an adult or near-adult individual based on relative size (~20% larger than UA 8678) and complete fusion of all neurocentral sutures. Finally, isolated postcranial axial elements are also included in the description, with specimen numbers noted. These include: FMNH PR 2293, second cervical (axis/C2) vertebra from MAD95-14; FMNH PR 2295, third cervical (C3) vertebra from MAD93-18; FMNH PR 2294, five distal caudal vertebrae (the last three of which are pathologically fused) from MAD93-18; UA 9089, four proximal caudal vertebrae from near MAD96-01. For descriptive and comparative studies of both the skull and appendicular skeleton of *Majungasaurus crenatissimus*, see Sampson and Witmer (this volume) and Carrano (this volume), respectively.

DESCRIPTION AND COMPARISONS

General Overview

Opisthocoelous cervical, weakly-amphicoelous dorsal, and amphicoelous caudal vertebrae characterize the vertebral column of *Majungasaurus*. Based on a near complete specimen (UA 8678), there is a presacral count of 23 with 10 cervical and 13 dorsal vertebrae. A partially preserved sacrum consists of two centra and three neural arches coossified as a single unit. However, five articular surfaces on the medial surface of each ilium indicate that additional vertebrae were incorporated into the sacral complex (Carrano, this volume). At present, the most complete tail yet recovered preserves 26 caudal vertebrae. Thus the regional count for *Majungasaurus* is 10 cervical, 13 dorsal, 3+ (probably 5) sacral, and >26 caudal vertebrae. All postaxial cervical centra are completely fused with their respective neural arches. The first two dorsal vertebrae exhibit partial fusion (i.e., the neurocentral suture is still visible) whereas the remainder of the presacral series is completely unfused. Although the preserved partial sacrum exhibits fused sacra and neural arches, it is clear that the remaining components of the sacrum were not completely fused as evidenced by intact sutural morphology rather than broken bone surfaces. Five proximal caudal vertebrae of UA8678 also retain unfused neural arches and centra in the first four elements of the series, with the fifth exhibiting bilateral asymmetry in sutural fusion.

Neural spines are relatively short throughout the presacral column, and the articulated cervical series exhibits the S-shaped curvature typical of most theropods. All postatlantal, precaudal vertebrae exhibit pneumatic features, minimally within the neural arch. There is no evidence of pneumaticity in the caudal vertebral series. Basivertebral foramina are absent on the dorsal surface of centra throughout the entire vertebral series.

Although generally well preserved, some elements exhibit slight to moderate postmortem damage and deformation; this is particularly apparent on the right side of the vertebral column. In specimen UA 8678, C4 (cervical 4) through D6 (dorsal 6) were preserved in direct articulation with one another. The cranial cervical and caudal dorsal vertebrae were slightly displaced (e.g., 5 to 50 cm) from the main articulated series. Numerous cervical and dorsal ribs were recovered, many still in direct articulation with their respective vertebrae. Midcervical ribs exhibit extensive pneumaticity in the neck and shaft, whereas pneumatic features are absent on dorsal ribs. There are no indications of dermal ossifications along the dorsal aspect of neural spines as has been reported for other basal neotheropod dinosaurs (e.g., *Ceratosaurus nasicornis* [USNM 4735]; Gilmore, 1920; *Ceratosaurus dentisulcatus* [UUVP 80]; Madsen and Welles, 2000). However, mid-dorsal and proximal-middle caudal neural spines exhibit both transverse and craniocaudal expansion at the dorsal end, typically characterized by extremely rugose surface texture. Standard vertebral metrics and indices for both UA 8678 and FMNH PR 2100 are listed in Tables 1 and 2.

Cervical Vertebrae

Majungasaurus possessed 10 cervical vertebrae (presacrals 1 to 10; Figs. 3–9). The post-axial cervical series is characterized by low, broad centra with the cranial articular surface dorsally elevated relative to the caudal surface. This offset promotes the S-shaped curve observed when the articulated cervical column is viewed laterally (Fig. 3). The degree of offset is most pronounced in the midcervical region, with C10 as the first vertebra of the series in which cranial and caudal articular surfaces assume equivalent dorsoventral positions. Mid cervical centra (C3-C6) are characterized by a length-height ratio ranging between 1.45 and 1.57 (CENL/CDCH calculated from Table 1). Cranial articular surfaces are generally flattened rather than convex as in tetanuran theropods. Postatlantal cervical centra exhibit marked opisthocoely that gradually decreases by C9. Postaxial neural spines are short and craniocaudally abbreviated throughout the cervical series. As in other abelisauroids generally, the epipophysis is notably enlarged. Epipophyseal expansion occurs caudally as in *Ilokelesia aguadagrandensis* (PVPH-35), whereas neither *Majungasaurus* nor *Ilokelesia* (Coria and Salgado, 1998) exhibit the cranial expansion observed in *Carnotaurus sastrei* (MACN-CH 894; Bonaparte et al., 1990). Transverse processes are oriented ventrolaterally rather than caudoventrolaterally as in many theropods (e.g., *Ceratosaurus nasicornis* [USNM 4735], *Allosaurus fragilis* [USNM 8367]). Additionally, the long axis of the transverse process forms an angle of 40° from the midsagittal plane (or dorsoventral vertebral axis) in the cranial cervical vertebrae, gradually shifting to an angle of 65° by C10 (Fig. 4B, C).

Zygapophyseal facets are well developed and horizontally oriented throughout the cranial portion of the cervical column. In the caudal cervical series, prezygapophyseal facets are oriented such that they face dorsomedially. The facets have transversely oriented major axes that exhibit craniocaudal expansion of the lateral portion of the articular surface (Figs. 7A, 8A), with similar morphology apparent in *Carnotaurus* (Bonaparte et al., 1990:fig. 9). There are numerous foramina located within both centra and neural arches, many of which are pneumatic in origin (Figs. 6–9). Foramina associated with the basivertebral venous system are not present on the dorsal surface of cervical centra (i.e., along the ventral aspect of the neural canal), unlike the condition in some other theropods (e.g., *Carcharodontosaurus saharicus* [CMN 41774]).

Atlas—The left neurapophysis of UA 8678 (Fig. 5) was discovered slightly displaced from the remainder of the cervical vertebral column. The right neurapophysis and atlantal intercentrum were not recovered. The atlantal centrum is fused to the axial intercentrum as the odontoid and is described below. The absence of a prezygapophyseal facet on the neurapophysis suggests that a proatlas was likely not present, or present only in a rudimentary form, in *Majungasaurus*.

The neurapophysis is elongate caudally and roughly similar to the 'L-shaped' condition described in *Ceratosaurus* (Gilmore, 1920:pl. 19), but unlike the subtriangular morphology observed in *Allosaurus* (Madsen, 1976). *Sinraptor dongi* (IVPP 10600) appears intermediate in form (Currie and Zhao, 1993:fig. 12). The pedicle tapers dorsally, forming a restricted neck (peduncular cervix) just ventral to the three main dorsal expansions—the

TABLE 1. Precaudal vertebral measurements (mm) in *Majungasaurus crenatissimus* (UA 8678). UA 8678 consists of 23 articulated/associated presacral vertebrae and a partial sacrum collected from locality MAD96-21.

Vertebra	CENL	CDCW	CDCH	MIDW	TOVH	NSH	NSL	NSW	IZW	IZL	IPPW	IDPW	PP/DP	EPL
C2	69.8‡	52.5	44.1	39.3	111.8	53.8*	82	—	79.4	57.6	54.6	63.8	0.86	29.3
C3	59.9	53.7	38.2	38.7	95.3	44	32.9	3.3	86.9	85.9	46.4	76.9*	0.60	35.2
C4	61.7	45.9	42.6	30.7*	109.1	50.9	23.3	6.6	84.5	84.4	47.6	85.5	0.56	37.5
C5	63.2	53.3	42.8	39.7	105.2	51.7	27.3	6.2	90.4	91.5	57.8	104.2	0.55	3.15
C6	65.5*	61.1	41.3*	45.6	102.9*	55.8	19.6	7.4	95.9	91.9	61.9	134.9	0.46	23.9
C7	60.1*	58.1*	†	36.1*	114.9*	†	15.1	9.5	89.3	81.6	53.5	133.4	0.40	17.7
C8	56.1*	60.2	55.7	40.9	122.6	61.3	13.1	12.7	85.1	82.3	57.1	132.5	0.43	13.2
C9	57.9	60.9	60.6	40.4*	131.9	61.1	12.5	14.8	83.8	78.1	56.5	132.3*	0.43	6.3
C10	58.4	56.8	62.1	36.8*	136.4	63.6	11.7	18.7	86.9	70.5	54.2*	134.3*	0.40	2.1
D1	59.3	53.5	60.6	33.1*	139.9	68.9	12.3	19.9	80.1	68.1	61.3	148.8*	0.41	—
D2	51.9*	54.3	62	†	148.2	73.1	14.3	23.4	†	62.1	†	148.9*	†	—
D3	55.2	51.1*	60.4	†	152.5	78.2	21.9	20.8	48.8	80.3	62.1	†	†	—
D4	51.6*	48.3*	59.8	21.7*	157.4	82.7	30.9	17.3	50.6	82.1	70.1	†	†	—
D5	58.9	52.4	57.6*	†	159.4	84.2	35.2	15.2	45.7	87.7	101.7	131.9	0.77	—
D6	59.7	57.9	66.6	†	159.1*	81.8*	43.8	13.9	42.7	93.3	120.7	140.9	0.86	—
D7	†	†	†	†	†	83.8	54.1	12.5	47.8	92.7	131.1	157.6	0.83	—
D8	67.4	63.4*	65.5*	25.4*	166.8	78.7	59.6	10.7	44.3	98.6	134.3	159.9	0.84	—
D9	67.1	70.6	64.2	34.1	153.6*	78.1	54.4	10.7	43.5	106.1	129.9	160.4	0.81	—
D10	†	†	†	†	†	88.5	53.3	10.8	53.2	101.1	129.3	159	0.81	—
D11	65.6	87.9	73.6	46.5	175.6	89.1	45.1	9.8	43.1	110.5	136.5	165.9	0.82	—
D12	†	†	†	†	†	90.6	40.3	10.3	43.6	103.4	†	†	—	—
D13	†	†	†	†	†	100.8	38.9	10.7	†	†	†	132.4	—	—
S1	†	†	†	†	†	†	†	†	†	†	†	†	†	†
S2	69.5	56.7	†	31.2	170.3	—	—	8.4	—	—	—	80.7	—	—
S3	79.1	64.6	49.1	32.9	173.4	—	—	9.5	—	—	—	54.8*	—	—
S4	†	†	†	†	†	†	†	†	†	†	†	†	†	†
S5	†	†	†	†	†	†	†	†	†	†	†	†	†	†

Notation: **CENL**, Centrum Length – maximum craniocaudal length; **CDCW**, Caudal Centrum Width – maximum width of caudal articular facet; **CDCH**, Caudal Centrum Height – maximum height of caudal articular facet; **MIDW**, Midcentral Width – width at central midlength; **TOVH**, Total Vertebral Height – dorsoventral extent of vertebra including centrum and neural spine; **NSH**, Neural Spine Height – dorsoventral extent of neural spine measured from dorsal aspect of neural canal; **NSL**, Neural Spine Length – craniocaudal extent of neural spine at spine midheight; **NSW**, Neural Spinal Width – transverse extent of neural spine at spine midheight; **IZW**, Interzygapophyseal Width – distance between lateral margin of postzygapophyses; **IZL**, Interzygapophyseal Length – distance from cranial margin of right prezygapophysis to caudal margin of right postzygapophysis; **IPPW**, Interparapophyseal Width – distance between lateral limit of parapophyses; **IDPW**, Interdiapophyseal Width – distance between lateral limit of diapophyses; **PP/DP**, Para-Diapophyseal Index – ratio of interparapophyseal width to diapophyseal width; **EPL**, Epipophyseal Length – distance from caudal margin of postzygapophyseal facet to caudalmost extent of epipophysis; *, incomplete measurement due to missing bone (e.g., partial breakage of a transverse process); †, unable to measure due to damaged/missing bone; ‡, centrum length of C2 includes axial centrum and intercentrum (axial centrum equals 50.3 mm); —, measurement not applicable for given vertebra.

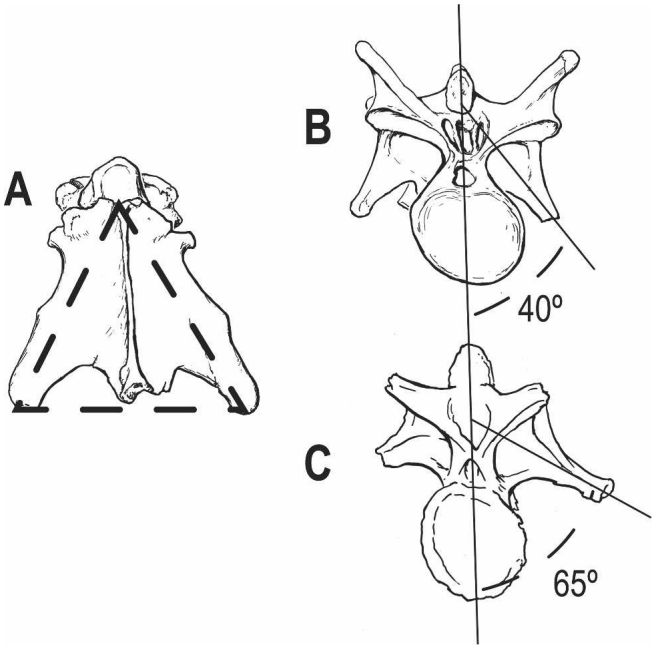

FIGURE 4. Schematic vertebral diagrams of *Majungasaurus crenatissimus*. **A**, second cervical vertebra (C2) in dorsal view; **B**, fifth cervical vertebra (C5) in caudal view; **C**, tenth cervical vertebra (C10) in caudal view. All illustrations are based on drawings of specimen UA 8678.

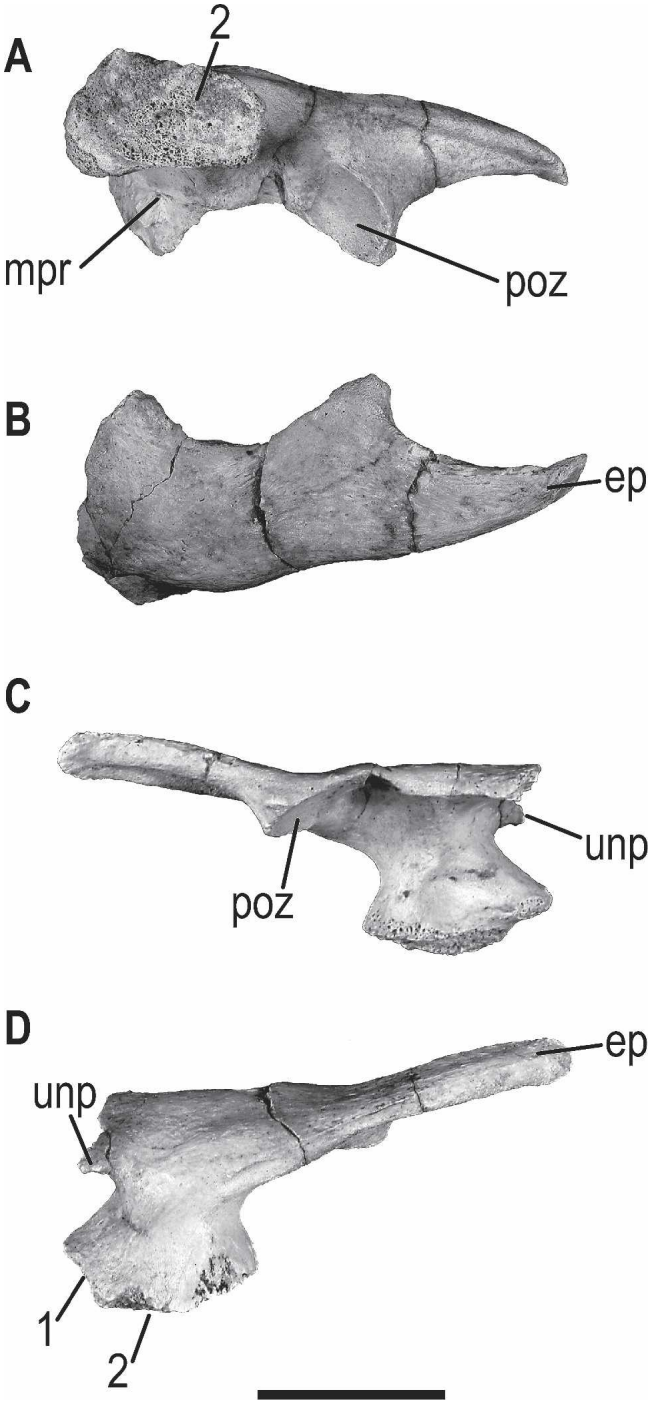

FIGURE 5. Left neurapophysis (UA 8678) of *Majungasaurus crenatissimus* in ventral (**A**), dorsal (**B**), medial (**C**), and lateral (**D**) views. **Notation**: **1**, contact surface for occipital condyle; **2**, sutural surface for atlantal intercentrum. See Appendix 1 for list of anatomical abbreviations used for this and subsequent figures. Scale bar equals 2 cm.

medial, uncinate, and postzygapophyseal processes. There is a small (~1.0 mm) vascular foramen set within a fossa on the medial surface of the pedicle (Fig. 5C). This does not appear to be present in *Dilophosaurus*, *Allosaurus*, or *Sinraptor*, and it is unclear if this feature is present in *Ceratosaurus* or *Carnotaurus*.

The postzygapophyseal process extends caudodorsally from the pedicle and approximates the crescentic emargination on the craniolateral aspect of the axial neural arch (Fig. 6A). The caudally expanded, falciform epipophysis is directed toward the midline. A similar condition is present in the basal theropod *Herrerasaurus ischigualastensis* (Sereno and Novas, 1993), but not in *Dilophosaurus wetherilli* (UCMP 37302), *Ceratosaurus* (USNM 4735), or more-derived theropods (e.g., *Allosaurus* or *Sinraptor*: Madsen, 1976; Currie and Zhao, 1993). Gilmore (1920:pl. 19) described and illustrated the epipophysis of *C. nasicornis* (USNM 4735) as being directed laterally (although, due to post-publication breakage of USNM 4735, it is no longer possible to ascertain this condition firsthand). The medial projection of the postzygapophyseal facet in *Majungasaurus* is similar to, but more developed than, the condition in *Ceratosaurus* and unlike that in *Sinraptor* and *Allosaurus*.

The medial process arches to form a partial roof over the dorsal aspect of the vertebral canal (Fig. 5A). Whereas it likely did not articulate directly with the corresponding element from the other side, rugose texturing on its ventromedial half suggests the presence of a substantial ligament connecting the medial process of each neurapophysis. The uncinate process consists of a small flange of bone extending cranioventrally from the craniolateral aspect of the peduncular crown, thereby forming a partial roof over the first cervical spinal nerve and its associated vasculature. A similar condition is present in *Sinraptor* (Currie and Zhao, 1993:fig. 12B) and to a lesser extent in *Ceratosaurus* (Gilmore, 1920:pl. 19, fig. 4).

Axis—The axis of UA 8678 (Fig. 6) was recovered in articulation with the third cervical vertebra, and these together were slightly displaced (15 cm) from the remainder of the articulated cervical series. This vertebra is moderately crushed on the right side of the centrum, and whereas there is slight torsion of the neural arch relative to the centrum, the overall shape of the vertebra is maintained. The axial intercentrum is firmly fused to the axial centrum, although a small, raised, circumferential ridge demarcates the line of fusion between the two elements. In lateral view, the ventral borders of both elements form a straight line (Fig. 6D), similar to the condition in many other theropods (e.g., *Ceratosaurus*, *Carnotaurus*, *Masiakasaurus*, and *Allosau-*

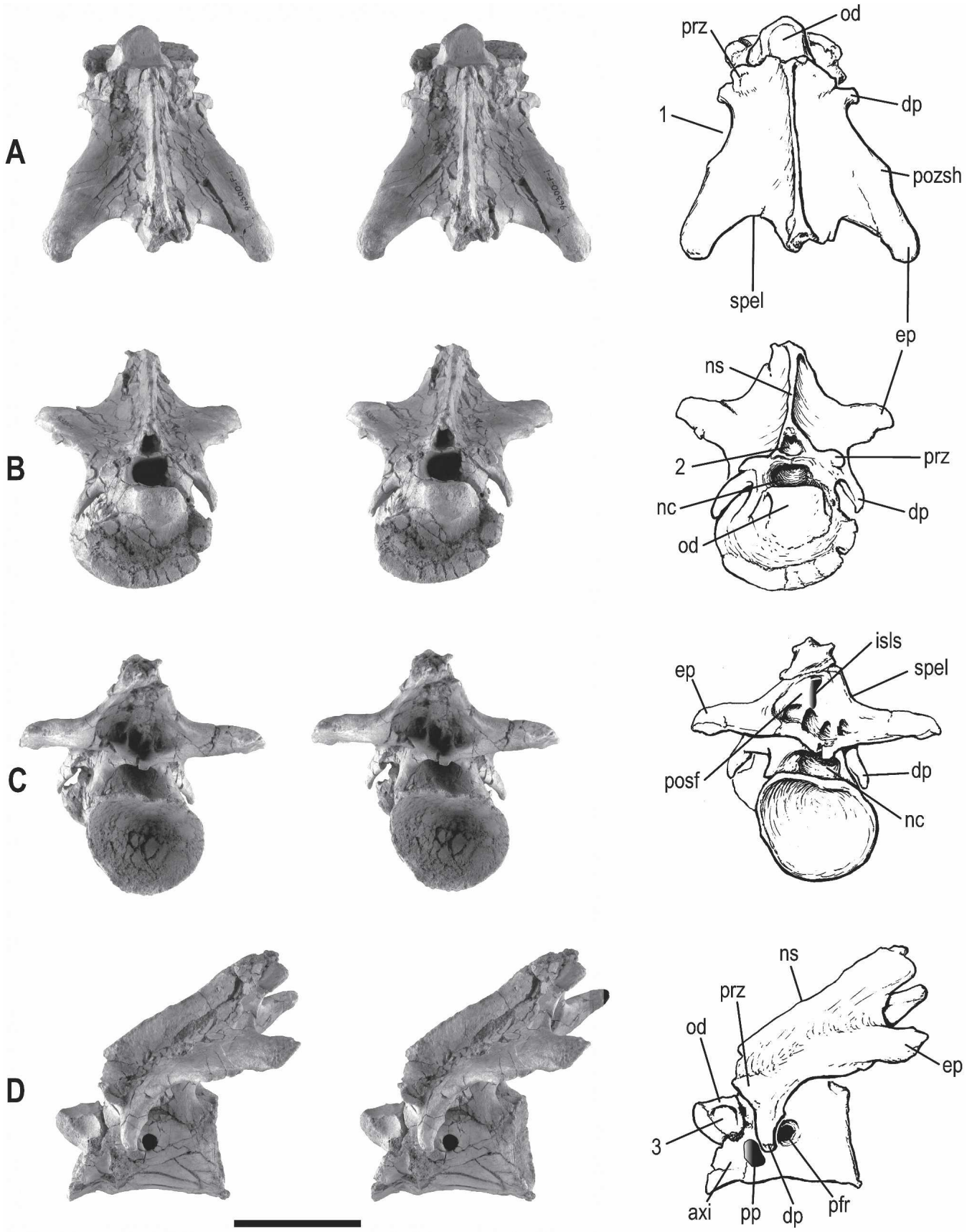

FIGURE 6. Second cervical (C2) vertebra (UA 8678) of *Majungasaurus crenatissimus* in dorsal (**A**), cranial (**B**), caudal (**C**), and left lateral (**D**) views. The left two images are stereophotographs, with the right interpretive drawing used for labeling purposes (the next five figures are arranged in a similar manner). **Notation**: **1**, crescent emargination of axial neural spine; **2**, pneumatic foramen? (see text for discussion); **3**, laterally flattened odontoid. See Appendix 1 for list of anatomical abbreviations. Scale bar equals 5 cm.

rus). Furthermore, the cranioventral margin of the intercentrum flares ventrally in a manner similar to that observed in *Masiakasaurus* and *Carnotaurus* (Bonaparte et al., 1990:fig. 8a), possibly representing a character shared by abelisauroid theropods. The odontoid (atlantal centrum) is partially fused to the craniodorsal aspect of the axial intercentrum, with an apparent open suture along the dorsal and dorsolateral margins of the element. This conformation is consistent with other features (e.g., unfused neurocentral sutures) indicative of the subadult status of this specimen.

The axial centrum is strongly opisthocoelous, with a caudal articular surface that is wider than high (Fig. 6C). The ventral surface of the centrum is broad, with only minimal development of a longitudinal ventral crest, similar to the condition in *Carnotaurus* but unlike the well-developed keel observed in *Herrerasaurus* (Sereno and Novas, 1993), *Ceratosaurus* (USNM 4735), and coelophysoids (e.g., *Dilophosaurus* [UCMP 37302]). Whereas axial centra of the allosauroid theropods *Sinraptor* and *Allosaurus* (e.g., MOR 693) also lack a well-defined ventral keel, they exhibit transverse pinching of the axial centrum near the centro-intercentral junction (Madsen, 1976:pl. 11; Currie and Zhao, 1993:fig. 13b). *Dilophosaurus* (UCMP 37302), *Ceratosaurus* (USNM 4735) and *Masiakasaurus* (FMNH PR 2445) also exhibit this feature. In contrast, in ventral view, abelisaurids maintain near parallel sides of the axial centrum-intercentrum throughout their length (e.g., Fig. 3), thereby highlighting a possible synapomorphy of the group. When viewed laterally (Fig. 6D), the caudal margin of the centrum forms a near-right angle with the ventral surface, similar to the condition in *Allosaurus*, but unlike the acute angle observed in other theropods (e.g., *Sinraptor*, *Carnotaurus*, *Ceratosaurus*). Abelisauroids show only minimal development of the concave ventral margin observed in most other noncoelurosaurian theropods. The laterally projecting parapophysis is located just above centrum mid-height, at the junction of the axial intercentrum and centrum. This condition appears unique among abelisauroids and more basal theropods, in which axial parapophyses tend to be ventrally placed on the craniolateral edge of the axial centrum and typically project ventrolaterally (e.g., *Herrerasaurus* [Sereno and Novas, 1993]; *Ceratosaurus* [USNM 4735]).

The odontoid is gently rounded on the ventral and cranial surfaces, with a shallow concavity along its dorsal aspect. The lateral surface of the odontoid is flat (Fig. 6D), rather than rounded as in many tetanurans (e.g., *Allosaurus* [UCMP 99094]) or concave as in coelophysoids (e.g., *Dilophosaurus* [UCMP 37302, UCMP 77270]). A single, round pneumatic foramen (~7 mm diameter) is present on the lateral surface of the centrum just caudodorsal to the parapophysis. In contrast, axial centra of *Masiakasaurus* (FMNH PR 2445) and *Carnotaurus* (Bonaparte et al., 1990) possess two pneumatic foramina on the lateral surface of the centrum, whereas *Sinraptor* exhibits asymmetry in these features, with two on the left and one on the right side (Currie and Zhao, 1993). The pneumatic foramen in UA 8678 is coplanar with the cortical surface and is not located within a large laterally-facing fossa as in forms like *Ceratosaurus* (USNM 4735) and *Allosaurus* (MOR 693, UCMP 99094). However, another, larger specimen of *Majungasaurus* (FMNH PR 2293) exhibits a large pneumatic foramen set within the confines of a large, laterally facing fossa; such differences in a single taxon likely represent ontogenetic variation in the development of pneumatic features. Generally, coelophysoids (e.g., *Dilophosaurus* [UCMP 37302]) and other basal theropods lack pneumaticity of the axial centrum (Rowe, 1989).

The neural arch is virtually complete with small, ventrally directed transverse processes, well-developed epipophyses, and a near-straight, extremely thin dorsal margin that slopes caudodorsally (Fig. 6). The transverse process tapers and is capped distally by a small diapophysis. In dorsal view, the plate-like neural arch exhibits lateral edges that sweep caudolaterally to such an extent that the epipophysis extends further caudally than the neural spine (Fig. 6A), thereby forming bilateral concavities along the caudodorsal aspect of the element. This condition is also present in *Carnotaurus* (Bonaparte et al., 1990:fig. 8b) and *Masiakasaurus* (FMNH PR 2445). Whereas epipophyseal expansion of the axis is known in other abelisaurid taxa in addition to the allosauroid *Sinraptor* (Currie and Zhao, 1993:fig. 13d), it is not present to the same degree in *Allosaurus* (MOR 693) and other tetanurans. Another shallow concavity is located along the cranial half of the lateral neural arch margin (Fig. 6A), demarcating the medial limit of the atlantal epipophysis when the two vertebrae are in articulation. Axial epipophyses are directed laterally such that a near-equilateral triangle, defined by the vertices at each epipophysis and the cranial limit of the neural spine (Figs. 4A, 6A), is formed when viewed dorsally. A similar situation exists in *Carnotaurus* (Bonaparte et al., 1990:fig. 8), but is in marked contrast to the condition in most other theropods (e.g., *Herrerasaurus*, *Ceratosaurus*, *Masiakasaurus*, *Allosaurus*), where epipophyses are located closer to the midline, thereby forming an isosceles triangle using the same three points. *Dilophosaurus* (UCMP 37302) also exhibits a broad axial neural arch with laterally divergent epipophyses, similar to the condition in *Majungasaurus* and *Carnotaurus*. However, the axis of *Dilophosaurus* is quite different from abelisauroids in having craniocaudally restricted epipophyses and an overall increase in relative vertebral height.

A small, dorsolaterally facing prezygapophysis is present for articulation with the atlantal neurapophysis. Similar to the condition in nontetanuran theropods (e.g., *Ceratosaurus*, *Carnotaurus*), the prezygapophysis is located just cranial to the base of the transverse process. In forms such as *Allosaurus*, the prezygapophysis is craniocaudally separated from the transverse process (MOR 693, UCMP 99094; Madsen, 1976:pl. 11). The postzygapophyseal facet is greatly enlarged, oriented horizontally, and exhibits a transversely-oriented major axis. Further, the facets are subtriangular in shape, with a craniocaudally expanded lateral margin. In lateral view, a straight spinous margin is present in both specimens of *Majungasaurus* that preserve the axial neural arch. The small-bodied abelisauroid *Masiakasaurus* (FMNH PR 2445) exhibits similar morphology, in contrast to the dorsally convex spinous margin in *Carnotaurus* and *Ceratosaurus.*

Similar to *Carnotaurus*, the caudodorsal end of the neural spine is forked. Bilateral spinoepipophyseal laminae extend from the caudodorsal aspect of the neural spine to each epipophysis (Fig. 6). These form the dorsolateral borders of a large postspinal fossa (postchonos of Welles, 1984) located on the caudal surface of the neural arch (Fig. 6C). The postspinal fossa is subdivided into a pair of fossae separated from one another on the midline by the interspinous ligament ridge. Bone within each fossa is texturally distinct in that it appears much smoother (i.e., less porous) than cortical bone from other areas of the vertebra.

Although crushing partially limits the identification of specific cortical structures, two pairs of foramina are positioned on the ventral surface of the neural arch. The first set is located just cranial to the postzygapophysis whereas the other is positioned medial to the base of the transverse process, forming infrapostzygapophyseal and infradiapophyseal foramina respectively. These foramina are similar to those described for *Carnotaurus* (Bonaparte et al., 1990). Unlike the condition in *Ceratosaurus* (USNM 4735) and *Allosaurus* (MOR 693), the axis of *Majungasaurus* does not possess foramina or fossae on the dorsal aspect of the neural arch. There is, however, a single, midline opening at the cranioventral end of the neural spine, just dorsal to the vertebral canal (Fig. 6B). Due to its broken edges, it appears that this structure is the result of postmortem breakage.

Postaxial Cervical Vertebrae—The third cervical (C3) vertebra of UA 8678 is virtually complete; however, it does exhibit considerable deformation of both the neural arch and centrum and is missing the distal end of the right transverse process. Fortunately, an additional, better-preserved specimen (FMNH PR 2295) was discovered at locality MAD 93-18 (Fig. 7). Aside from size differences, the two third cervical vertebrae known for *Majungasaurus* (UA 8678 and FMNH PR 2295) are virtually identical. The centrum of C3 is strongly opisthocoelous, with a flat cranial articular surface. Additionally, the cranial articular surface is positioned dorsal relative to the caudal surface, a situation that exists in vertebrae between position C3 and C9. A slight crest is present on the gently rounded ventral surface of the centrum. Whereas the crest on this vertebra represents the maximal development of a 'ventral keel' throughout the vertebral column, it is in marked contrast to the prominent condition present in many other theropods (e.g., *Herrerasaurus*; Sereno and Novas, 1993; *Ceratosaurus* [USNM 4735]). Midcervical vertebrae of *Dilophosaurus* (UCMP 37302) and other coelophysoids (e.g., *Liliensternus liliensterni* [MB 2175.2]) also lack prominent keels, but, in contrast to the gently rounded condition of abelisauroids, possess a flat ventral surface. The parapophysis of C3 projects ventrolaterally and is notably ovoid, with its major axis oriented craniodorsal to caudoventral, as in *Carnotaurus* (Bonaparte et al., 1990:fig. 9). The major axis is oriented from cranioventral to caudodorsal in many other nontetanuran theropods (e.g., *Herrerasaurus*, *Dilophosaurus*, *Ceratosaurus*, *Ilokelesia*), whereas more derived taxa (e.g., *Allosaurus*, *Sinraptor*) have a parapophyseal orientation similar to *Majungasaurus* and *Carnotaurus*. The parapophysis remains close to the lateral surface of the centrum and hence does not possess the distinct pedestal present in forms such as *Dilophosaurus* (UCMP 77270), *Herrerasaurus* (Sereno and Novas, 1993), and *Rajasaurus* (Wilson et al., 2003:fig. 5B).

A pneumatic foramen is located in the caudal half of the lateral surface of the centrum. The foramen is positioned at the cranial end of a craniocaudally-oriented sulcus at mid-height of the centrum. This condition differs from that in the third cervical vertebra of *Carnotaurus*, where "two small pleurocoels are present on the rather flat lateral side of the centrum" (Bonaparte et al., 1990:12). *Ilokelesia* also possesses a pair of 'pleurocoels' in the lateral central surface (Coria and Salgado, 1998). Whereas there is a small (<1 mm) slit located dorsal to the parapophysis in C3 of *Majungasaurus* (possibly corresponding to the cranial pair of features in other abelisauroids), it is unclear what type of soft-tissue structure (e.g., vasculature, air sac diverticula, etc.) may have been associated with this opening.

The neural arch is intact and characterized by enlarged epipophyses, laterally expanded postzygapophyses, a transversely narrow and caudodorsally directed neural spine, and numerous foramina communicating with internal pneumatic chambers. Pre- and postzygapophyseal facets are nearly horizontal, with their major axes oriented transversely. Epipophyseal expansion in *Majungasaurus* reaches its maximum in C3–C4 and, similar to the condition in *Ilokelesia* (Coria and Salgado, 1998), occurs in the caudal direction only. It appears that, whereas cranial expansion of postaxial cervical epipophyses may characterize Carnotaurini (Bonaparte et al., 1990; Coria and Salgado, 1998; Coria et al., 2002), caudal expansion characterizes a more inclusive group of abelisauroids (e.g., *Majungasaurus*, *Ilokelesia*, *Carnotaurus*, *Noasaurus*). Caudal expansion is also present in certain tetanurans such as *Sinraptor* (Currie and Zhao, 1993:fig. 13). In general, the smaller-bodied abelisauroids (e.g., *Masiakasaurus* [FMNH PR 2140]; *Laevisuchus indicus* [ISI K27/696]) do not exhibit caudal expansion of the epipophysis in the cervical series (Carrano et al., 2002:fig. 7A-C). *Noasaurus* (PVL 4061) is the exception, exhibiting both cranial and caudal epipophyseal expansion similar to that in carnotaurines (Bonaparte and Powell, 1980).

The C3 neural spine is higher than the epipophysis (Fig. 7D). Moreover, the neural spine tapers dorsally (i.e., it possesses nonparallel cranial and caudal margins) and is caudally positioned rather than being located over the mid-portion of the centrum as in forms such as *Ceratosaurus* and *Allosaurus*. *Majungasaurus* shares both of these features with *Carnotaurus* (Bonaparte et al., 1990:fig. 9B). The prespinal fossa is large (Fig. 7A) with dorsolateral margins defined by distinct spinoprezygapophyseal laminae. Prezygoepipophyseal laminae span the entire length of the neural arch (Fig. 7A). These features have received considerable attention by other authors, particularly with reference to the degree to which they demarcate the dorsal and lateral surfaces of the neural arch (e.g., see Bonaparte et al., 1990; Coria and Salgado, 1998; Sereno et al., 2004). Specifically, a well-defined prezygoepipophyseal lamina has been featured as a purported synapomorphy of Abelisauridae (Coria and Salgado, 1998). Interestingly, two different specimens of *Majungasaurus* preserving the third cervical vertebra show differential development of this feature. One specimen (FMNH PR 2295:Fig. 7D) has a sharp ridge running from the prezygapophysis to the epipophysis, and is thereby consistent with the description for other abelisaurids. Another specimen (UA 8678) lacks a well-defined ridge and exhibits a gently rounded border between the dorsal and lateral surfaces of the neural arch. Whereas the significance of this difference remains unclear, the second specimen is ~10% smaller than the first, and the absence of a sharply defined border may represent ontogenetic variation. The majority of the succeeding postaxial cervical vertebrae (C4–C7) of UA 8678 exhibit sharply defined borders separating the dorsal and lateral aspects of the arch (Fig. 8A–D). The lateral margin of each postzygapophysis extends lateral to the prezygoepipophyseal lamina, making it visible in dorsal view (Fig. 7A). This forms a postzygapophyseal shelf that projects from the lateral arch surface. Succeeding vertebrae in the series do not exhibit this feature.

Numerous, well-defined fossae and foramina are present on the neural arch. Most prominent are those on the ventral surface just cranial to the postzygapophyses (Fig. 7C, D). In caudal view, a diamond-shaped postspinal fossa is present dorsal to the neural canal at the junction of the neural spine and postzygapophyses. The dorsolateral borders of this diamond are formed by spinopostzygapophyseal laminae whereas the ventrolateral borders are formed by the two postzygapophyses and the intrapostzygapophyseal lamina. Within the fossa a pair of dorsoventrally elongate foramina connects with neural arch pneumatic cavities. Each foramen is positioned just lateral to the ventralmost attachment of the interspinous ligament (Fig. 7C). Although similar foramina are present on the axis (Fig. 6C), those on C3 are considerably more restricted. A similar situation is described in *Carnotaurus* (Bonaparte et al., 1990), whereas *Ilokelesia* exhibits a fossa in this location (Coria and Salgado, 1998:fig. 5). Additionally, a round laminopeduncular pneumatic foramen (cranial peduncular foramina of Britt, 1993) is located on the craniodorsal aspect of each pedicle (Fig. 7B). Due to the extraordinary preservation of this specimen, it is clear that all abovementioned foramina communicate with a series of large cavities within the neural arch and centrum. Fortuitous breaks in this specimen reveal continuity of internal chambers, including both dorsal expansion into the epipophysis (Fig. 7C) and communications between the neural arch and centrum via the pedicles. Noticeably absent are foramina located medial to the base of the transverse process. This condition differs from that in C3 of *Ilokelesia*, in which large infradiapophyseal foramina are present at this location (Coria and Salgado, 1998).

Although similar in overall proportions to C3, the fourth cervical vertebra is more robust, particularly within the transverse processes. Whereas this vertebra retains most of its three-

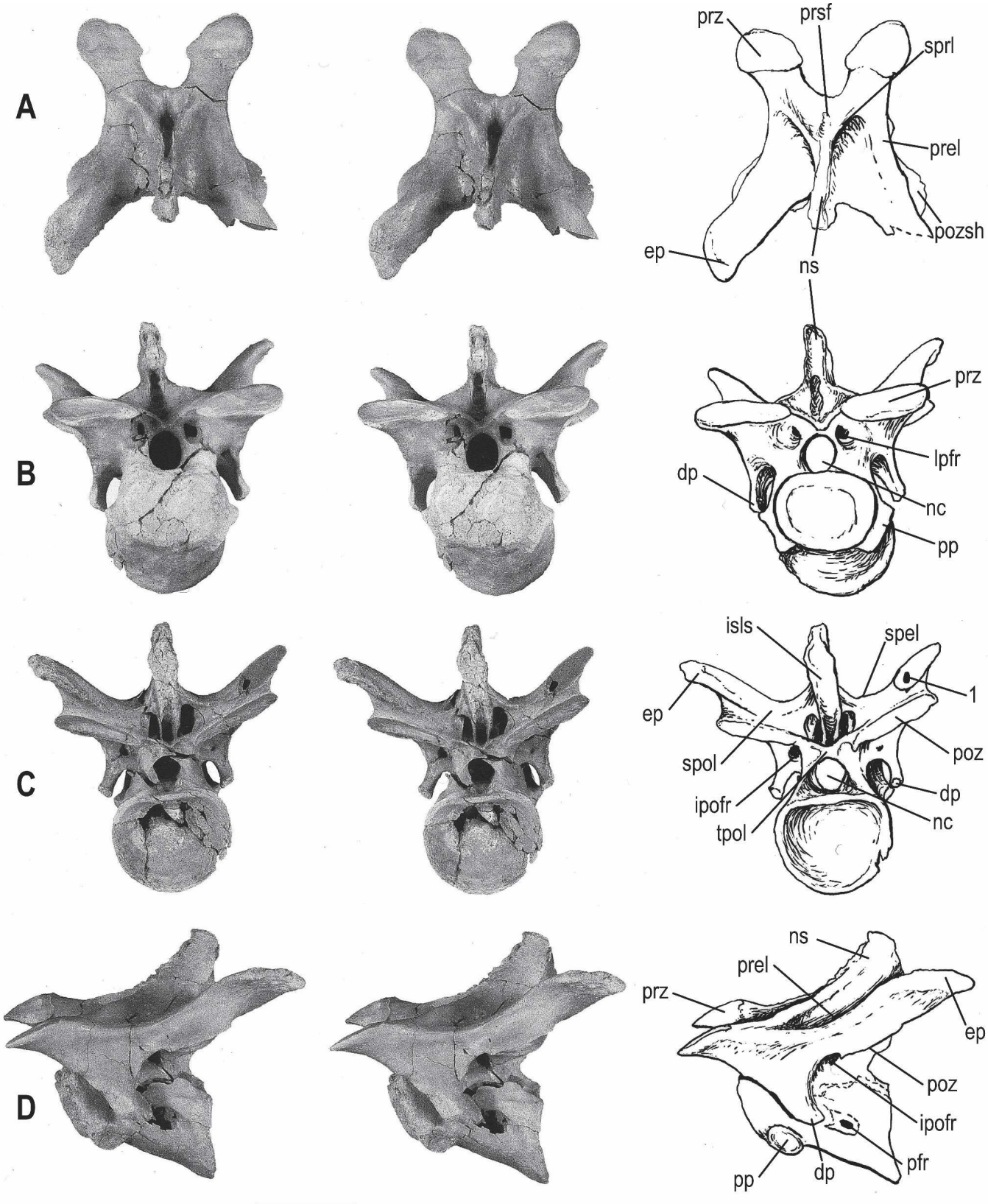

FIGURE 7. Third cervical (C3) vertebra (FMNH PR 2295) of *Majungasaurus crenatissimus* in dorsal (**A**), cranial (**B**), caudal (**C**), and left lateral (**D**) views. **Notation**: **1**, pneumatic cavity within right epipophysis. See Appendix 1 for list of anatomical abbreviations. Scale bar equals 5 cm.

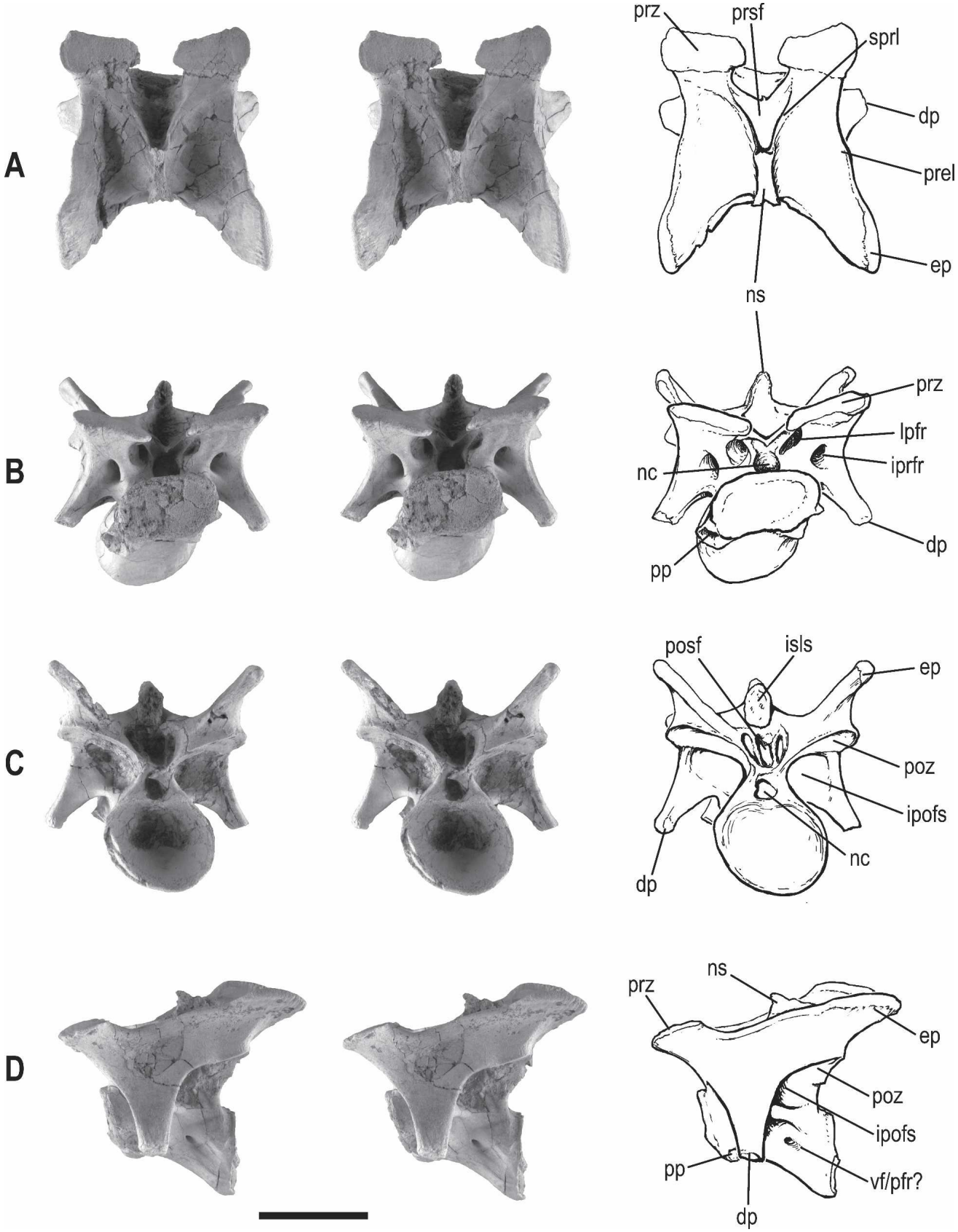

FIGURE 8. Fifth cervical (C5) vertebra (UA 8678) of *Majungasaurus crenatissimus* in dorsal (**A**), cranial (**B**), caudal (**C**), and left lateral (**D**) views. See Appendix 1 for list of anatomical abbreviations. Scale bar equals 5 cm.

dimensional shape, the left side of the centrum and dorsal surface of the neural arch are slightly crushed. Similar to C3, the centrum is opisthocoelous, with a flat cranial articular surface offset dorsally relative to the caudal surface. The ventrolaterally directed parapophyses are oriented with the long axis running from craniodorsal to caudoventral. The ventral surface of the centrum is flat with no evidence of a keel. However, a small interparapophyseal crest spans transversely between the parapophyses. Whereas poor preservation of the left surface of the centrum precludes the identification of specific cortical features, the right side clearly shows the absence of any large (>1 mm) foramina. There is a craniocaudally-oriented sulcus at mid-height on the caudal half of the centrum, similar to the situation in C3. Although no distinct foramen is associated with this sulcus, a small slit-like opening is present. There is also a small (<1 mm) supraparapophyseal slit located at central mid-height. The neural arch of C4 is similar in many respects to that of C3 in possessing enlarged epipophyses and a reduced neural spine. Pre- and postzygapophyseal facets retain transversely oriented long axes, but are no longer horizontal. The articular surface of the prezygapophyseal facet is oriented dorsomedially, rather than dorsally as in the preceding vertebra. There is a concomitant change in the surface orientation of postzygapophyseal facets, such that the ventrolaterally facing facets are oriented ~15–20° relative to the horizontal. This change in facet orientation continues into the caudal cervical vertebrae, similar to the condition in other theropods. The neural spine is laterally compressed, and its maximum height equals that of the epipophysis. The cranial and caudal borders of the neural spine are parallel, as in the remainder of the presacral vertebrae. Similar to the condition in C3 (and in C5), the craniocaudal extent of the neural spine is restricted dorsally over the caudal half of the centrum, and a large triangular prespinal fossa is present on the craniodorsal surface of the arch. A well-developed prezygoepipophyseal lamina is present and clearly demarcates the dorsal and lateral surfaces of the arch. The surfaces of each ventrolaterally directed transverse process are defined to such a degree that the dorsolateral and caudal surfaces meet each other at approximately 90°, similar to that of succeeding cervical vertebrae (see Fig. 8D). In lateral view, the transverse process has near-parallel cranial and caudal borders throughout most of its length. This condition differs substantially from that in other abelisaurids (e.g., *Ilokelesia*, *Carnotaurus*), in which the transverse process appears as a large, flat triangular plate in lateral view (Bonaparte et al., 1990:fig. 10; Coria and Salgado, 1998:fig. 5). The caudal centrodiapophyseal lamina of *Majungasaurus* joins the centrum around midlength, similar to the condition in *Carnotaurus*. This conformation differs from that in *Ilokelesia*, in which the caudal centrodiapophyseal lamina attaches further caudally (Coria and Salgado, 1998:fig. 5). The caudodorsal surface of the transverse process is transversely expanded, with its medial edge forming the lateral rim of the infrapostzygapophyseal fossa. In general, the fossae and foramina of C4 are similar in shape and location to those of C3, with the addition of foramina located just medial to the base of each transverse process. The caudal aspect of the neural arch retains the diamond-shaped postspinal fossa and its associated foramina.

The fifth cervical vertebra (UA 8678; Fig. 8) is better preserved and considerably more robust than the fourth. Notable differences between the two include a shorter, craniocaudally expanded neural spine, and a shorter but wider epipophysis in C5. Features related to the centrum (e.g., opisthocoelous with flat cranial surface, lack of ventral crest, offset articular facets) remain similar. However, there is no interparapophyseal crest on the ventral surface of C5, nor is this feature present on any succeeding vertebrae. The parapophysis retains a ventrolaterally facing articular surface. In lateral view, a concavity is apparent on the ventral surface of the centrum of C5. A fossa is present on the caudal half of the centrum, and an obliquely positioned canal enters the centrum at the cranial end of the fossa (Fig. 8D). Unlike the preceding two vertebrae, a supraparapophyseal foramen/slit is absent.

The neural arch of C5 is characterized by a short neural spine that is craniocaudally elongate compared to C4. Indeed, the neural spine of C5 possesses the greatest absolute length of all the cervical neural spines. The neural spine is also transitional in that the caudal surface, and thus the attachment surface for the interspinous ligament, is ~30% larger than the cranial surface. This feature no doubt relates to the fact that successively more caudally positioned osseous and ligamentous structures must support a proportionately larger mass than preceding structures. Similar to C4, the neural spine is located over the caudal half of the centrum, and attains a maximum height equal to that of the epipophysis. Whereas the epipophysis is slightly reduced in length relative to C4, it is wider (i.e., laterally expanded) and more substantially built. The transverse process is directed ventrolaterally and is craniocaudally restricted. There is an increase in width of the postzygapophysis compared with C4, and pneumatic features are generally similar in position to those described for preceding vertebrae. However, foramina at the base of each transverse process are significantly enlarged, as are fossae positioned at the cranial edge of each postzygapophysis (Fig. 8C, D). Infraprezygapophyseal foramina are dorsoventrally elongate (Fig. 8B), and laminopeduncular foramina are apparent just dorsolateral to the neural canal (Fig. 8B).

The sixth cervical vertebra, aside from being slightly larger, is similar in most regards to C5. Subtle differences include a decrease in the craniocaudal length of the neural spine and slight dorsal elevation of the transverse process. Unlike C5, a supraparapophyseal slit is present on the left side of the centrum of C6. Notably absent are fossae or foramina on the caudal half of the lateral central surface. Continuing the trend observed in the preceding two vertebrae, the epipophysis exhibits a reduction in length and an increase in width. The neural spine is centered dorsal to mid-centrum length, rather than over the caudal half of the centrum. Related to cranial migration of the neural spine is the loss of a distinct diamond-shaped postspinal fossa. In its place is a large pyramidal depression with the interspinous ligament scar forming its cranial limit. Foramina are present on the ventrolateral surface of the depression, adjacent to the attachment site of the interspinous ligament. Canals passing from each foramen lead cranially into the neural arch. Similar to the condition described for caudal arch fossae of the axis, smooth-textured bone is apparent adjacent to the opening of each canal. Whereas the craniocaudally narrow transverse process is still directed ventrolaterally, it does exhibit the onset of dorsal migration observed in mid- to caudal cervical vertebrae of most other theropods.

The seventh cervical vertebra is slightly crushed along the dorsoventral axis, with most damage localized to the pedicles. Most other components of the neural arch are intact and preserved in three dimensions. The low, broad centrum is generally similar to preceding centra in being opisthocoelous, with a flat cranial articular surface that is offset from the caudal surface. Additionally, the ventral margin of the centrum is concave in lateral view and an ovoid parapophysis is directed ventrolaterally. Cortical surfaces of the centrum are poorly preserved; however, a craniocaudally oriented fossa is apparent on the lateral centrum surface at mid-height, similar to those identified in C3–5. Due to poor preservation, it is unclear whether foramina are present within the fossa. The supraparapophyseal slit is replaced by a sizable foramen (>4 mm) located dorsal to each parapophysis. Reduced epipophyses and a neural spine that is craniocaudally shorter, yet higher and transversely expanded relative to the neural spine of C6, characterize the neural arch of C7. The overall length of the arch is reduced (as measured by the interzygapophyseal length;

see Table 1). Due to its crushed condition, it is impossible to characterize the exact nature of cortical features.

The eighth cervical vertebra is intact and preserves much of its three-dimensional shape, although the neurocentral junction is slightly crushed at the cranial end. The caudal articular surface of the centrum is round, in contrast to the transversely oval condition exhibited by preceding vertebrae. The cranial and caudal articular surfaces are offset, but to a lesser degree than in C7 (Fig. 3). In lateral view, two large foramina are present at midcentrum height. The caudally positioned foramen enters the centrum at the cranial end of the craniocaudally oriented fossa. The other foramen is positioned on the cranial half of the centrum just dorsal to the parapophysis. The epipophysis is further reduced in C8 whereas the neural spine is higher and transversely expanded, similar to that in C7. As compared with *Carnotaurus* (Bonaparte et al., 1990), the dorsal surface of the arch is reduced in area and a distinct prezygoepipophyseal lamina is absent. Notably different from preceding vertebrae are the enlarged, pyramid-shaped infrapostzygapophyseal fossae. Each fossa is defined by three laminae: the caudal centrodiapophyseal lamina ventrally, the centropostzygapophyseal lamina medially, and the postzygodiapophyseal lamina cranially. Multiple foramina pierce the neural arch at the ventromedial border of the fossa. The transition from distinct infrapostzygapophyseal foramina to enlarged infrapostzygapophyseal fossae occurs between C5 and C7. Due to poor preservation of the preceding two vertebrae (C6–7), however, the exact nature (e.g., abrupt vs. gradual change) of this transition is unclear. Infradiapophyseal foramina are present and transversely elongate.

The ninth cervical vertebra is well preserved and undistorted. Although the right surface of the centrum is slightly crushed, the distal end of the left diapophysis is the only portion completely missing. The centrum is taller and rectangular in cross-section, rather than oval as observed in preceding vertebrae. The ventral surface of the centrum lacks a keel, in stark contrast to the condition of C9 in *Carnotaurus* (Bonaparte et al., 1990). The cranial and caudal articular surfaces are round and only slightly offset. Whereas the cranial articular surface remains flat, the degree of opisthocoely is reduced relative to preceding vertebrae. In lateral view, the ventral surface of the centrum is concave and the parapophysis is directed laterally, unlike the ventrolaterally directed parapophyses observed in more cranially-positioned vertebrae. Pneumatic foramina are present on the lateral surface of the centrum. The right side of the centrum is similar to that of C8, with two foramina located at midcentral height. The left surface contains only a single foramen dorsal to the parapophysis. The neural arch exhibits the continuation of trends described for preceding vertebrae, including increased neural spine height and width, a further reduced epipophysis, and a dorsally elevated transverse process. This is the first vertebra caudal to C3 for which the neural spine height exceeds that of the epipophyses. The ninth cervical vertebra of *Carnotaurus* is drastically different in this regard, as the epipophyses are significantly higher than the dorsal extent of the neural spine (Bonaparte et al., 1990:fig. 12).

An increase in diameter of the transverse process, associated with the dorsal migration of the element, is accompanied by the development of a large fossa (infradiapophyseal fossa) on the ventral surface of the neural arch. In preceding vertebrae (C4–C8), the base of the transverse process contains a distinct foramen on its ventral surface. As the process increases in size and assumes a more lateral trajectory, large fossae are defined between the cranial and caudal centrodiapophyseal laminae (i.e., infrapre- and infrapostdiapophyseal laminae respectively; e.g., Owen, 1856; Britt, 1993). Thus, a pattern exists where pneumatic features occur as distinct foramina cranially and transition to fossae in more caudal elements of the series. Additional foramina are present on the ventromedial surface of the transverse process. A large, pyramidal infraprezygapophyseal fossa is present on the cranial aspect of the neural arch, bounded by the centroprezygapophyseal lamina dorsomedially, the cranial centrodiapophyseal lamina ventrally, and the prezygodiapophyseal lamina dorsolaterally. Similar to the transition described for the infradiapophyseal region, infraprezygapophyseal pneumaticity exists as foramina cranially (Fig. 8B) and fossae caudally (Fig. 9B) within the cervical series. Infrapostzygapophyseal fossae are similar to those described in C8. Cranial and caudal laminopeduncular foramina are also present on this vertebra.

Similar to the ninth cervical vertebra, the tenth is well preserved and retains its three-dimensional shape (Fig. 9). The right side of the centrum is slightly crushed and the arch is missing the distal half of the left transverse process. In contrast to other cervical vertebrae, central articular surfaces are only slightly offset from each other and, in lateral view form right angles with the horizontal axis of the vertebra. A similar condition exists in *Carnotaurus* (Bonaparte et al., 1990:fig. 13). The cranial articular surface remains flat, whereas the caudal surface is slightly concave. The centrum is nearly rectangular in cross section and a ventral concavity is apparent in lateral view. The parapophysis is located on the cranioventral aspect of the centrum and is directed laterally, similar to C9. There is an incipient, rounded sagittal crest on the ventral surface, rather than a significant ventral keel. On the left side an enlarged foramen (>12 mm) is positioned immediately dorsal to the parapophysis. Within the aperture of this foramen are numerous trabeculae that resemble pneumatic architecture found in the vertebrae of many extant bird groups (O'Connor, 2004, 2006). Foramina located on more cranial vertebrae (with the exception of the axis) are only 1/4 to 1/3 this size. C10 lacks a caudally positioned foramen or fossa on the left side. Moreover, the crushed nature of the right surface of the centrum precludes identification of specific cortical features. Two distinct pairs of foramina are present on C10 of *Carnotaurus* (Bonaparte et al., 1990:fig. 13].

The neural spine has a transverse notch around the dorsal margin (Fig. 9D) and the transverse process is directed ventrolaterally at an angle of 65° angle relative to the dorsoventral axis (Figs. 4C, 9C). Neural arch fossae are generally similar to those described for C9. However, due to the exquisite preservation of this vertebra, numerous accessory laminae are apparent within many of the fossae (e.g., Fig. 9D). Laminopeduncular foramina are present cranially, but absent caudally. Of note is the presence of an enlarged foramen on the cranial surface of the right transverse process (Fig. 9B).

Dorsal Vertebrae

General—*Majungasaurus* possessed 13 dorsal vertebrae (Figs. 3, 10–13). Whereas some authors use the designation of 'pectoral' to describe morphology intermediate between that of cervical and dorsal vertebrae (e.g., Welles, 1984; Madsen and Welles, 2000), this term will not be used here. A pectoral vertebra is typically characterized by the positioning of parapophyses on both the centrum and neural arch (i.e., bridging the neurocentral suture). Only a single vertebra (presacral 14) of *Majungasaurus* exists with this configuration. By using this framework, *Majungasaurus* would be characterized as possessing 13 cervical, one pectoral, and nine dorsal vertebrae. Such a description would no doubt promote more confusion than clarity on the issue of regional vertebral number in theropods. For simplicity, the boundary between cervical and dorsal vertebrae is defined by the abrupt increase in parapophyseal size and diapophyseal robusticity, both indicative of the increased rib size that coincides with encasement of thoracic structures and articulation with the sternum. The last dorsal vertebra of the series (presacral 23) formed part of the sacral complex, as indicated by an articular contact

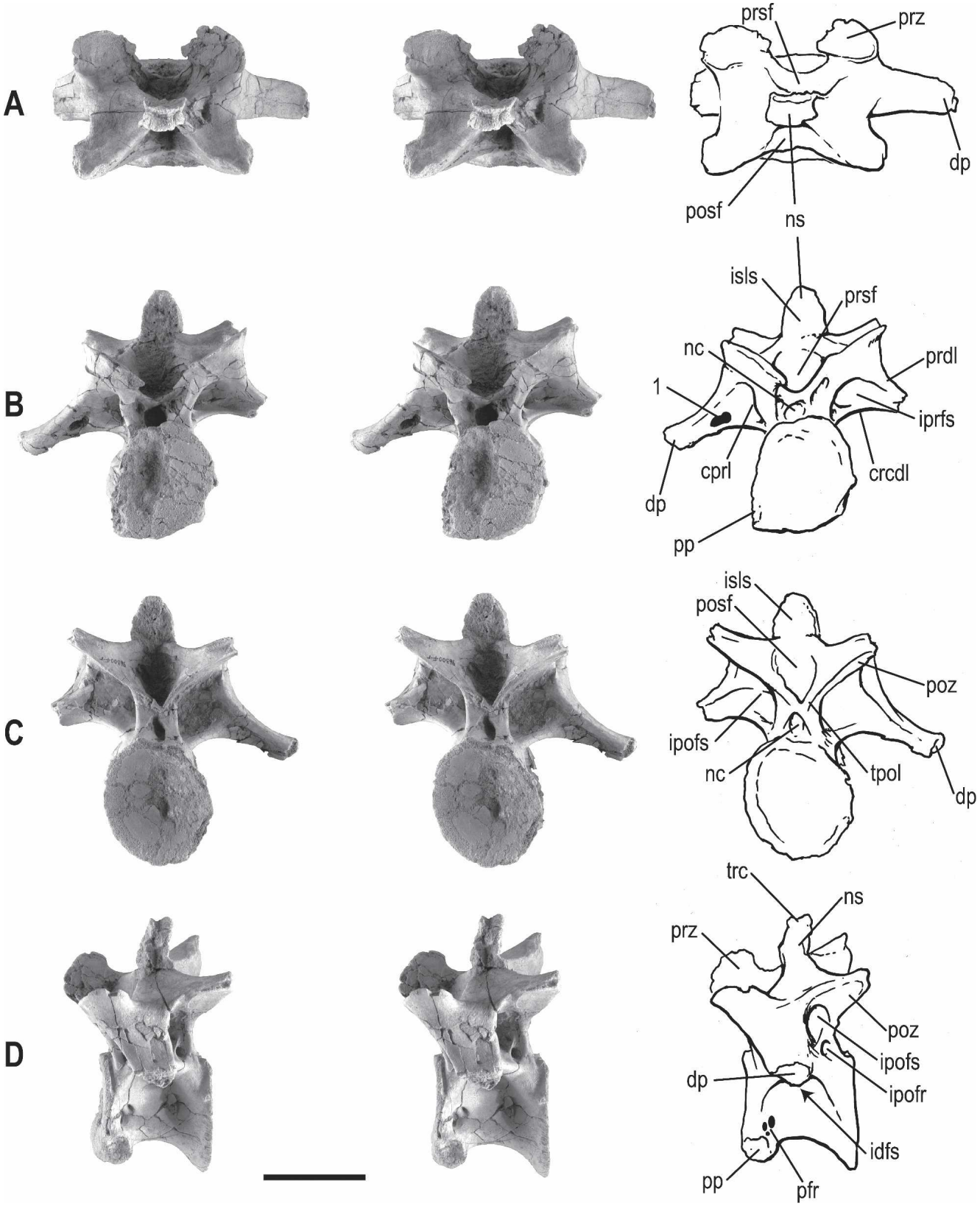

FIGURE 9. Tenth cervical (C10) vertebra (UA 8678) of *Majungasaurus crenatissimus* in dorsal (**A**), cranial (**B**), caudal (**C**), and left lateral (**D**) views. **Notation**: **1**, pneumatic foramen on cranial surface of right transverse process. See Appendix 1 for list of anatomical abbreviations. Scale bar equals 5 cm.

between its diapophysis and the preacetabular iliac blade (see below). For the purposes of description, D1–6 are referred to as 'cranial dorsals' and D7–13 as 'caudal dorsals,' although there is no abrupt transition within the dorsal column.

Generally, dorsal vertebrae of *Majungasaurus* are characterized by short, weakly amphicoelous centra and low, stout neural spines. The length-height ratio of centra throughout the dorsal column ranges between 0.90 and 1.05 (Table 1). Vertebrae of the cranial dorsal series exhibit articular faces that are dorsoventrally ovoid, whereas articular surfaces in the caudal dorsals are nearly circular. Centra are transversely narrow throughout most of their length, giving each a characteristic pinched (spool-shaped) appearance. Neural arches and centra of UA 8678 are fused in the first two dorsal vertebrae (presacral 11 and 12), although the neurocentral suture is clearly visible. Vertebrae caudal to this position remain completely unfused (Fig. 3). In the mid- and caudal dorsals, prezygapophyseal facets are directed dorsolaterally rather than dorsomedially. The first hyposphene is incipiently present on the second dorsal vertebra (presacral 12). All successive presacral vertebrae (presacrals 13–23) exhibit hyposphene-hypantrum articulations characteristic of saurischian dinosaurs (Gauthier, 1986). Whereas neural spine height increases relative to the cervical series, spines are still relatively short as compared with most nonabelisauroid theropods (e.g., *Ceratosaurus dentisulcatus* [UUVP 48], Madsen and Welles, 2000; *Sinraptor*; Currie and Zhao, 1993; *Allosaurus* [USNM 8367]).

Cranial dorsal (D3–6) neural arches appear triangular in dorsal view, whereas the arches of D7–11 are subrectangular (Figs. 3, 9, 10). Neural spines gradually increase in length throughout the series with a concomitant reduction in transverse width. A related feature is the attachment for the interspinous ligament, which, in contrast to the condition in most theropods, extends to the dorsal limit of each neural spine (Figs. 10, 11). Postspinal fossae are particularly well developed throughout the dorsal series, with distinct spinopostzygapophyseal laminae demarcating their lateral borders. Distinct prespinal fossae are also present, but are not as well defined as their postspinal counterparts. Neural spines of mid-dorsal vertebrae exhibit transverse expansion of the caudodorsal tip and are characterized by extremely rugose bone texture, as in *Carnotaurus* (Bonaparte et al., 1990). Transverse processes are triangular in cross-section in D1–2 and assume flat, plate-like cross-sections in more caudally positioned vertebrae. The transverse process of D13 is rectangular in cross-section, with a robust diapophysis for articulation with the preacetabular portion of the ilium.

As is typical of nonavian theropods, dorsal vertebrae of *Majungasaurus* exhibit a dorsal migration of the parapophysis (i.e., from centrum to neural arch), moving cranial to caudal through the series. However, beginning with D4, the parapophysis progressively shifts laterally, ultimately approaching the lateral limit of the transverse process at D12. The PP/DP index (interparapophyseal width/interdiapophyseal width) ranges from 0.41 in D1 to ~0.80 in the caudal dorsal series, and equals ~1.0 in D12, where the parapophysis and diapophysis unite to form a single pleuropophysis (see Table 1). Such lateral displacement of the parapophysis characterizes abelisaurids (e.g., *Carnotaurus*, *Ilokelesia*) and likely represents a synapomorphy of the group. As the parapophysis shifts laterally, a series of variably present laminae connect it with other portions of the neural arch, thereby forming the boundaries of numerous neural arch fossae (e.g., infraprezygapophyseal fossa; Figs. 10, 11). As noted for cervical vertebrae, neural arch fossae are characterized by relatively smooth bone texture, particularly near points where foramina pierce the cortical surface and connect with internal chambers of the neural arch.

The following is a general discussion of vertebral laminae in dorsal neural arches of *Majungasaurus*, particularly as related to parapophyseal migration. Vertebra-specific modifications are discussed in the following sections. A single lamina buttresses the parapophysis ventromedially, connecting along the centroprezygapophyseal lamina near the neurocentral suture (cranial [anterior] centroparapophyseal lamina). In the mid-dorsal series (D5–D10), two laminae also connect the parapophysis to different points on the transverse process (Figs. 3, 11). The first is a transversely oriented lamina (the caudal paradiapophyseal lamina) that extends between the parapophysis and the caudal centrodiapophyseal lamina. The second (the dorsal paradiapophyseal lamina) extends dorsally to connect the parapophysis with the ventral surface of the prezygodiapophyseal lamina, giving the appearance that the former is suspended from the latter (Figs. 10D, 11D). And finally, a lamina present only on D4 and D5 (the prezygoparapophyseal lamina) connects the parapophysis dorsomedially with the prezygapophysis (Fig. 10D).

Cranially-positioned pneumatic foramina are present bilaterally on D1–D3 just caudal to the parapophysis, whereas the centrum of D4 exhibits a foramen on the right side only. Foramina occupying a caudal position on the lateral surface of the centrum are absent on all dorsals. This pattern of pneumaticity in dorsal centra (i.e., cranial foramina on D1–D4) is similar to that present in many theropods, such as *Spinostropheus gautieri* (MNN TIG6), *Allosaurus* (Madsen, 1976), and *Sinraptor* (Currie and Zhao, 1993), yet unlike the condition reported for *Carnotaurus* (Bonaparte et al., 1990) and *Acrocanthosaurus atokensis* (Harris, 1998), in which central foramina are found in the series through at least D10 (see below for additional discussion on variation in postcranial pneumaticity among nonavian theropods). Similar to the cervical vertebral series, paired basivertebral foramina are absent on dorsal vertebra of *Majungasaurus*. However, small (<1 mm), irregularly-placed foramina are found on the dorsal surface of larger, apneumatic centra (e.g., D9, D11).

Cranial Dorsal Vertebrae—The first dorsal vertebra (presacral 11) consists of a fused centrum and neural arch and is missing the distal end of the left transverse process (Fig. 3). Although firmly fused to each other, a suture line is clearly evident at the junction of the centrum and neural arch. The flat cranial articular surface of the centrum is subcircular whereas the slightly concave caudal surface is dorsoventrally elongate, reflecting the transitional nature of this vertebra. The parapophysis is located just caudal to the cranial articular surface at midcentral height. It is directed laterally and is significantly larger than that of C10. There are large (10.3 mm wide × 9.1 mm high) pneumatic foramina located caudodorsal to each parapophysis, similar in size and position to those in C10. Caudally positioned foramina are absent on the lateral surface of the centrum. The centrum is rectangular in cross section and a slight longitudinal ridge is present on the ventral surface. This condition differs from the ventral keel observed in forms such as *Allosaurus* (Gilmore, 1920). It is also unlike the condition in *Dilophosaurus* (UCMP 77270) and *Sinraptor* (Currie and Zhao, 1993), where a distinct hypapophysis is present on the cranioventral midline of the centrum.

The neural arch is similar in overall size to that observed in C10. Notable differences include a slight increase in neural spine height, a complete lack of epipophyses, and a significant increase in size of the transverse process and diapophysis. The transverse process is oriented laterally (i.e., 90 degrees relative to the dorsoventral axis), rather than ventrolaterally as in preceding vertebrae. Zygapophyseal facets increase in size transversely and are oriented horizontally. The centroprezygapophyseal lamina intersects the prezygapophysis close to its medial end. This condition contrasts with that present in many other theropods (e.g., *Allosaurus*, *Carnotaurus*, *Sinraptor*), in which the lamina intersects the prezygapophysis laterally, or at least as far laterally as the midpoint of the prezygapophysis. Neural arch fossae are similar to those described for C10, with many exhibiting acces-

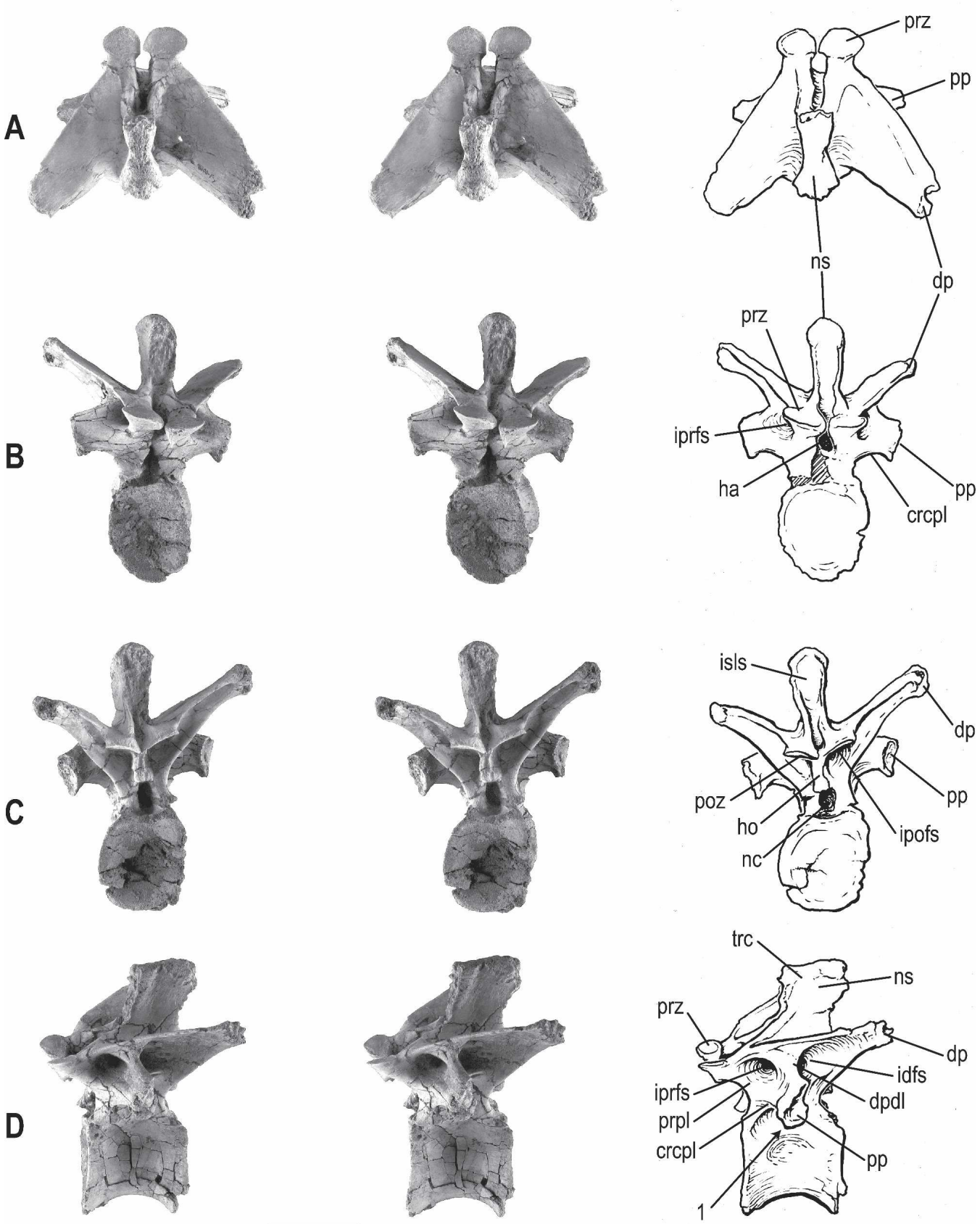

FIGURE 10. Fifth dorsal (D5) vertebra (UA 8678) of *Majungasaurus crenatissimus* in dorsal (**A**), cranial (**B**), caudal (**C**), and left lateral (**D**) views. **Notation**: **1**, arrow pointing to location of deep infradiapophyseal fossa (medial to the parapophysis). See Appendix 1 for list of anatomical abbreviations. Scale bar equals 5 cm.

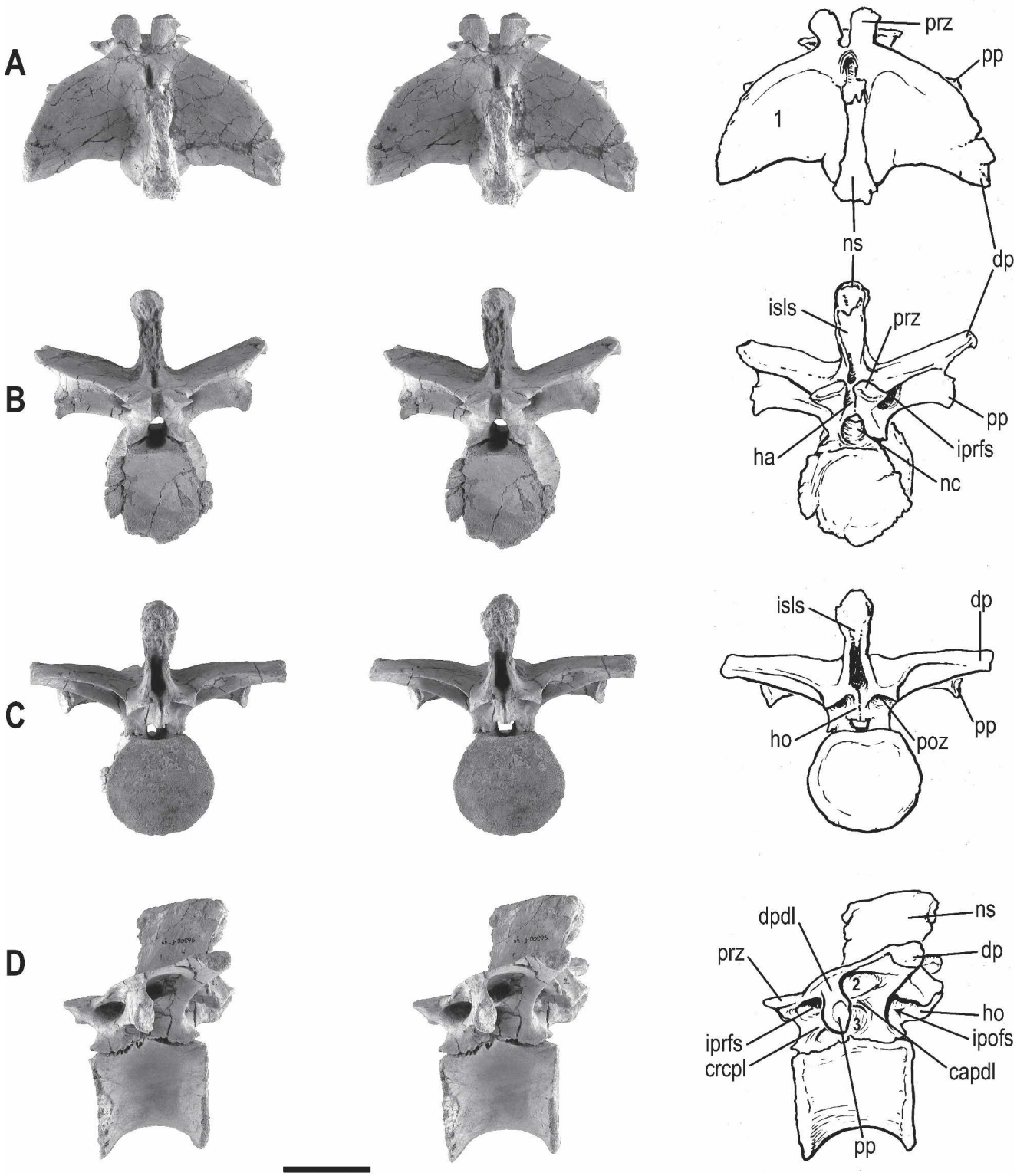

FIGURE 11. Ninth dorsal (D9) vertebra (UA 8678) of *Majungasaurus crenatissimus* in dorsal (**A**), cranial (**B**), caudal (**C**), and left lateral (**D**) views. **Notation**: **1**, craniocaudally expanded transverse process; **2**, dorsal portion of infradiapophyseal fossa; **3**, ventral portion of infradiapophyseal fossa. See Appendix 1 for list of anatomical abbreviations. Scale bar equals 5 cm.

sory pneumatic foramina leading to internal cavities within the arch.

The second dorsal vertebra is represented by a fused centrum and neural arch, with the neurocentral suture clearly evident along the length of the vertebra. It is moderately well preserved, with a partially crushed centrum and right diapophysis; the distal half of the left diapophysis was not recovered. The cranial articular surface is poorly preserved except for a small portion

adjacent to the left parapophysis. The centrum is slightly opisthocoelous, with a dorsoventrally elongate articular surface. Due to poor preservation, it is difficult to assess the exact shape (e.g., flat or concave) of the cranial articular surface. However, by comparison with adjacent vertebrae, it can be assumed that the cranial articular surface was transitional between the flat surface in D1 and the slightly concave surface of D3. Articular surfaces of vertebrae in this region of *Carnotaurus* differ in being round rather than dorsoventrally elongate (Bonaparte et al., 1990:figs. 14, 15). The parapophysis is directed laterally and is positioned slightly above midcentral height. On the left side, a large pneumatic foramen (~9 mm diameter) is located just caudal to the dorsal end of the parapophysis. Additionally, a shallow, craniocaudally oriented fossa is located on the upper third of the centrum just caudal to the pneumatic foramen. Poor preservation of the right surface of the centrum precludes identification of surface features. The centrum is subrectangular in cross-section with only incipient development of a longitudinal ventral keel. Neural arch elements are more robust than those observed in D1 (e.g., the neural spine of D2 is more than twice the length of D1) and the neural spine exhibits a transverse cleft around its dorsal margin (Fig. 3)). The transverse process is laterally directed and forms a right angle with the dorsoventral axis of the vertebra, unlike the dorsolaterally directed transverse process exhibited in the same vertebra of *Carnotaurus* (Bonaparte et al., 1990:fig. 14). The laterally facing diapophysis is quadrangular in lateral view and attains the largest size of any in the presacral column. Zygapophyses are transversely elongate, but lack the craniocaudal expansion of the lateral margins that characterizes preceding vertebra. In addition, as observed in other theropods, zygapophyses are medially positioned, and an incipient hyposphene is associated with the postzygapophyses. *Carnotaurus* exhibits an identical pattern of hyposphene development (i.e., the first hyposphene is located on D2; Bonaparte et al., 1990); this condition differs from that in many other theropods (e.g., *Sinraptor*, present on all dorsals, Currie and Zhao, 1993; *Allosaurus*, lacking on D1–D5, Madsen, 1976) and may reflect clade specific character variation. As in D1, the centroprezygapophyseal lamina intersects the prezygapophysis near its medial end. Infraprezygapophyseal, infradiapophyseal, and infrapostzygapophyseal fossae are all well developed, with pneumatic foramina piercing the neural arch at the deepest point of each fossa.

The third dorsal vertebra consists of an unfused centrum and neural arch. The centrum is crushed on the right side and the neural arch is missing the distal half of the left transverse process. The distal third of the right transverse process was also not preserved. Both cranial and caudal articular facets are slightly concave and dorsoventrally elongate. The parapophysis, dorsally shifted relative to the position in D2, is directed laterally and spans a height from the neurocentral suture to a position just below midcentral height. A small (~5 mm) pneumatic foramen is located just caudal to the parapophysis. Similar to D2, a shallow fossa is located on the dorsal half of the lateral surface of the centrum. Rather than rectangular in cross-section (as observed in the preceding four vertebrae), the centrum exhibits the constriction typical of dorsal vertebrae in theropods. Such centra are characterized by peripherally flared cranial and caudal articular facets with a narrow middle portion, giving rise to the often described 'spool-shaped' centrum. Significant changes characterize the neural arch, including a dorsoventrally-flattened transverse process, an increase in neural spine robusticity, and the presence of a hypantrum on the prezygapophysis. Relative to D2, the neural spine is more elongate, yet it retains the transverse cleft around the dorsal margin. A dorsal cleft is preserved through the succeeding four vertebrae, but is less marked than in the cranial dorsal series. The dorsal half of the neural spine consists of rugose bone that is expanded transversely relative to the ventral half (i.e., the neural spine flares dorsally). Whereas the transverse process is laterally directed in preceding vertebrae, it sweeps caudolaterally in D3. Zygapophyses are reduced in transverse dimensions, oriented ~35° from the horizontal, and contribute to the formation of both hypantrum and hyposphene accessory articulations. In contrast to the condition in D2, the centroprezygapophyseal lamina joins the prezygapophysis near its transverse midpoint. Associated with a decrease in the dorsoventral dimension of the transverse process, delicate laminae extend from the ventral surface to the pedicles, thereby better defining the series of ventral neural arch fossae. Furthermore, there is a general increase in neural arch length, as measured by the interzygapophyseal length (Table 1). Pneumatic features of the arch are similar to those described for D2, with the exception that the infraprezygapophyseal fossa exhibits a considerable increase in volume. This feature is related to both dorsoventral thinning of the transverse process and increased neural arch length.

The fourth dorsal vertebra consists of a well-preserved unfused centrum and neural arch. The centrum of D4 is similar to that of D3 in that it is weakly amphicoelous, with dorsoventrally-elongate articular surfaces. One notable difference is that the parapophysis spans the neurocentral contact and preserves evidence of the neurocentral suture. The parapophysis exhibits slight lateral displacement from its position on the preceding vertebra. A large (~9 mm) pneumatic foramen is located on the centrum just caudal to the parapophysis on the right side only, whereas the left side of the centrum does not exhibit any pneumatic openings. Similar to D3, a shallow, craniocaudally-oriented fossa is present just ventral to the neurocentral suture. This feature is found throughout the remainder of the dorsal vertebral series, and likely does not represent a pneumatic feature, but rather a basic architectural feature present in many archosaurian taxa (e.g., dinosaurs, crocodyliforms, *Marasuchus*; Sereno and Arcucci, 1994). General trends described for the first three dorsal neural arches are continued in D4 (e.g., increased neural spine length, caudolaterally-directed transverse process, increased development of hyposphene-hypantrum facets, etc.; Fig. 3). In contrast to D3, however, the transverse process exhibits a slight dorsal elevation. The prezygapophysis is oriented ~25° relative to the horizontal, whereas the postzygapophysis is nearly horizontal in orientation. Pneumatic features consist of large infraprezygapophyseal fossae with foramina opening on the craniolateral aspect of the arch, and small infradiapophyseal foramina set within their respective fossae. Infrapostzygapophyseal foramina are not present, although a small, blind fossa is located just cranial to the postzygapophyseal facet. Finally, cranial laminopeduncular foramina are present dorsolateral to the neural canal, whereas caudal laminopeduncular foramina are absent on this and all succeeding presacral vertebrae.

The fifth dorsal vertebra consists of a complete centrum and neural arch (Fig. 10). Although collected in articulation, the neurocentral suture is completely unfused. The spool-shaped centrum is weakly amphicoelous, with dorsoventrally-elongate articular facets and no evidence of pneumaticity. Whereas there is an increase in both length and height of the neural spine relative to more cranial dorsal vertebrae, there is a slight reduction in width. Similar to previous vertebrae, the dorsal tip of the neural spine is formed of rugose bone that is transversely expanded (Fig. 10B). Transverse processes are caudodorsolaterally-oriented, with nearly straight cranial and caudal margins, and appear triangular in dorsal view (Fig. 10A). The parapophysis is located entirely on the neural arch, with a ventrolaterally facing facet. This parapophysis is laterally and dorsally shifted relative to its position in D4, and is connected to other portions of the arch via a system of thin laminae (Fig. 10D, Table 1). Lateral displacement of the parapophysis in D5 is similar to that described for *Carnotaurus* (Bonaparte et al., 1990), but unlike the condition in many tetanurans (e.g., *Allosaurus*, *Sinraptor*, *Tor-*

vosaurus), where it maintains a medial position on the neural arch (Madsen, 1976; Britt, 1991; Currie and Zhao, 1993).

The sixth dorsal vertebra is represented by a complete centrum and neural arch, with the neurocentral suture completely unfused. Whereas the sixth neural arch was collected in near-articulation with both the fifth and seventh arches, the centrum was recovered ~30 cm away. Corresponding sutural morphology allows a confident association between the two elements. The sixth dorsal vertebra is virtually identical to D5, with the only notable differences being a slightly longer neural spine and a parapophysis with its articular facet facing caudoventrolaterally rather than ventrolaterally. The dorsal tip of the neural spine is transversely expanded and rugose, particularly along its caudal margin. Similar to other theropods, the usual series of infraprezyga-, infrapostzyga-, and infradiapophyseal fossae are present, typically associated with foramina that penetrate into the neural arch. However, the laterally positioned parapophysis and the caudal paradiapophyseal lamina subdivide the infradiapophyseal fossae into two distinct fossae, a feature that is serially maintained through D10 (Fig. 3). Similar arch morphology has been described in *Ilokelesia* (Coria and Salgado, 1998), appears to be present in *Carnotaurus* (Bonaparte et al., 1990:figs. 16, 17), and may be diagnostic of Abelisauridae.

Caudal Dorsal Vertebrae—The seventh dorsal vertebra is represented solely by its neural arch. Although the centrum was not recovered, sutural grooves on the ventral surface of each pedicle reveal that the two were not yet fused. Notable features of the arch include transverse processes with a convex cranial margin, resulting in a craniocaudally expanded middle portion of the process. Further, the caudal margin of the transverse process is caudally concave. This differs from the condition in preceding dorsal arches, in which the cranial and caudal margins are formed by near-straight edges (Fig. 3). The neural spine is increased in length and also exhibits transverse expansion along its caudodorsal margin. Prezygapophyseal facets are directed dorsally, rather than dorsomedially as in preceding vertebrae. The parapophyseal facet is shifted further laterally and directed caudolaterally. Ventral arch laminae and pneumatic features are generally consistent with those described for D6. Numerous mediolaterally-oriented striations are preserved on the dorsal surface of the right transverse process (Fig. 3).

The eighth dorsal vertebra consists of a complete, unfused neural arch and centrum. The centrum is amphicoelous, with dorsoventrally elongate articular surfaces, and lacks pneumatic foramina. It is spool-shaped and retains the craniocaudally elongate fossa on the lateral central surface just ventral to the neurocentral suture. The neural arch is generally similar to that of D7, with slight differences that include a slightly longer neural spine and a laterally displaced parapophysis. The prezygapophysis is directed dorsolaterally, rather than dorsally or dorsomedially as in most other theropods, a trait shared with *Carnotaurus* (Bonaparte et al., 1990).

The ninth dorsal vertebra preserves an unfused centrum and neural arch, neither of which exhibit any significant deformation (Fig. 3, 11). Whereas the amphicoelous centrum has a dorsoventrally elongate cranial articular facet similar to vertebrae more cranial in the series, the caudal surface is subcircular, similar to those through the remainder of the dorsal series. As noted previously, paired basivertebral foramina are not present on centra of *Majungasaurus.* However, the ninth centrum does exhibit variably-placed, small (<1 mm) foramina passing obliquely through the cortical bone adjacent to the medial border of the neurocentral suture. These likely represent osteological correlates of vertebral vasculature (e.g., tributaries of the internal vertebral venous sinus) and not pneumatic diverticula. The ninth neural arch is generally similar to those adjacent to it, but stands out in having the longest (craniocaudally) neural spine of the presacral series. The neural spine also exhibits the transverse expansion of its caudodorsal end, but not to the degree observed in preceding vertebrae. The parapophyseal facet is reduced in size compared to D8; however, it maintains an equivalent mediolateral placement on the arch. Additionally, it has shifted dorsally, thereby decreasing the length of the dorsal paradiapophyseal lamina.

The tenth dorsal vertebra is represented only by a neural arch. The neural spine is higher, narrower, and reduced in length relative to D9, with only a slight transverse expansion of its caudodorsal end. The prezygapophyseal facet is directed dorsolaterally to a degree unsurpassed in any other dorsal vertebra. The ventral surface of the pedicle exhibits distinct sutural grooves, similar to those of other presacral neural arches; however, the ventral surface is expanded and represents the largest sutural contact of the presacral series. Ventral arch laminae and pneumatic features are similar to those described for other mid-dorsal vertebrae.

The eleventh dorsal vertebra preserves both neural arch and centrum. The weakly amphicoelous, spool-shaped centrum exhibits circular articular surfaces and is considerably more robust than centra located more cranially in the series. Numerous small vascular foramina are located on the dorsal aspect of the centrum. Similar vascular foramina are present only on larger, apneumatic centra of the presacral series (i.e., D9 and D11; note that, as preserved, D10 and D13 lack centra, and the centrum of D12 is severely crushed). Hence, it appears that there is a correlation between the presence of macroscopic nutrient foramina within the neural canal and larger, more dense vertebral centra (see Discussion). The neural spine is higher, reduced in length, and exhibits a significantly reduced dorsal expansion relative to D10. The prezygapophysis retains a dorsolaterally facing facet. The parapophysis is both laterally displaced and dorsally shifted so as to merge with the ventral aspect of the transverse process, resulting in the loss of the paradiapophyseal lamina. As such, the infradiapophyseal fossa is no longer subdivided into two separate fossae (Fig. 3C). The cranial centroparapophyseal lamina is retained and forms the caudoventral boundary of a deep infraprezygapophyseal fossa that opens via a foramen into the neural arch. Large infrapostzygapophyseal and small infradiapophyseal foramina are also present on this arch. A ventrally directed flange of bone emanates from the caudal centrodiapophyseal lamina, thereby delimiting the lateral border of the infrapostzygapophyseal fossa.

The twelfth dorsal vertebra consists of an unfused neural arch and centrum (Fig. 12). Whereas the arch is well preserved and intact in three dimensions, the centrum is badly crushed and missing the ventral half of the element (Fig. 3; due to the severity of damage, the D12 centrum was not figured). The distal third of the left transverse process was also not preserved. Although incomplete ventrally, the centrum is increased in overall size relative to D11 and lacks pneumatic features. The neural arch is characterized by a tall, narrow neural spine that exhibits further reduction in the expansion of its dorsal tip. The transverse process differs significantly in that it is no longer craniocaudally expanded at its distal end, and is triangular in dorsal view (Fig. 12A). Moreover, the parapophyseal and diapophyseal facets have coalesced into a single structure (pleuropophysis) at the distal end of the transverse process (Fig. 12C). Based on its position when articulated with succeeding vertebra, the transverse processes would have been positioned between the cranial edges of the preacetabular iliac blades. Pre- and postzygapophyseal facets are similar to preceding vertebrae, and well-developed hyposphene/hypantrum articulations are present. Ventral arch laminae are reduced such that only slight cranial and caudal centrodiapophyseal laminae are present. Concomitant with the reduction in neural arch laminae, pneumatic foramina are only present immediately adjacent to the postzygapophyses.

The thirteenth dorsal vertebra is represented by its neural arch (Figs. 13, 14). Notable features include a tall, thin neural spine

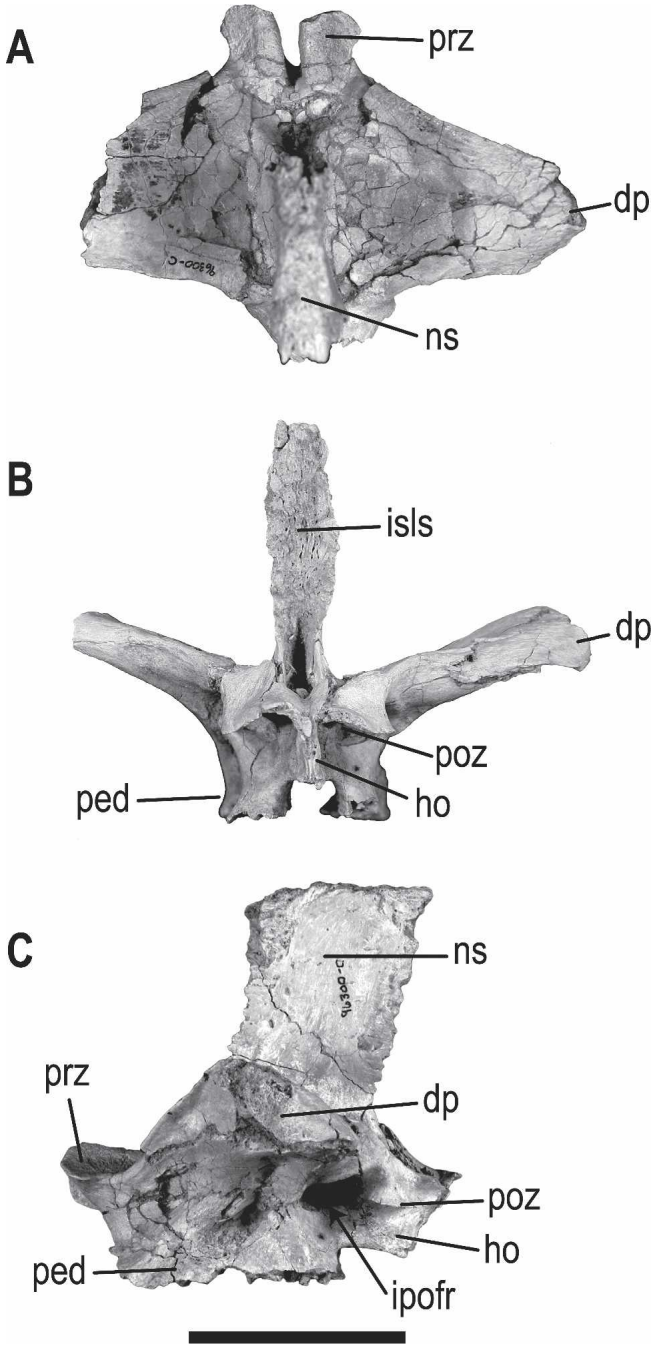

FIGURE 12. Twelfth dorsal (D12) vertebra (UA 8678) of *Majungasaurus crenatissimus* in dorsal (**A**), caudal (**B**), and left lateral (reversed for image) (**C**) views. See Appendix 1 for list of anatomical abbreviations. Scale bar equals 3 cm.

and a dorsolaterally-directed transverse process with an expanded lateral end. The enlarged diapophysis articulates with the preacetabular portion of the ilium, resulting in functional 'sacralization' of D13. It does not appear that the centrum of D13 would have articulated with the ilium. As such, this element will be classified as a dorsal rather than a sacral vertebra (see below for a discussion of elements comprising the sacral complex). The prezygapophyseal facet faces dorsolaterally and the hypantrum is well-developed. The caudal surface of the neural arch is incompletely preserved (Fig. 13A), but it is apparent that typical postzygapophyses were not present, and that the element was likely fused with the first sacral neural arch. The pedicle is high, with a ventral surface (sutural contact) that is transversely broad at the cranial end and transversely narrow at the caudal end (Fig. 3). The neural canal is significantly larger (~20%) than in the preceding dorsals. Pneumatic features are limited to small, infrapostzygapophyseal foramina. In overall shape, this vertebra resembles sacral vertebra one (S1) of both *Carnotaurus* (Bonaparte et al., 1990:fig. 20) and *Sinraptor* (Currie and Zhao, 1993:fig. 17c). However, S1 of *Majungasaurus* differs from that of *Carnotaurus* in that its neural spine is relatively longer (craniocaudally) and its transverse process is not directed cranially.

Sacral Vertebral Complex

The sacrum is represented by a single, partially preserved specimen (UA 8678; Figs. 13, 14) consisting of the second and third sacral centra (primordial sacrals 1 and 2) and the second through fourth neural arches (primordial sacrals 1 and 2 and caudosacral 1) completely fused to one another. Although the sacrum is incomplete, articular facets preserved on both ilia indicate areas of attachment for five sacral vertebrae (Carrano, this volume). These contacts include distinct facets for both sacral ribs and transverse processes.

Collected as a single, co-ossified specimen, sutures are still evident between individual centra and neural arches and between adjacent neural arches. The two preserved centra (S2–S3) are firmly coossified, with flat articular surfaces. It is apparent from the preservation of the exposed cranial and caudal surfaces that adjacent centra were not yet fused at the time of death. This interpretaion is consistent with observations by others that primordial sacral vertebrae are the first units of the sacral system to co-ossify, followed by additional elements of the complex (Currie and Zhao, 1993).

The centra are D-shaped and exhibit a flattened dorsal surface, similar to sacral centra of *Masiakasaurus* (Carrano et al., 2002). In lateral view the two centra have similar profiles in that each exhibits a ventrally concave surface. However, the two vertebrae together do not indicate the ventral arching apparent in other abelisauroids such as *Carnotaurus* (Bonaparte et al., 1990:fig. 20C) and *Masiakasaurus* (Carrano et al., 2002:fig. 9A); nevertheless, a full complement of sacral centra would be necessary to assess this characteristic adequately. The centra are transversely constricted as in other nontetanuran theropods, but not to the degree observed in *Ceratosaurus* (Gilmore, 1920:pl. 21) and *Carnotaurus* (Bonaparte et al., 1990:fig. 20B). Sacral centra lack pneumatic foramina and have a flat ventral surface (i.e., they lack a longitudinal groove found in other theropods; e.g., ornithomimids, see Gilmore, 1920:fig. 67).

Although the first sacral centrum and neural arch are not preserved, the position of articular facets on each ilium indicates that the first sacral rib likely maintained contact with the first sacral centrum. A sutural contact for the second left sacral rib is present on the craniodorsal aspect of the S2 centrum, although the sacral rib was not recovered. The third and fourth sacral ribs are preserved on the left side and exhibit transitional morphology with the third maintaining contact with the second and third sacral centra (Fig 13A). The third sacral rib consists of a nonspecialized lateral protuberance that articulates with the medial surface of the ilium just dorsal to the acetabular midpoint (Fig. 14). The fourth sacral rib is a laterally-projecting cylinder bearing a circular articular facet for the medial surface of the ilium (Fig. 13A). The articular surface of the rib projects laterally to a point just past the caudolateral margin of the third sacral centrum. Unlike the condition of the second and third sacral ribs, the fourth sacral rib does not maintain contact with sacral centra, as evidenced by the clear suture lines (Fig. 13A).

The preserved intervertebral foramina are located dorsal to midcentral length, rather than between adjacent centra. How-

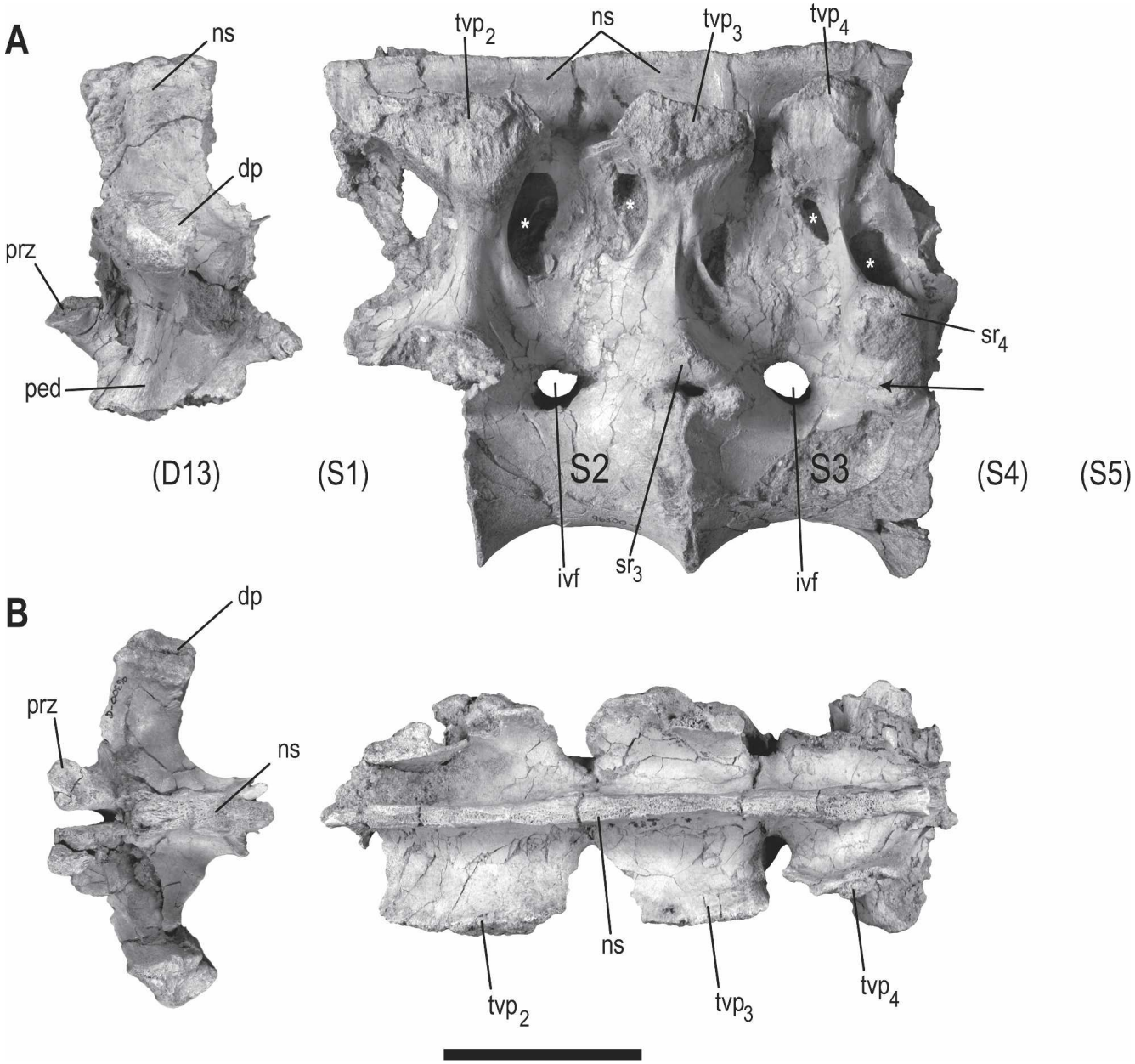

FIGURE 13. Sacral complex (UA 8678) of *Majungasaurus crenatissimus* in left lateral (**A**) and dorsal (**B**) views. Note: the isolated element on the left side of each row is the thirteenth dorsal (D13) vertebra, which represents the cranialmost portion of the sacral complex in *Majungasaurus*. Vertebral centra of D13, S1, S4, and S5 were not preserved with the specimen, nor were complete neural arches of S1, S4, and S5. **Notation**: **S2**, **S3**, second and third sacral centra respectively; (**D13**), (**S1**), (**S4**), and (**S5**) indicate inferred positions of vertebral centra that were not recovered with the specimen; white asterisks denote pneumatic features in sacral neural arches; black arrow indicates a sutural line between the third sacral centrum and fouth sacral neural arch. See Appendix 1 for list of anatomical abbreviations. Scale bar equals 5 cm.

ever, the foramina retain their normal position with respect to neural arches (i.e., at the junction of the ventral end of adjacent arches). A similar situation exists in *Masiakasaurus* (FMNH PR 2142; Carrano et al., 2002:fig. 9). The shifted position of these foramina relative to centra results from the cranial translation of neural arches relative to centra within the sacral complex. Such arch translation facilitates the formation of multipart sacral ribs at the junction of adjacent sacral centra and neural arches (e.g., the caudodorsolateral edge of the S2 centrum and the craniodorsolateral edge of the S3 centrum along with the ventral portion of the S3 neural arch; Fig. 13A). The cranial shifting (i.e., translation) of sacral neural arches results from the formation of a craniocaudally restricted S1 neural arch, similar to that found in other theropods such as *Tyrannosaurus* (Brochu, 2003:fig. 57).

The three sacral neural arches are coossified, although suture lines are evident, revealing the individual components of the fused arch system (Fig. 13). Adjacent neural spines are fused to one another, forming a midline plate of bone that extends the length of the sacrum. Transverse processes are directed dorsolaterally, extending almost to the dorsal limit of the fused neural spines, and articulate with the iliac blade via expanded distal ends (Fig. 13A). A lamina connects the neural spine with the dorsomedial portion of the transverse process, forming a prominent shelf (sacral shelf) along the length of the sacrum (Fig.

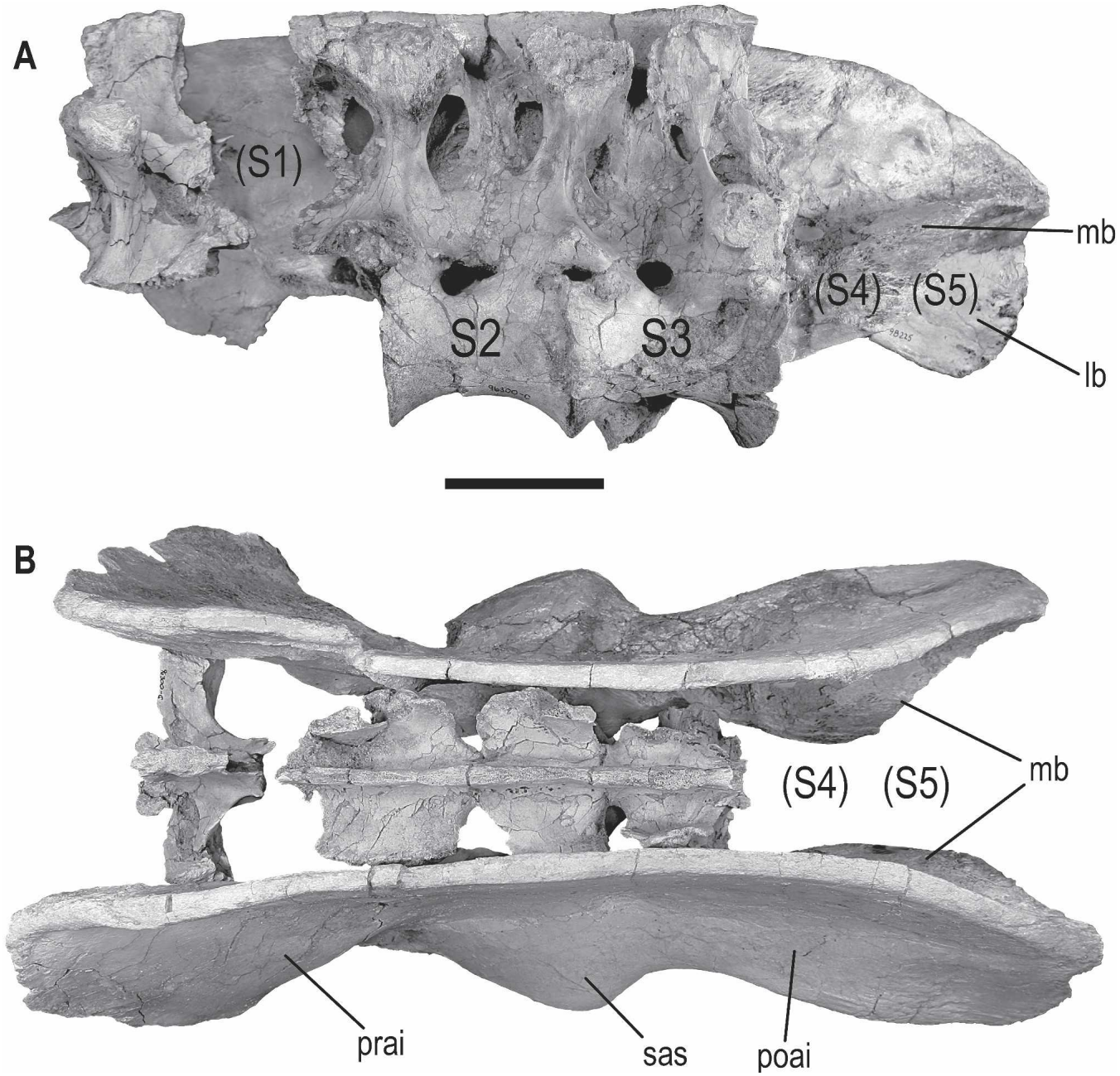

FIGURE 14. Articulated pelvic complex (UA 8678) of *Majungasaurus crenatissimus* in left lateral (**A**) and dorsal (**B**) views (cranial to the left). **Notation**: **S2**, **S3**, second and third sacral centra respectively; (**S1**), (**S4**), and (**S5**) indicate inferred positions of other components of the sacral complex based on articular facets on medial surface of ilium. See Appendix 1 for list of anatomical abbreviations. Scale bar equals 5 cm.

13B). The shelf is interrupted segmentally at intervertebral junctions, allowing passage of neurovasculature between the intervertebral foramina and the dorsal body wall.

Of particular note is the elaborate pneumaticity present within sacral neural arches. Numerous well-defined fossae are located adjacent to each transverse process on the dorsolateral portion of each arch (Fig. 13A). These are found on both the cranial and caudal aspect of each transverse process. Similar pneumatic fossae are present in the sacrum of *Masiakasaurus* (Carrano et al., 2002:fig. 9A). Generally, abelisauroids differ from tetanurans (e.g., *Allosaurus*) in that sacral transverse processes attain a dorsal position subequal to that of the coossified neural spines, and together these extend slightly above the dorsal margin of the ilium (Fig. 14).

Caudal Vertebrae

Caudal vertebrae of *Majungasaurus* (Figs. 15–18) are preserved from numerous localities throughout the Berivotra field area. Of particular relevance are five articulated proximal caudal vertebrae, the first elements of UA 8678 recovered from MAD 96-21 (hence the partial erosion and bleached neural spines; Fig. 15A). Like the dorsal vertebrae preserved with the same specimen, caudal centra and neural arches are variably fused. Neural arches and centra are unfused in the first vertebra of the series, partially fused in the second and third vertebrae (i.e., neurocentral sutures remain visible on the cortical surface; Fig. 15A), and asymmetrically fused in the fourth vertebra; the right side of Ca4 is partially-fused (neurocentral suture visible), whereas the left

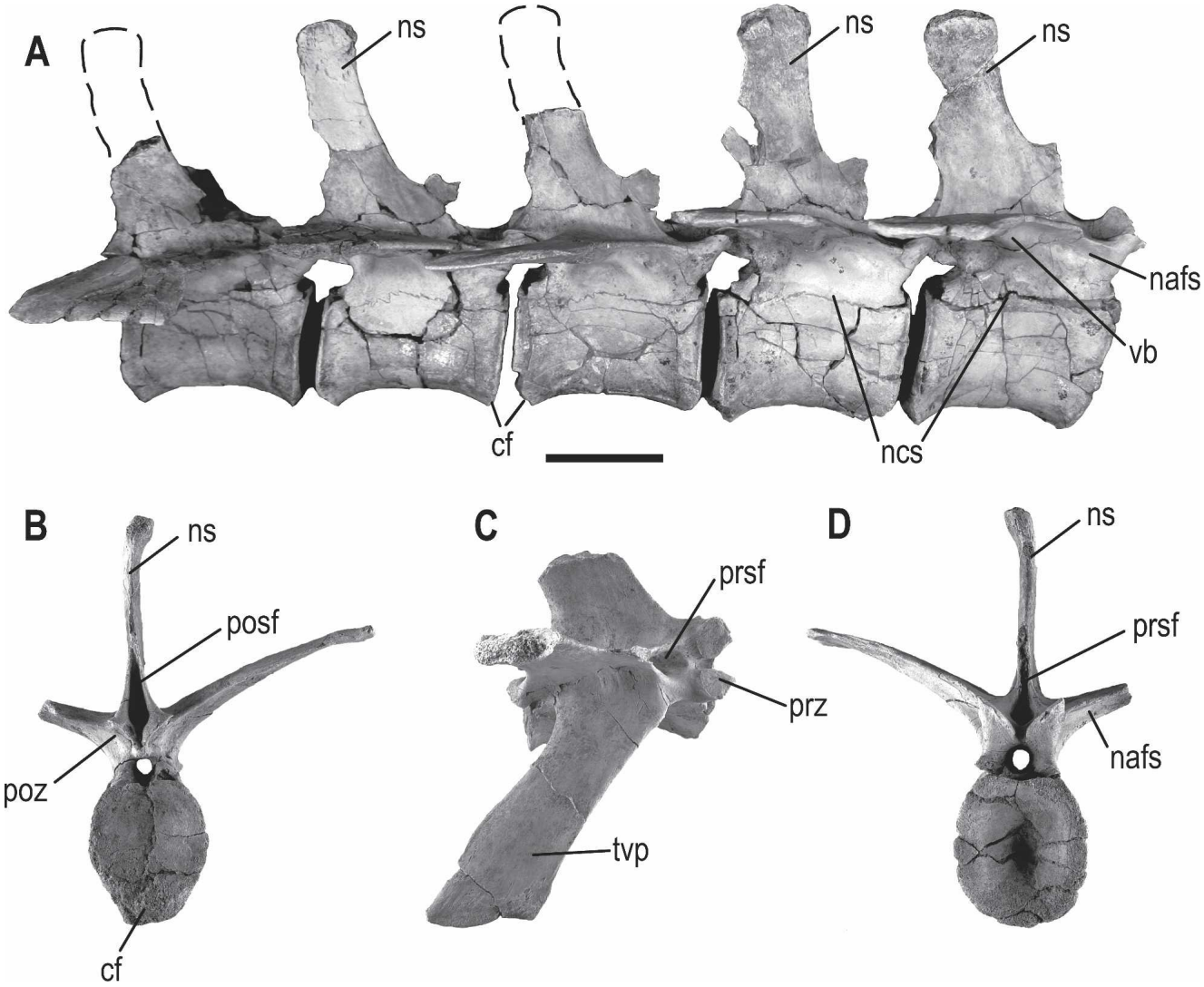

FIGURE 15. Proximal caudal vertebrae (UA 8678) of *Majungasaurus crenatissimus* in right lateral (**A**) view (cranial is to right of image); **B**–**D** are alternative views of cranialmost vertebra in **A** in caudal (**B**), dorsal (**C**), and cranial (**D**) views. See Appendix 1 for list of anatomical abbreviations. Scale bar equals 5 cm.

side exhibits a partially obliterated neurocentral suture in which the cranial half of this contact is still evident and the caudal half is obliterated. In the only vertebra preserved caudal to this point, the neural arch and centrum are fully co-ossified, with no remaining trace of the suture. Given the position of the fifth sacral vertebra of UA 8678 (inferred based on articular surfaces on the ilium; Fig. 14), it is likely that the first caudal vertebra was positioned at least partially between the postacetabular iliac blades. Although transverse processes of the first caudal vertebra laterally embrace the caudal iliac margin in carnotaurine abelisaurids (Coria et al., 2002), incomplete preservation of this region precludes direct assessment of this characteristic in *Majungasaurus*.

Additionally, 25 near-sequential caudal vertebrae, ranging from the proximal to the mid-distal region of the tail, were collected in association with a skull of *Majungasaurus* (FMNH PR 2100; Fig. 16). A single distal caudal vertebra was also recovered but, based on the relative size of this specimen and the remainder of the FMNH PR 2100 series, it is apparent that a number of intervening vertebrae were not preserved. All vertebrae in the preserved sequence exhibit fusion of the neurocentral sutures (Figs. 16–18). Although the preserved series likely represents a near-continuous sequence based on both size and shape criteria (Fig. 16; Table 2), it remains possible that certain individual vertebrae were not recovered. Nonetheless, FMNH PR 2100 preserves the most complete tail skeleton of *Majungasaurus* yet recovered. A number of the vertebrae in this series exhibit extensive tooth marks that are consistent with scavenging events prior to burial (see below). A sequence of four, poorly preserved, proximal caudal vertebrae (UA 9089) was also recovered from 'near' the MAD96-01 locality in 1989 (Ravoavy, 1991), and may pertain to FMNH PR 2100. In support of such an association, both shape and size analyses would place this sequence of vertebrae at the cranial end of the FMNH PR 2100 series. However, ambiguity surrounding specimen provenance of UA 9089 precludes a definitive association at this time. Due to the incomplete nature of the four vertebrae, they are not figured here. An additional specimen (FMNH PR 2294) preserves five articulated distal caudal vertebrae with two chevrons. The distal three vertebrae exhibit extensive hyperostosis with complete fusion of adjacent centra and neural arches (O'Connor, 2003:fig. 4–15; Farke and O'Connor, this volume:fig. 1).

All caudal centra are amphicoelous, with no evidence of pneu-

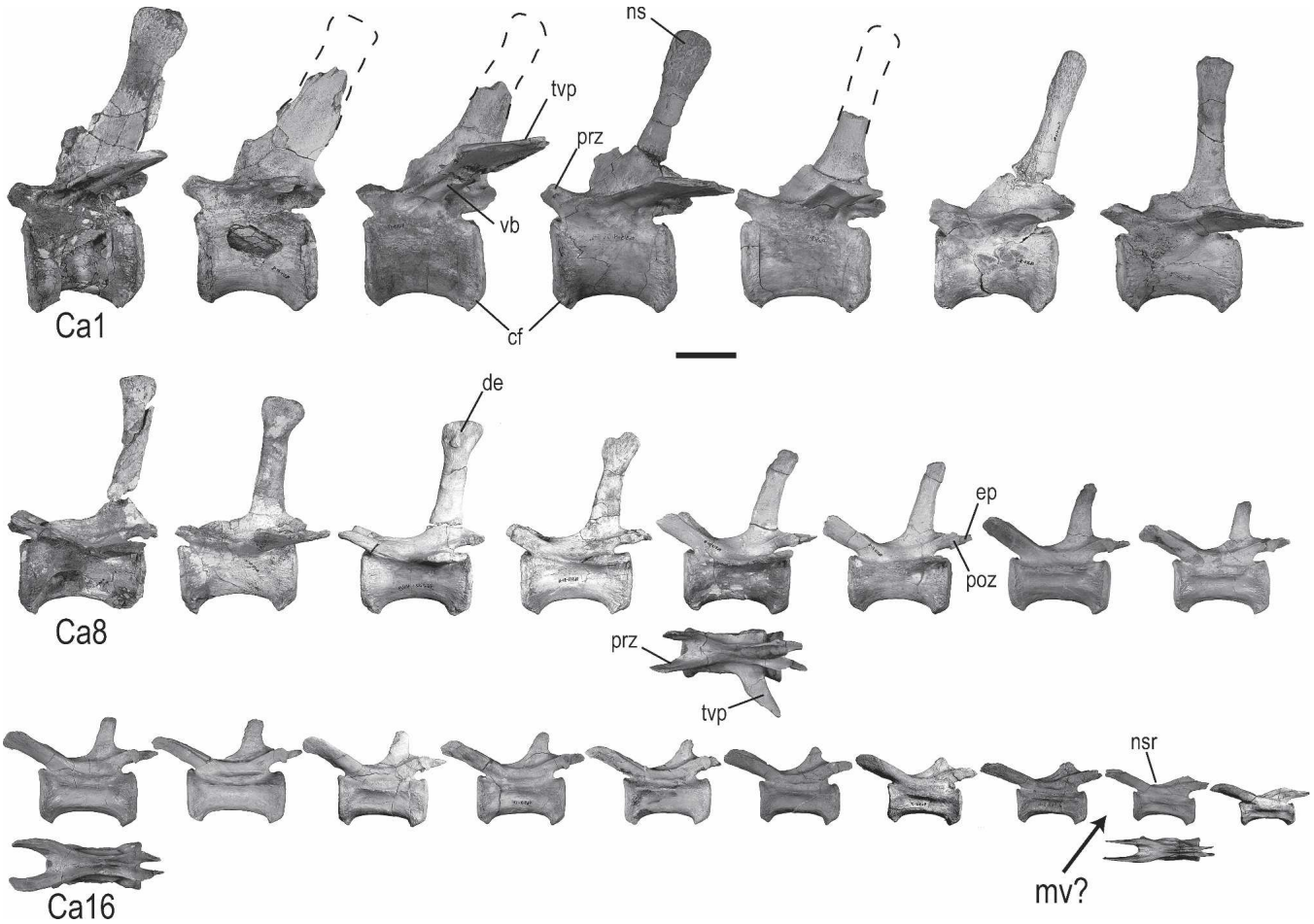

FIGURE 16. Caudal vertebral series of *Majungasaurus crenatissimus* (FMNH PR 2100) in left lateral view (cranial to caudal progression in each row from left to right); dorsal views of selected vertebrae (Ca12, Ca16, Ca24) are provided below the corresponding lateral image. All images are reversed to provide consistency with views used in Figure 3. **Notation**: **Ca1**, first caudal vertebra; **Ca8**, eighth caudal vertebra; **Ca16**, sixteenth caudal vertebra. See Appendix 1 for list of anatomical abbreviations. Scale bar equals 5 cm.

maticity. Proximal caudal centra are transversely narrow, with elliptical articular facets oriented dorsoventrally (Fig. 15B, C), unlike the round facets observed in *Carnotaurus* (Bonaparte et al., 1990:fig. 21) or *Masiakasaurus* (Carrano et al., 2002). Generally, chevron facets are prominent throughout the entire vertebral series, such that the ventral border of the centrum exhibits both cranioventrally and caudoventrally oriented articular surfaces (Figs. 15–18). A shallow longitudinal sulcus is present on the ventral surface of proximal caudal centra, whereas the deep fossae present on the dorsolateral surface of the centrum in forms such as *Ceratosaurus* (Gilmore, 1920:pl. 22) are absent in *Majungasaurus*.

Proximal caudal neural arches generally resemble those of other medium-sized theropods, with the development of both pre- and postspinal fossae and a caudolaterally directed transverse process. Both pre- and postspinal fossae are bounded by distinct spinozygapophyseal laminae, resulting in relatively deep fossae on the cranial and caudal surfaces of the neural spine base (Fig. 15B–D). Zygapophyseal facets are inclined 30–40° from vertical and do not have the distinct accessory hyposphene-hypantrum articulations observed in other abelisaurids (e.g., *Aucasaurus*; Coria et al., 2002) and some non-abelisaurid basal theropods (e.g., *Dilophosaurus*; Welles, 1984). Indeed, proximal caudal vertebrae in *Majungasaurus* appear intermediate in form, with zygapophyses that exhibit a gentle bend at the midpoint such that facets possess a slight biplanar articular surface (Fig. 15D). The neural spine is L-shaped and positioned dorsal to the caudal half of the centrum (Fig. 15A, 16). It does not sweep caudodorsally to the degree observed in *Ceratosaurus* (Gilmore, 1920:pl. 22) or *Carnotaurus* (Bonaparte et al., 1990:fig. 21). The dorsal half of the neural spine is reduced craniocaudally compared to the ventral portion (Fig. 15A), similar to the condition in *Masiakasaurus* (Carrano et al., 2002). The morphology of the neural spine transitions between ~Ca5 and Ca7, being laminar proximal to this point and assuming a columnar appearance distal to it. Proximal caudal neural spines variably exhibit both transverse and craniocaudal expansion of the dorsal margin (Fig. 15B, 16), similar to the condition described for the middle presacral and middle caudal series.

The transverse process exhibits only slight (~20° from the horizontal) dorsal elevation (Fig. 15B, D), yet it does sweep caudally well past the caudal margin of the centrum (Fig. 15C, 16). This contrasts with the dorsally elevated transverse processes observed in the proximal caudal series of many other abelisauroids such as *Masiakasaurus* (Carrano et al., 2002), *Carnotaurus* (Bonaparte et al., 1990:figs. 21–23), and *Aucasaurus* (Coria et al., 2002:fig. 2A). For example, *Carnotaurus* possesses transverse processes that exceed 50º relative to the horizontal axis of the vertebra. The length of the transverse process on proximal caudal vertebrae far exceeds centrum length (in some cases ~1.6 times centrum length; see Table 2). An increase in length of the proximal caudal transverse processes, a character present in both

TABLE 2. Caudal vertebral measurements (mm) of *Majungasaurus crenatissimus* (UA8678 and FMNH PR 2100).

Vertebra	CENL	CDCW	CDCH	MIDW	TOVH	NSH	NSL	NSW	IZW	IZL	IDPW	TP/CN
						UA 8678						
~Ca 1	71.3	52.3	58.8	30.3	176.1	106.4	28.2	8	26.3	90.9	233.2	1.64
Ca 2	69.6	50.2	55.7	29.3	174.3	105.7	29.4	7.2	27.2	91.8	223.2	1.60
Ca 3	70.8	45.2	51.6	25.1*	†	†	24.5	7.4	25.2	91.5	204.5	1.44
Ca 4	73.2	44.9	48.9	30.8	159.7	101.6	21.6	6.1	28.8	95.2	†	†
Ca 5	75.2	42.8	48.1	26.4	†	†	†	†	†	†	†	†
						FMNH PR 2100						
~Ca 5**	84.9	69.9	73.5	33.5*	235.2	154.8	43.5	8.6	32.3	110.3	†	†
Ca 6	95.7	67.5	76.7	34.1	232.5*	†	†	†	29.4	114.9	†	†
Ca 7	98.1	62.1	69.6	33.1	230*	†	†	†	31.6	114.8	252.6*	1.29
Ca 8	98.1	57.9	65	31	228.3	150.7	33.5	11.4	32	116.4	†	†
Ca 9	97	57.5	62.9	29.1	218*	†	†	9.1	31.1	118.4	†	†
Ca 10	93.1*	56.9	59.4	27.4*	210.4	139.4	23.3	12.9	31.9	112.3	†	†
Ca 11	96	†	†	†	194	137	22.96	15.9	†	113.5	174.6*	0.91
Ca 12	96.7	52.6*	52.5*	28.4	185.7	135.3	21.8	13	29.5*	115.2	†	†
Ca 13	95.6	48.3	53.1*	†	178.2	117.7	20.9	11.6	25.4	†	146*	0.77
Ca 14	94.2	44.6	51.2	24.7	171.8	114.3	21.8	11.7	23	118.9	†	†
Ca 15	91.4	51	49.6	36.6	156.4	989.6	21.2	10.1	†	112.1	†	†
Ca 16	91.5	48.3	50.1	37.7	144.5	87.1	18.8	11.5	26.8*	102.4	107.2	0.59
Ca 17	90.4	48.4	49.7	36.1	139.4	82.9	17	11.2	28.6	106.6	95.2	0.53
Ca 18	91.1	50.9	49.1	38	122.9	66.4	18.7	10.22	30.5	107.4	65.6	0.36
Ca 19	90.9	48.8	51	35.8	110.6	52.1	15.9	7.9	27.9	106.7	—	—
Ca 20	88.7	46.8	50.1	34.4	100.3	46.4	15.1	6.3	28	101.7	—	—
Ca 21	86.6	45.8	48	33.2	95.8	41.2	16.5	5.7	27	98.1	—	—
Ca 22	83.5	44	46.9	31.6	93.1	39.7	17.26	6.1	26.5	99.4	—	—
Ca 23	81.6	42.6	44.2	33.3	87.2	38	15.2	5.6	26	92.4	—	—
Ca 24	79.2	41.6	42.1	32.7	81.3	33.3	13.8	4.5	23.3	92.7	—	—
Ca 25	79	37.9	40.8	32.1	79.5	31.6	14.9	4.1	22	89.4	—	—
Ca 26	76.6	37.3	40.3	30.3	72.4	28.3	—	—	17.7	86.5	—	—
Ca 27	74.6	34.2	36	30.9	66.7	26.5	—	—	15.6	86.9	—	—
Ca 28	70.8	30.1	32.1	28.1	57.4	19.8	—	—	12.2	79.1	—	—
Ca 29	67.5	25.8	27.1	15.3	46.9	18.3	—	—	9.9	104.4	—	—
Ca X***	36.5	9.7	10.5	6.4	20.4	—	—	—	†	†	—	—

UA 8678 consists of five articulated proximal caudal vertebrae (~Ca 1–5) collected from locality MAD96-21. FMNH PR 2100 consists of 25 associated, near-sequential caudal vertebrae (?Ca 5–Ca29) and one distalmost caudal vertebra collected from locality MAD96-01. Notation: **CENL**, Centrum Length – maximum craniocaudal length; **CDCW**, Caudal Centrum Width – maximum width of caudal articular facet; **CDCH**, Caudal Centrum Height – maximum height of caudal articular facet; **MIDW**, Midcentral Width – width at central midlength; **TOVH**, Total Vertebral Height – dorsoventral extent of vertebra including centrum and neural spine; **NSH**, Neural Spine Height – dorsoventral extent of neural spine measured from dorsl aspect of neural canal; **NSL**, Neural Spine Length – craniocaudal extent of neural spine at spine midheight; **NSW**, Neural Spinal Width – transverse extent of neural spine at spine midheight; **IZW**, Interzygapophyseal Width – distance between lateral margin of postzygapophyses; **IZL**, Interzygapophyseal Length – distance from cranial margin of right prezygapophysis to caudal margin of right postzygapophysis; **IDPW**, Interdiapophyseal Width – distance between lateral limit of diapophyses; **TP/CN**, Transverse Process/Centrum Index – ratio of transverse process length to centrum length; *, incomplete measurement due to missing bone (e.g., partial breakage of a transverse process); **, indicates first vertebra of the associated series, not necessarily the first caudal vertebra; ***, indicates a substantial gap between the last two vertebrae; †, unable to measure due to damaged/missing bone; —, measurement not applicable for given vertebra.

Carnotaurus (Bonaparte et al., 1990) and *Aucasaurus* (Coria et al., 2002), has been posited as an abelisaurid synapomorphy (Rauhut et al., 2003).

The transverse process also exhibits a prominent ridge of bone along its ventral surface, with well-defined fossae positioned adjacent to it (Fig. 15A). A similar strut design is present in many other theropods (e.g., *Aucasaurus*) and likely serves a mechanical role in ventral buttressing of the elongate transverse process. The distal portion of the transverse process is only slightly expanded craniocaudally (Fig. 15C). This condition differs considerably from the variety of modifications exhibited by other abelisaurid taxa. For example, the cranial 'uncinate' processes of *Carnotaurus* (Bonaparte et al., 1990:fig. 21) or the cranially directed 'awl-like projections' of *Aucasaurus* (Coria et al., 2002:fig. 2) are not present on transverse processes of *Majungasaurus*.

In contrast to the condition in most theropods, relatively long transverse processes on proximal caudal vertebrae indicate that the base of the tail of *Majungasaurus* was transversely broader than tall, indicative of a relatively expanded connection between tail and trunk. This conformation is consistent with other aspects of axial morphology in this taxon (e.g., stout cervical region with interlocking cervical ribs) and in abelisaurids generally, suggesting that members of this clade possessed a robust axial core.

Middle caudal centra (Fig. 16–17) are amphicoelous with subcircular articular facets. Prezygapophyseal processes extend craniodorsally past the cranial limit of the centrum, whereas the prezygapophyseal facets are located at the cranial margin of the centrum. Zygapophyseal facets are oriented ~140° relative to the dorsoventral axis of the vertebra, thereby allowing extensive flexion-extension in this region of the tail. The postzygapophysis is located just dorsal to the caudal margin of the centrum. An expanded epipophysis is present in the mid-caudal region, a trait that is rare among theropods and has been described in only a limited number of taxa, including the abelisauroid *Masiakasaurus* (FMNH PR 2126; Carrano et al., 2002:fig. 10A). This morphology is consistent with the generally 'hyper-ossified' condition apparent in many elements (cranial and postcranial) of *Majungasaurus* (see below; also see Sampson and Witmer, this volume). The transverse processes are reduced in size relative to those in preceding vertebrae, and they originate from the caudal one-quarter of the fused neurocentral suture. The neural spine is craniocaudally restricted and projects dorsally over the caudal quarter of the centrum, in line with the transverse process. Mid-caudal neural spines are characterized by variably-shaped expansions of bone at the dorsal end (Fig. 16, 17). These last two traits are minimally shared with some other basal neotheropods (e.g., *Ceratosaurus* [UUVP 375–378]; Madsen and Welles, 2000:pl. 18B).

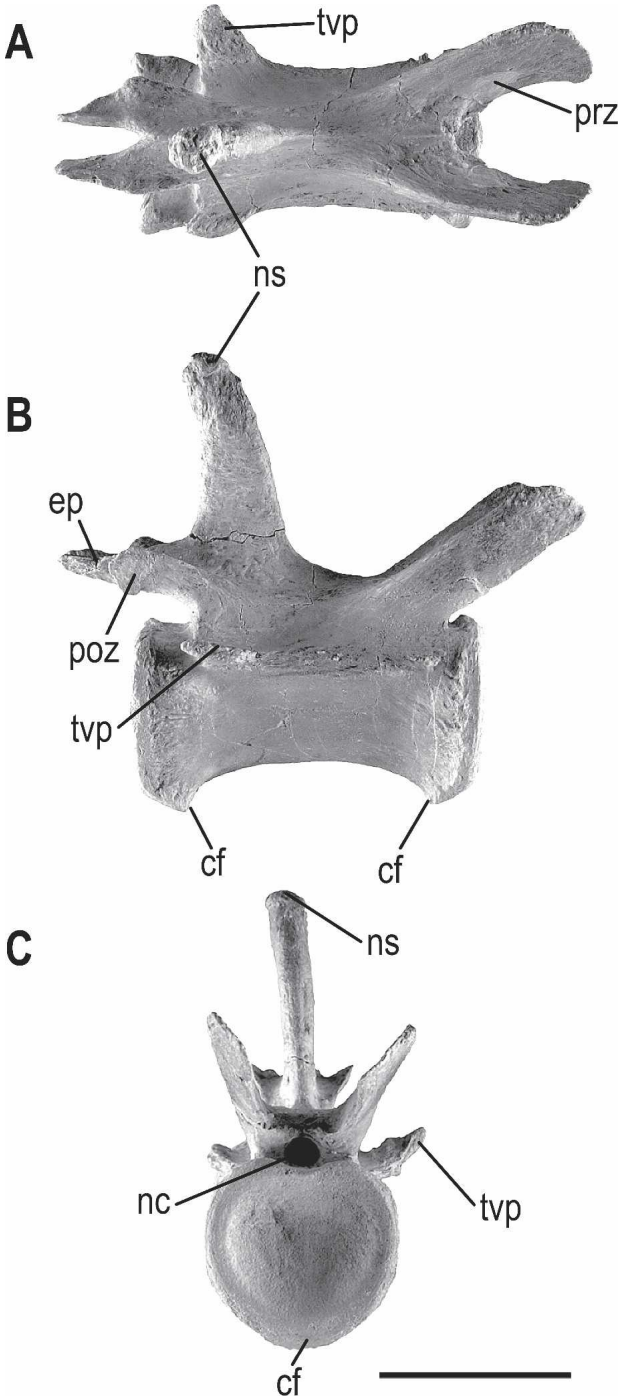

FIGURE 17. Middle caudal vertebra (FMNH PR 2100) of *Majungasaurus crenatissimus* in dorsal (**A**), right lateral (**B**), and cranial (**C**) views. See Appendix 1 for list of anatomical abbreviations. Scale bar equals 5 cm.

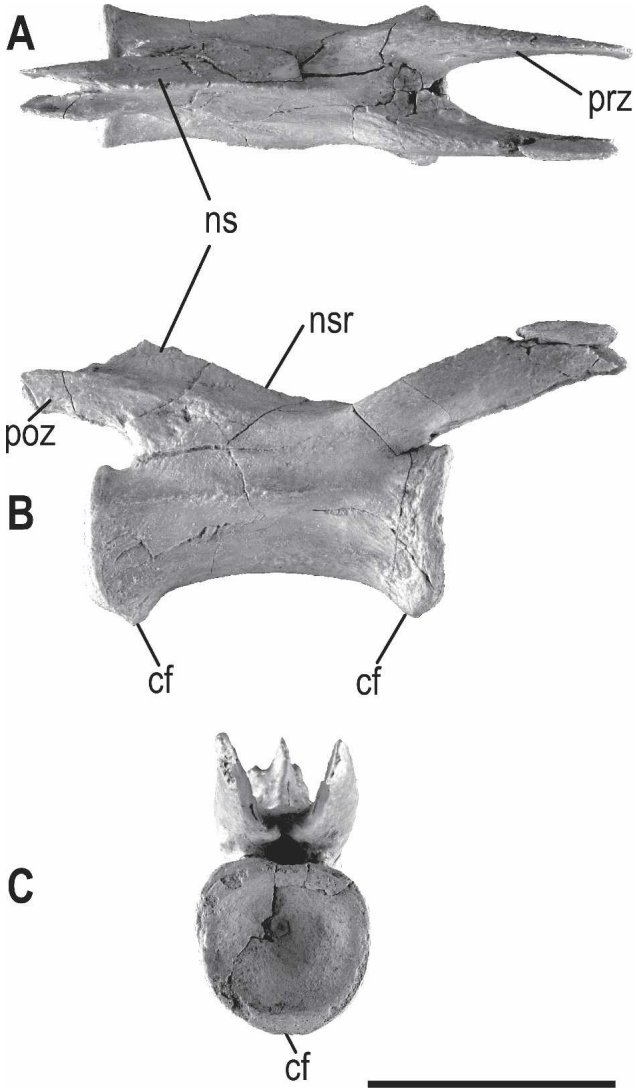

FIGURE 18. Distal caudal vertebra (FMNH PR 2100) of *Majungasaurus crenatissimus* in dorsal (**A**), right lateral (**B**), and cranial (**C**) views. See Appendix 1 for list of anatomical abbreviations. Scale bar equals 5 cm.

Distal caudal vertebrae (Figs. 16, 18) are amphicoelous, with elongate centra (centrum length approximately twice centrum height) bearing nearly circular articular facets. The prezygapophyseal process projects craniodorsally well past (>½ total centrum length) the cranial limit of the centrum. In contrast to middle caudal vertebrae, the prezygapophyseal facet is located well cranial of the cranial margin of the centrum (Fig. 18A). The transverse process and neural spine are reduced to low ridges of bone, and an abbreviated neural spine ridge passes cranially along the dorsal aspect of the neural arch. The zygapophyses are oriented in a manner similar to those of the middle caudal vertebrae and epipophyses are absent. Distinct chevron facets are still present, even in distal caudal vertebrae.

Haemal Arches

Numerous chevrons are preserved from throughout the caudal series, many with abundant tooth marks indicative of scavenging (FMNH PR 2100; Fig. 19N, O; Rogers et al., 2003, this volume). Chevrons from the proximal portion of the tail are rod-shaped, similar to those described in other abelisaurids (e.g., *Aucasaurus*, *Carnotaurus*, *Ilokelesia*). Although the dorsal half of the shaft is typically cylindrical, the ventral end is transversely compressed, with variably-sized tendon attachment scars (Fig. 19A, B). The first chevron is preserved in UA 8678 and exhibits a single dorsally concave articular surface (Fig. 19J-M), similar to first chevron morphology noted in other theropods (e.g., tyrannosaurids; Brochu, 2003:fig. 68A). Chevrons from more caudal in the series possess two distinct articular facets, craniodorsal and caudodor-

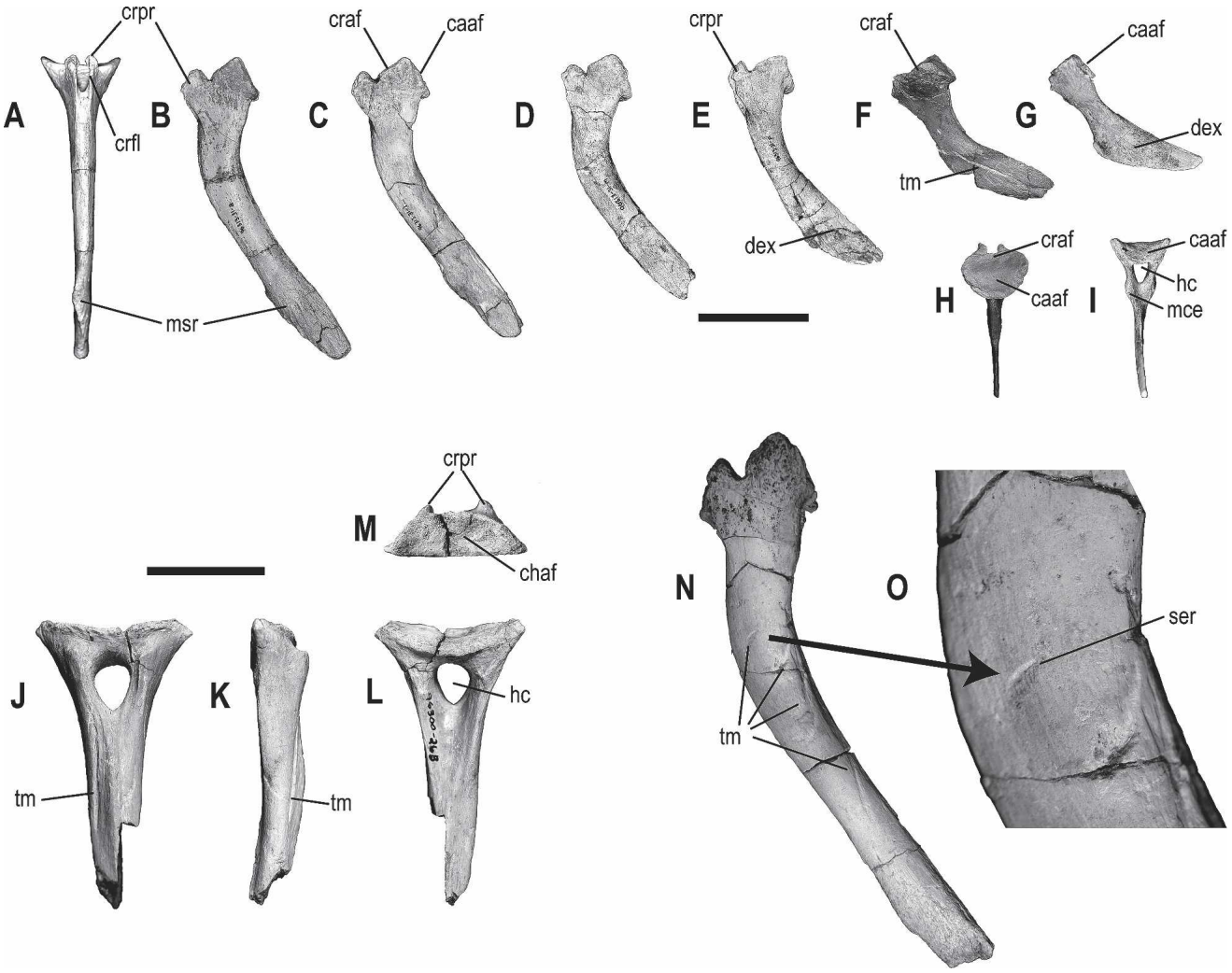

FIGURE 19. Haemal arch morphology of *Majungasaurus crenatissimus*. (**A**–**I**, **N**–**O**) FMNH PR 2100, (**J**–**M**) UA 8678. (**B**–**G**) Representative haemal arches in left lateral view, cranial to caudal progression from left to right in image (note: this does not represent a continuous series). Additional images include cranial view (**A**) of haemal arch in **B**; dorsal view (**H**) of haemal arch in **F**; and caudal view (**I**) of haemal arch in **G**. (**J**–**M**) First haemal arch (UA 8678) in cranial (**J**), right lateral (**K**), caudal (**L**), and dorsal (**M**) views. (**N**–**O**) Proximal (i.e., cranial within the series) haemal arch with numerous tooth marks [including close-up (**O**) illustrating serrations from denticle drag]. See Appendix 1 for list of anatomical abbreviations. Scale bar equals 5 cm in **A**–**I**; 4 cm in **J**–**M**; **N**–**O** not to scale.

sal, that serve as contact points for vertebrae, rather than one as described for *Ilokelesia* (Coria and Salgado, 1998) and figured for *Carnotaurus* (Bonaparte et al., 1990:fig. 26). The craniodorsal facet is relatively larger than the caudodorsal surface; thus each chevron articulates predominantly with the cranial member of the vertebral pair. This conformation is consistent with the relative sizes of the chevron facets on caudal vertebrae (i.e., distal chevron facets are larger than proximal facets; Figs. 15A, 17B, and 18B). The haemal canals are closed dorsally, as in *Carnotaurus* (Bonaparte et al., 1990:fig. 26) and *Ilokelesia* (Coria and Salgado, 1998:fig. 12), and in contrast to the open condition in *Aucasaurus* (Coria et al., 2002). Thin flanges of bone form the craniolateral borders of the haemal canal. Each flange terminates in a cranially directed prong adjacent to the craniodorsal vertebral facet of the chevron (Fig. 19). Chevrons from the middle portion of the tail are transversely compressed, with a ventral half that angles caudally and expands dorsoventrally (Fig. 19F, G). Although reduced in size, a cranially-directed prong is still evident on chevrons from the middle region of the tail. In contrast to the condition described for *Carnotaurus* (Bonaparte et al., 1990), the tails of *Majungasaurus* and *Aucasaurus* (Coria et al., 2002:fig. 2A) are not compressed dorsoventrally.

Costal Elements

Cervical Ribs—Cervical ribs (CR) of *Majungasaurus* (Figs. 20) are preserved from C3 through C10 on the right side of UA 8678, whereas ribs of only C4, C8, and C9 were recovered from the left. Although many ribs (e.g., right CR7-10) were recovered in direct articulation with their respective vertebrae, there is no evidence of rib-vertebra fusion. The delicate nature of cervical ribs preserved in UA 8678 (Fig. 20A) highlights the preservational potential of the Maevarano Formation.

Middle and caudal cervical ribs (CR4–CR10) possess large, shallow concavities on the dorsolateral and ventromedial surfaces. Furthermore, multiple, enlarged pneumatic foramina are positioned on the cranio- and caudomedial aspects of the neck on CR4-CR9. The shafts of CR4–CR7 are distally bifurcate (Fig. 20B–E), a condition otherwise known only in *Carnotaurus*

among theropods (S. Sampson, pers. comm., October, 2006). The shafts are convex laterally and clearly overlap adjacent ribs, thereby forming part of an interlocking osseoligamentous cervical complex.

It is unclear whether an atlantal rib was present in *Majungasaurus*. There were no single-headed ribs identified from the MAD 96-21 quarry, nor was the atlantal intercentrum with its potential articular surfaces recovered. *Carnotaurus* retains an atlantal rib (Bonaparte et al., 1990), as do more primitive taxa such as *Herrerasaurus* (Sereno and Novas, 1993) and *Megapnosaurus* (formerly *Syntarsus*; Rowe, 1989). However, more derived taxa such as *Sinraptor* (Currie and Zhao, 1993) and *Allosaurus* (Madsen, 1976) do not possess atlantal ribs. Many slender fragments of bone were found near the axis; however, none could be confidently identified as axial ribs. As the axis has well-developed para- and diapophyses, a double-headed axial rib was no doubt present in this taxon.

The third cervical rib (Fig. 20A) is double-headed, with a long slender shaft that extends caudally to the level of C5. The capitulum is robust, whereas the tuberculum displays only minimal development. Pneumatic foramina are absent on this rib; however, a large fossa is located on the medial surface of the shaft just distal to the capitulotubercular plane (Fig. 20A). A small craniolateral process is present (Fig. 20B).

The fourth cervical rib possesses an expanded proximal region, including a distinct capitulum and well-developed tuberculum connected via a short capitulotubercular web (Fig. 20B). The capitulum has a convex articular surface for contact with a concave parapophysis, whereas the tuberculum has a concave articular surface for contact with a convex diapophysis. This morphology is consistent through the remaining cervical rib series. The cranial process is significantly expanded relative to the previous rib, and a large (11.5 mm high × 13.3 mm wide) pneumatic foramen is present in the cranial surface of the capitulotubercular web (Fig. 20B). A smaller pneumatic fossa is set within the caudal surface of the web. The shaft is mediolaterally expanded along its proximal half, with ventrolaterally convex and dorsomedially concave surfaces. The shaft bifurcates distally into two distinct portions; the dorsolateral process extends approximately one half the total length of the rib, whereas the ventromedial styliform process continues distally as a thin, oval piece of bone (Fig. 20B). The dorsolateral process corresponds to the 'aliform process' identified in mid-cervical ribs of *Carnotaurus* (Bonaparte et al., 1990:fig. 24), whereas the ventromedial styliform process likely represents an ossified tendon of cervical musculature (e.g., M. longus coli lateralis). Such ossified tendons and/or hyper-ossified muscle attachment sites of the postcranium (e.g., hypertrophied cervical and caudal epipophyses) characterize *Majungasaurus* and other abelisauroids. Together with several features of the craniofacial skeleton, these structures suggest a clade-specific trend toward ossification and/or mineralization of soft tissues (see Discussion and Sampson and Witmer, this volume).

The fifth cervical rib is larger, particularly within the proximal half of the shaft (Fig. 20C). The capitulotubercular web is perforated both cranially and caudally by pneumatic foramina. The well-developed craniolateral process contains a large pneumatic fossa in its dorsomedial surface. The dorsolateral process of the costal shaft is enlarged, notched caudally, and exhibits a pronounced pneumatic fossa on the dorsomedial surface adjacent to the tubercular lamina. The caudal portion of the dorsolateral process thins considerably and forms a lateral buttress for the cranial process of the succeeding cervical rib. Related to this arrangement, a craniocaudally-oriented groove is present on the concave dorsomedial surface (Fig. 20C). This groove would have received the craniolateral process of the succeeding cervical rib upon lateral flexion of the cervical vertebral column. This condition exists through the remainder of the cervical rib series and no doubt contributed to general stability of the neck in addition to limiting extreme lateral flexion during cervical movements. Consistent with the overall increase in size, the styliform process is more robust than on the preceding rib. Due to remarkable preservation, it is apparent that the styliform process ossifies separately, as evidenced by the presence of a distinct suture at the point of contact with the main rib shaft (Fig. 20C).

The sixth and seventh cervical ribs resemble the fifth in most pneumatic features and general morphology (Fig. 20D, E). Significant differences include an increase in the distance between the capitulum and tuberculum (related to diapophyseal elevation through the cervical vertebral series) and a reduction in size of both the dorsolateral and styliform processes of the rib. Notably, CR7 (Fig. 20E) does not preserve the distal end of the styliform process, but does retain a clear separation proximally between the two components of the rib shaft. Due to incomplete preservation, the large internal pneumatic sinus is exposed on CR6 (Fig. 20D).

The eighth and ninth cervical ribs (Fig. 20F, G) are similar to one another, characterized by a shaft that tapers distally. This tapering is accomplished in two ways; first, by a reduction in the dorsal margin of the dorsolateral process, and second, by progressive reduction of the styliform process. As the capitulotubercular web increases in size, distinct fossae are formed along its cranial and caudal surfaces (Fig. 20G). These pre- and postcostal fossae contain pneumatic foramina that allow communication with one another via pneumatic sinuses within the rib. Although not recovered, it is clear that the styliform processes were present, but not completely fused, to the rib shafts (Fig. 20F, G). The neck-shaft angle gradually transitions from ~90 degrees on CR5–8 to ~120 degrees on CR9 (Fig. 20E–G, inset diagrams).

The tenth cervical rib is clearly transitional in nature, with an increased distance between the capitulum and tuberculum (Fig. 20H). The precostal fossa is large, with a pneumatic foramen penetrating the cortical surface and communicating with the internal cavity of the rib shaft. Although incomplete distally, the shaft is long and does not taper as in preceding ribs. Further, when articulated with C10, the rib shaft is directed caudoventrally, rather than caudally as in preceding ribs. The craniolateral process remains distinct and does not exhibit the marked reduction or loss characteristic of many theropods (e.g., reduced in *Carnotaurus* [Bonaparte et al., 1990] and *Sinraptor* [Currie and Zhao, 1993]; absent in *Monolophosaurus* [Zhao and Currie, 1993]). The neck-shaft angle on the CR10 approaches 130 degrees (Fig. 20H, inset diagram).

Dorsal Ribs—UA 8678 preserves dorsal ribs (DR) 2–4, 6, and 11 from the left side and DR1–6, 8, 10, and 11 from the right, most being incomplete distally (Fig. 21). Numerous other rib fragments (e.g., left DR10) were also recovered from the MAD 96-21 quarry. Similar to cervical ribs, some dorsal ribs were articulated with their respective vertebrae and exhibit tooth marks indicative of scavenging. It is unclear if a rib was associated with dorsal vertebra 12, as the parapophysis and diapophysis coalesce (pleuropophysis) to form a single articulation. When articulated with adjacent vertebrae, the combined pleuropophysis of D12 would have been located at the cranial edge of the preacetabular ilium; thus, if a rib was present, it was likely vestigial in nature. The thirteenth dorsal vertebra (presacral 23) lacked a rib altogether and articulated directly with the medial surface of the preacetabular ilium.

In general morphology, dorsal ribs of *Majungasaurus* are similar in most regards to those of other medium-to-large bodied theropods. The capitulum and tuberculum are separated by a distinct neck, which narrows to a thin sheet of bone (capitulotubercular web) toward its medial edge. A shallow depression is present in the caudomedial surface of the web. However, contra

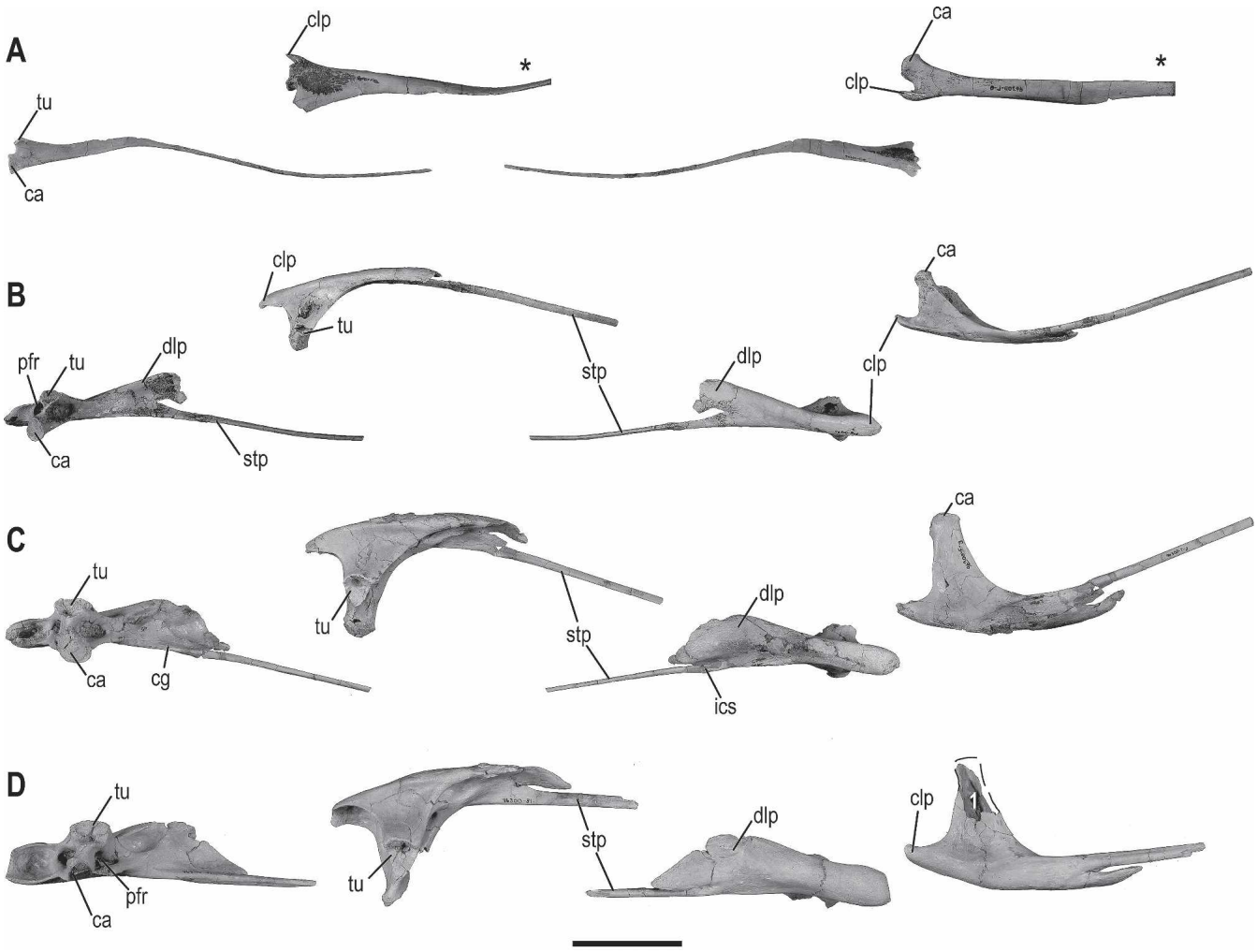

FIGURE 20. Right cervical rib series (UA 8678) of *Majungasaurus crenatissimus* in medial, dorsal, lateral, and ventral views (from left to right). Elements figured include the third (**A**), fourth (**B**), fifth (**C**), sixth (**D**), seventh (**E**), eighth (**F**), ninth (**G**), and tenth (**H**) cervical ribs. The ninth cervical rib (**G**) imaged here is the reversed ninth left cervical rib. **Notation: 1**, pneumatic cavity visible in broken section of sixth cervical rib. See Appendix 1 for list of anatomical abbreviations. Asterisk (*) in **A** indicates images that have been scaled up ~30% relative to other views on the figure to emphasize detail. For all other images, scale bar equals 5 cm.

Tykowski and Rowe (2004), no pneumatic foramina are present near tubercula, in contrast to the situation reported in other basal theropods (e.g., *Ceratosaurus dentisulcatus*—Madsen and Welles, 2000; *Sinraptor*—Currie and Zhao, 1993). Furthermore, numerous fortuitous breaks reveal that none of the ribs possess hollow shafts. The tuberculum is well separated from the capitulotubercular web (Fig. 21), even in the most caudal dorsal ribs, similar to the situation in *Sinraptor* (Currie and Zhao, 1993:fig. 19). This conformation differs markedly from the condition in *Carnotaurus* (Bonaparte et al., 1990:fig. 25), *Allosaurus* (Madsen, 1976:pls. 39, 40), and *Monolophosaurus* (Zhao and Currie, 1993:fig. 5). The costal neck shortens in more caudal dorsal ribs, corresponding to the approximation of para- and diapophyses in caudal dorsal vertebrae (Fig. 21I–K). A similar condition has been described in *Carnotaurus* (Bonaparte et al., 1990), and likely represents a feature shared by other abelisaurids. In relation to parapophyseal migration, caudal dorsal rib shafts project caudoventromedially rather than ventromedially as in most theropods.

As is typical of theropods, rib shafts are gently curved in the cranial portion of the series (DR2, 3) and approach a near-right angle with the axis of the costal neck (Fig. 21A, B), whereas shafts more caudal in the series exhibit higher curvature and an increased shaft-neck angle (Fig. 21C–F). Shafts of DR2 and 3 exhibit a mediolaterally flattened distal portion that terminates in a blunt, squared-off end (Fig. 21A), rather than tapering to a point as in more caudal ribs (Fig. 21C–E). Significantly, these are also the most robust elements of the series, representing those ribs that articulated with the sternal complex (not preserved in this specimen) via a system of sternal ribs and/or costal cartilages. The cranial intercostal ridge extends proximally to reinforce the tuberculum (Fig. 21A, B), as in *Sinraptor* and other theropods in general (Currie and Zhao, 1993). Dorsal ribs 10 and 11 have prominent caudomedial flanges along the proximal third of the shaft (Fig. 21K). This may represent a unique feature of *Majungasaurus*. Many of the costal elements exhibit tooth marks consistent in size with known teeth of *Majungasaurus* and suggest intraspecific scavenging between members of this species (Rogers et al., 2003; this volume).

Gastralia—Many slender pieces of bone were collected from the quarry at MAD96-21 and likely pertain to gastral elements. However, none are sufficiently complete for confident identification, let alone formal description.

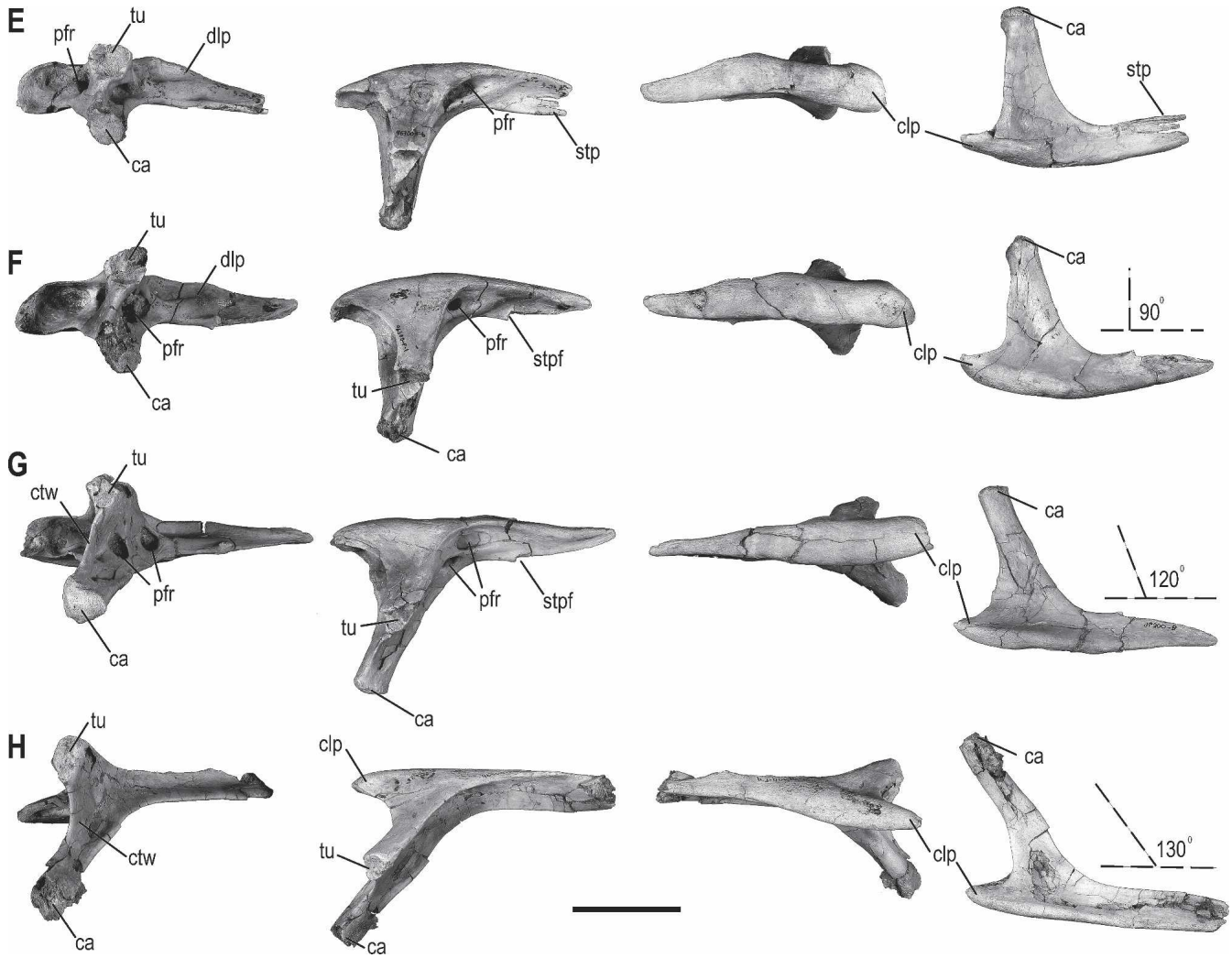

FIGURE 20. *(Continued)*

DISCUSSION

Phylogenetic Characters of the Postcranial Axial Skeleton

The quality of preservation, combined with the completeness of numerous specimens of *Majungasaurus*, makes it possible to identify new and refine existing characters useful for phylogenetic analysis. Many of these characters diagnose clades within Ceratosauria, particularly Abelisauridae, and may further assist with elucidating phylogenetic relationships among basal theropod taxa. Listed below are characters derived from the postcranial axial skeleton of *Majungasaurus*, along with their distribution among abelisauroids and abelisaurids. These warrant consideration in future phylogenetic analyses.

The postcranial axial skeleton of *Majungasaurus* possesses the following features also present in most abelisauroids: axial centrum and intercentrum with straight ventral margin in lateral view; axial intercentrum with ventrally-flared cranial margin; axial neural spine with (near) straight dorsal margin; axial neural spine with deep concavities along caudal margin; mid-cervical vertebrae with short, craniocaudally-restricted neural spines positioned over the caudal half of the centrum; mid-cervical vertebrae with distinct prezygoepipophyseal lamina; enlarged, caudally-directed cervical epipophyses (no cranial expansion); D-shaped sacral centra (similar to *Masiakasaurus*); distinct intercentral articulations in sacrum, similar to those in some abelisauroids (e.g., *Masiakasaurus*, unnamed Indian forms [GSI K27/533, GSI K27/554]; Novas et al., 2004) and unlike the coalesced, rod-shaped sacrum of *Carnotaurus*; sacral neural arches exhibiting extensive pneumaticity; sacral transverse processes subequal in height to co-ossified neural spines; proximalmost caudal vertebrae with L-shaped neural spines positioned over caudal half of centrum (Carrano et al., 2002); and middle caudal vertebrae with prominent epipophyses.

Majungasaurus shares the following characteristics with at least some abelisaurids: straight, parallel-sided axial centrum and intercentrum (Fig. 3C), unlike most other theropods that exhibit transverse pinching of the lateral sides near the centrointercentral suture; odontoid with flat lateral surface; axial neural spine forming an equilateral (rather than isosceles) triangle in dorsal view; cervical zygapophyses with craniocaudal expansion of lateral half; postaxial cervical parapophyses notably ovoid, with long axis oriented craniodorsal to caudoventral (as in *Carnotaurus*); caudal centrodiapophyseal lamina of mid-cervical vertebrae connecting to centrum at mid-length; third cervical vertebra with nonparallel cranial and caudal neural spine margins; laterally-expanded, ventrally-buttressed dorsal parapophysis (caudal to D3); dorsolaterally-facing prezygapophysis in mid-dorsal series; mid-dorsal vertebrae with centroprezygapophyseal lamina inter-

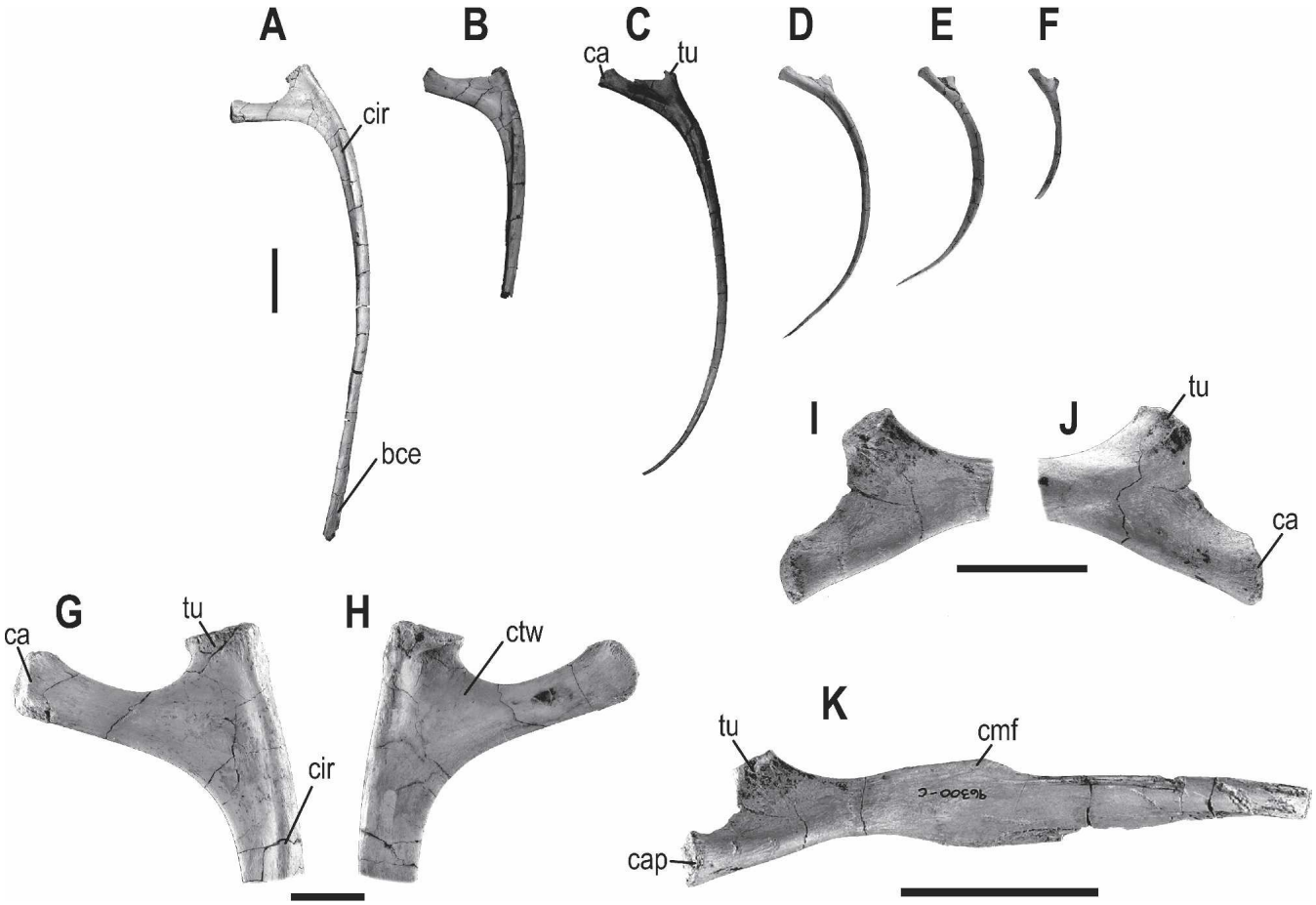

FIGURE 21. Dorsal (vertebral) rib series (UA 8678) of *Majungasaurus crenatissimus*, with examples of representative rib morphology from throughout the series. Elements figured include the second (**A**), fourth (**B**), and sixth (**C**) left dorsal ribs in cranial view; the eighth (**D**), tenth (**E**), and eleventh (**F**) right dorsal ribs in craniolateral view (elements reversed in image); (**G**, **H**) close-up of proximal end of second left dorsal rib in cranial (**G**) and caudal (**H**) views; (**I**, **J**) close-up of proximal end of eleventh right dorsal rib in (**I**) medial and (**J**) lateral views; (**K**) near-complete eleventh right dorsal rib in medial view. See Appendix 1 for list of anatomical abbreviations. Scale bar equals 5 cm for **A**–**F** and **K**; 3 cm for **G**–**J**.

secting medial end of prezygapophysis; infradiapophyseal fossa of middle-caudal dorsal vertebrae subdivided by caudal paradiapophyseal lamina; interspinous ligament scar extending to dorsal limit of neural spine; proximal-middle caudal vertebrae with columnar neural spine capped by an enlarged dorsal expansion; caudal transverse process >1.4 times centrum length (also, see Rauhut, 2003); and caudally-bifurcate cervical ribs with broad dorsolateral process and long, thin styliform process (shared with *Carnotaurus*).

The following characteristics present in *Majungasaurus* are variably shared by other basal (non-coelurosaurian) theropods: axial parapophysis located at centrum mid-height (similar to some basal tetanuran taxa, but unlike the condition in most non-tetanuran neotheropods); incipient hyposphene-hypantrum articulations on proximal caudal vertebrae (but not to the extent observed in *Aucasaurus* and *Carnotaurus*); and dorsal ribs with tubercula well-separated from capitulotubercular web. Given their variable distribution within basal theropods, the phylogenetic significance of these characters can only be assessed through additional cladistic analyses.

Within Abelisauroidea, *Majungasaurus* appears unique in the following characteristics: long, falciform atlantal epipophysis; mid-cervical transverse processes with parallel cranial and caudal borders (in lateral view); cranial dorsal vertebrae with dorsoventrally-elongate articular surfaces; mid-dorsal transverse processes with convex cranial and concave caudal margins; dorsally-expanded (both transversely and craniocaudally) neural spines in dorsal vertebral series; transverse cleft around dorsal tip of cervical and dorsal neural spines; dorsally-directed caudal neural spines (rather than caudodorsal as in most abelisauroids); proximal caudal centra elliptical in shape (also in *Masiakasaurus*?); cervical ribs pierced by multiple, enlarged pneumatic foramina on medial surface of shaft and accessory pneumatic foramina on cranial and caudal surfaces of capitulotubercular web; CR10 with distinct craniolateral process; and caudal dorsal ribs with distinct ventromedial flange. However, it must be noted that several of these characters currently cannot be assessed for various abelisaurid taxa; thus additional discoveries may demonstrate broader distributions of some of these features within the clade.

Majungasaurus does not possess the following characters previously cited as syapomorphies of Abelisauridae (Coria and Salgado, 2000; Coria et al., 2002): proximal-middle caudal vertebrae with distally-modified transverse process (e.g., uncinate processes of *Carnotaurus* or *Ilokelesia*, overlapping awl-like projections of *Aucasaurus*); dorsally-elevated proximal caudal transverse processes; and proximal caudal vertebrae with distinct hyposphene-hypantrum accessory articulations (perhaps incipiently present, see above).

Cervical Robustness, Hyperossification, and Reduced Forelimbs

Enlarged (hypertrophied) epipophyses combined with a robust, tightly-interlocking cervical rib series indicate that the neck

region of *Majungasaurus* formed a sturdy axial core relative to the condition in most other theropods. Concomitant enlargement of the caudal surfaces of the skull (e.g., large nuchal crest and parietal eminence) have also been noted in *Majungasaurus* and other abelisaurids (Sampson et al., 1998; Sampson and Witmer, this volume), suggesting increased areas of attachment for cervical musculature. These features have also been suggested to correlate with decreased forelimb size in abelisaurids (Tykoski and Rowe, 2004). Taken together, these specializations in *Majungasaurus* (and perhaps abelisaurids in general) indicate the presence of an extremely robust cervicocephalic complex, and underscore likely foraging/feeding adaptations. For example, increased cervical and cervicocephalic musculature may have proved beneficial to animals engaged in 'rip and tear' scavenging, particularly of large-bodied prey items. It has been documented that *Majungasaurus* commonly engaged in scavenging behavior on various vertebrate taxa preserved in the Maevarano Formation, including not only the large-bodied titanosaurian *Rapetosaurus,* but similarly-sized conspecifics (Rogers et al., 2003; this volume). Whereas morphological features of the skull and cervical column of *Majungasaurus* suggest possible feeding adaptations, perhaps correlated with decreased forelimb size (and minimally consistent with available taphonomic data from the Maevarano Formation), the functional and ecomorphological significance of such characteristics awaits further study. Other large-bodied nonavian theropods (e.g., tyrannosauroids) also exhibit extremely reduced forelimbs in conjunction with a hypertrophied cervical skeleton, and may prove useful for analyzing independently derived character correlations for comparisons with abelisaurids.

Sutural Fusion and Maturity Status

One specimen (UA 8678) of *Majungasaurus* exhibits considerable variation in sutural fusion throughout the vertebral column, indicating the specimen had not reached somatic maturity at the time of death. Due to the near-complete nature of this immature specimen, it is possible to begin assembling a larger view on the patterning of suture fusion in this taxon (Fig. 3). All postaxial cervical centra and neural arches are fused with one another, possessing completely obliterated neurocentral sutures. The only incompletely fused cervical elements are the atlas, consisting solely of the left neurapophysis (Fig. 5), and the axis, which retains not only a partially-open neurocentral suture but a clearly open suture between the odontoid and axial intercentrum (Fig. 6). In no instances are cervical ribs fused to their respective vertebrae. The first two dorsal vertebrae exhibit partial fusion of centra and neural arches. Whereas the elements are firmly attached to one another, sutures are evident at the cortical surface. Remaining elements of the dorsal series (D3–D13) lack fusion between centra and neural arches (Figs. 3, 10–12). Indeed many dorsal centra of UA 8678 were displaced from their corresponding arches, and three dorsal centra (D7, D10, and D13) represent the only missing elements of the entire postatlantal, presacral vertebral column. The sacral complex consists of two partially fused centra and three neural arches, all with sutures clearly visible. Moreover, there is a fused fourth sacral rib on the left side with an unfused one on the right. Articular surfaces on the two sacral centra are well preserved and indicate that adjacent centra were not fused to these at the time of death. The five proximal caudal vertebrae recovered with this specimen include a mixture of fused and unfused elements. The neural arch and centrum of the first vertebra in the series are unfused, with the second and third exhibiting partially-fused sutures. The fourth vertebra exhibits asymmetry in fusion, with a visible suture on the right side and a partially obliterated one on the left. The fifth vertebra consists of a fused neural arch and centrum, with completely obliterated neurocentral sutures on both sides.

Based upon the unique preservation of UA 8678, it is clear that fusion proceeds from at least three different focal areas of the vertebral column, including the cervical, sacral, and caudal regions. The complete fusion of the postaxial cervical series, along with the absence of fusion of the axis and atlas, suggests a caudal to cranial progression in this region. Patterns of fusion within the dorsal series indicate a cranial to caudal progression. Taken together, these results suggest that fusion initiates at the cervico-dorsal transition and proceeds cranially and caudally within the presacral series. Fusion of the two primordial sacral vertebrae and their neural arches likely pertains to the functional necessity of transmitting body weight through the sacral complex. The 26 associated caudal vertebrae (FMNH PR 2100; Fig. 16), collected as part of a specimen ~20% larger than UA 8678, display complete fusion between centra and neural arches.

Vertebral fusion in *Majungasaurus* appears more complex than that reported for extant nonavian archosaurs (crocodylians), in which neurocentral suture fusion proceeds from caudal to cranial through the vertebral series (Brochu, 1996). Indeed the pattern observed in *Majungasaurus* (i.e., variable fusion in different regions of the column) more closely resembles that reported for other extant nonarchosaurian sauropsids (Rieppel, 1992a, 1992b, 1993); thus it appears that extant crocodylians are not a good model for use in comparisons with theropod dinosaurs when inferring other attributes (e.g., growth, maturity status, reproductive potential, etc.) based on vertebral fusion schemes. Prior to the formulation of inferences in fossil archosaur groups based on these traits, additional work is necessary, particularly relating to birds, in order to examine large-scale patterns of vertebral fusion within Archosauria. In sum, based on incomplete fusion of many vertebral elements in UA 8678, this specimen is here classified as a subadult individual. In this context, 'subadult' indicates merely that an individual had not completed somatic growth (i.e., it had not attained its upper growth asymptote), and does not pertain specifically to reproductive potential.

Soft Tissue Inferences

Nonpneumatic Soft Tissues: The Basivertebral Venous System—A number of soft-tissue systems (e.g., pulmonary, muscular, vascular) are known to significantly influence vertebral morphology in archosaurs (O'Connor, 2003, 2006). Notable among these is the basivertebral venous system and its osteological correlates, basivertebral foramina. Paired foramina on the dorsal surface of vertebral centra are ubiquitous among both extant and fossil (e.g., *Mahajangasuchus insignis* [UA 8654]) crocodyliforms, and represent osteological correlates of paired veins that exchange blood between vertebral centra and the longitudinal internal vertebral venous sinus (IVVS) (O'Connor, 2006:fig. 9). Basivertebral foramina are absent in vertebral centra of *Majungasaurus* and certain other theropods (e.g., *Masiakasaurus* [FMNH PR 2140]), including extant birds. However, other nonavian theropods (e.g., *Carcharodontosaurus* [CMN 41774]) possess distinct basivertebral foramina in at least some regions of the vertebral column, implying a pattern of vertebral vascularization similar to that in crocodyliforms. Functional hypotheses to account for such variation in theropods include differential vascularization as a function of body size and/or relative degree of vertebral pneumaticity. Both factors would place different demands on the amount of vasculature required for a given volume of bone. For example, relative to pneumatic bone, apneumatic bone represents an increase in tissue density per unit volume (Schepelmann, 1990; O'Connor, 2006), and would require a higher amount of vascularization to accommodate the metabolically expensive bone marrow. Alternatively, the presence of this system in certain theropod groups and not others may reflect nothing more than clade specificity. Nonetheless, the basiverte-

bral venous system (represented in fossils by basivertebral foramina) warrants both functional and systematic consideration in future studies of theropod dinosaurs.

Postcranial Pneumaticity—In this study, postcranial pneumaticity was identified by the presence of distinct cortical features, specifically foramina and/or fossae in centra, neural arches, and ribs that are continuous with large, internal chambers within these elements (Fig. 22). Postcranial pneumatic features have formed the basis for inferring the presence of an avian-like pulmonary air sac system in nonavian theropods, and have been the subject of a number of recent studies (Britt, 1993; O'Connor, 2003, 2006; O'Connor and Claessens, 2005). Using the above definition, all postatlantal, precaudal vertebrae of *Majungasaurus* exhibit extensive pneumaticity, more so than is typical of many nonavian theropods. Sacral pneumaticity in *Majungasaurus* is restricted to neural arches. Moreover, cervical ribs 4–10 also display extensive pneumaticity bilaterally (Figs. 20, 22). Pneumatic caudal vertebrae are not present in *Majungasaurus*.

Pneumatic features in the postcranial axial skeleton of *Majungasaurus* range in size from small foramina in cervical centra (Fig. 8D) to elaborate fossae and foramina in the mid-dorsal vertebral series (Fig. 11). Throughout the vertebral series, the usual complement of infraprezygapophyseal, infradiapophyseal, and infrapostzygapophyseal fossae and foramina are present. The postaxial cervical and cranial dorsal vertebrae typically possess both cranial and caudal laminopeduncular foramina (Fig. 8B). Of note is the considerable variation in pneumatic features both within and between vertebral regions. For example, within cervical centra, C8 has two foramina per side piercing the centrum (one positioned cranially, the other on the caudal half), a character often cited as a synapomorphy of Ceratosauria (Rowe and Gauthier, 1990; Tykoski and Rowe, 2004). Yet other cervical vertebrae (C2, C5) possess only the cranialmost foramen on each side, and another (C4) lacks central foramina altogether. Moreover, significant size and shape variation of pneumatic features is present within vertebral centra. Neural arch pneumaticity is generally more consistent in morphology and serial organization. The subadult status of UA 8678 may contribute to the high levels of variation (ontogenetic variability?) observed in this specimen; although, certain extant birds are known to exhibit high levels of intraspecific variation in pneumatic morphology (O'Connor, 2006). Thus, collection of additional materials is necessary to rigorously assess these characteristics in *Majungasaurus* specifically and, more generally, among theropods.

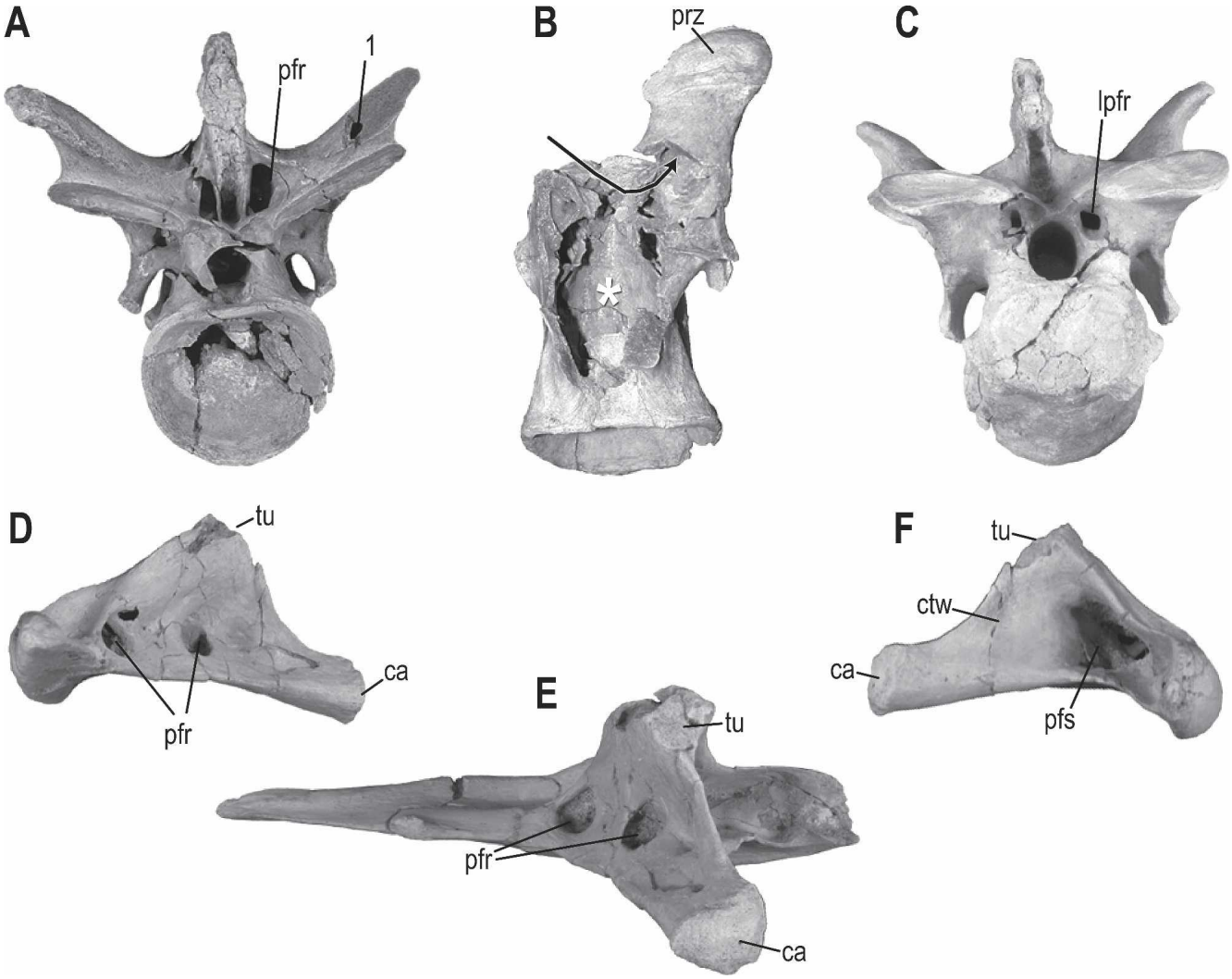

FIGURE 22. Pneumatic features preserved in vertebral and costal elements of *Majungasaurus crenatissimus*. (**A**–**C**) Third cervical vertebra (FMNH PR 2295) in caudal (**A**), dorsal (**B**), and cranial (**C**) views (dorsal view is of centrum with neural arch removed). (**D**–**F**) Ninth left cervical rib (UA 8678) in caudal (**D**), medial (**E**), and cranial (**F**) views. **Notation**: **1**, pneumatic cavity within right epipophysis; white asterisk in **B** indicates large pneumatic cavity within vertebral centrum; black arrow in **B** indicates continuity of pneumatic cavity between the pedicle and prezygapophyseal process. See Appendix 1 for list of anatomical abbreviations. Images not to scale: see Fig. 6 for scale of **A**–**C** and Fig. 18G for scale of **D**–**F**.

Dorsal vertebrae of *Majungasaurus* exhibit neural arch pneumaticity that is present through the entire series. Within dorsal centra, however, large (3–10 mm) pneumatic foramina are located bilaterally just caudal to the parapophysis on the first three dorsal centra and unilaterally on the fourth, being present only on the right side. Vertebral centra caudal to D4 do not exhibit pneumatic foramina. Other taxa displaying this general pattern (i.e., pneumaticity restricted to centra of D1–4) include *Spinostropheus* (MNN TIG6), *Sinraptor* (Currie and Zhao, 1993), and *Allosaurus* (Madsen, 1976). An isolated caudal dorsal vertebra of the abelisaurid *Ilokelesia* is reported to lack central pneumatic features ('pleurocoelic foramina') altogether (Coria and Salgado, 1998), consistent with the state in *Majungasaurus*. The only other abelisaurid preserving an intact presacral column (*Carnotaurus*) is described as possessing pneumatic foramina in the dorsal series through centrum D10 (Bonaparte et al., 1990). Pneumatic centra are found throughout the dorsal series in some large-bodied tetanurans, including *Acrocanthosaurus atokensis* (SMU 74646; Harris, 1998), *Baryonyx walkeri* (BMNH R9951), *Neovenator salerii* (BMNH R.10001), and *Tyrannosaurus rex* (FMNH PR 2081). In contrast, pneumaticity of dorsal centra is typically reduced in the smaller-bodied coelurosaurs (e.g., Hwang et al., 2002, dromaeosaurids). Given this range of variation, statements concerning general patterns of pneumaticity (e.g., "[in] most theropods where dorsal vertebrae are known, a pleurocoelic foramen is present in the lateral side of the centrum throughout the dorsal series" [Coria and Salgado, 1998:94]) remain premature until a broader survey of taxa has been conducted (see Britt [1993] for a review of pneumaticity patterns in a subset of nonavian theropods).

Generally, basal neotheropods exhibit a wide range of relative pneumaticity states, with abelisauroids possessing increased levels relative to coelophysoid taxa. For example, *Dilophosaurus* (UCMP 37302) lacks axial pneumaticity, whereas *Ceratosaurus*, *Carnotaurus*, *Majungasaurus*, and *Masiakasaurus* all possess extensive pneumaticity of both the axial centrum and neural arch. Interestingly, coelophysoids (e.g., *Liliensternus* [MB 2175.2], *Dilophosaurus* [UCMP 37302, 77270]) exhibit extensive pneumaticity of the postaxial cervical series, similar to that of most abelisauroids (and *Spinostropheus* [MNN TIG6]). The absence of axial pneumaticity in *Dilophosaurus* (and other coelophysoids) thus remains intriguing. Coelophysoids exhibit pneumaticity of centra in the cranialmost dorsal series, with the remainder of dorsal centra caudal to this point being apneumatic. Neural arch pneumaticity, however, is present through most of the dorsal series, similar to that of many other theropods, including abelisauroids (see Britt, 1993). Only in the largest theropods (e.g., spinosauroids, carcharodontosaurids, tyrannosauroids) are dorsal centra commonly pneumatized throughout the entire series, suggesting that the relative extent of vertebral pneumaticity may be correlated with body size (Carrano and O'Connor, 2005; O'Connor, 2006). This relationship has even been suggested in a size range of species restricted to a given clade (e.g., tyrannosauroids, Xu et al., 2004).

Whereas postcranial pneumaticity in nonavian theropods is generally restricted to the axial skeleton, one unequivocal case of appendicular pneumaticity is that reported by Makovicky et al. (2005), where a pneumatic furcula (based on both external and internal morphology) is preserved in the dromaeosaurid *Buitreraptor*. Previous reports have suggested the presence of appendicular pneumaticity in other nonavian theropods (e.g., *Piatnitzkysaurus*, Bonaparte, 1986; carcharodontosaurids, Alcober et al., 1998); however, a more thorough examination of these materials is necessary to ascertain their soft-tissue associations.

Although considerable serial variation exists in the distribution of skeletal pneumatic features (e.g., reduced dorsal vertebral pneumaticity in deinonychosaurs; Hwang et al., 2002; Xu et al., 2004), this variation mirrors levels observed in birds and likely pertains to the variety of factors known to influence relative pneumaticity in the living descendents of theropod dinosaurs (e.g., body size, clade specificity; Groebbels, 1932; O'Connor, 2003, 2004, 2006). Clearly a systematic survey of nonavian theropods is warranted to elucidate large-scale patterns of pneumaticity throughout the group, particularly prior to making character assessments based on incomplete and/or poorly preserved specimens.

Finally, based on inferred postcranial pneumaticy in fossil archosaurs (e.g., saurischian dinosaurs, pterosaurs, basal archosauriforms), several workers have promoted the idea that an avian-style lung and air sac system was responsible for such features (Owen, 1856; Janensch, 1947; Britt, 1993, 1997; Britt et al., 1998; Gower, 2001; O'Connor, 2003, 2006; Wedel 2003; O'Connor and Claessens, 2005). Indeed many osteological traits are morphologically consistent with pneumatic features identified in extant bird skeletons (Fig. 22). And whereas it is anatomically reasonable that such features resulted from a pulmonary air sac system, the degree of structural or functional similarity between such a system in fossil groups and that in extant birds remains a point of inquiry. A recent study by O'Connor and Claessens (2005), using *Majungasaurus* (UA 8678) and other nonavian and avian theropods, concluded that both cranial and caudal sets of pulmonary air sacs were likely present early in the evolutionary history the neotheropod clade. The presence of both sets of air sacs highlight the anatomical prerequisite for flow-through ventilation of the pulmonary apparatus, a trait previously considered to be unique among living birds (or perhaps their closest extinct maniraptoran relatives), and one key element responsible for high levels of gas exchange required for sustained metabolic activity. Importantly, the pneumatic furcula reported by Makovicky et al. (2005), if confirmed, represents the best evidence available for the presence of a clavicular air sac in a nonavian theropod, underscoring yet another component of avian-like pulmonary organization in the group. For an additional discussion of these points and specific details regarding pulmonary reconstructions in other fossil archosaurs, see Janensch (1947), Britt (1993), Perry and Reuter (1999), Wedel (2003), O'Connor (2003, 2006), Perry and Sander (2004), and O'Connor and Claessens (2005).

CONCLUSIONS

Recently discovered, remarkably preserved specimens of the theropod dinosaur *Majungasaurus crenatissimus* highlight the preservational potential of the Upper Cretaceous Maevarano Formation in northwestern Madagascar. Until now, only limited anatomical research has been performed on this taxon, with an emphasis on cranial material. This paper provides a detailed description of the postcranial axial skeleton of *Majungasaurus* and places it within a comparative framework among nontetanuran and basal tetanuran theropods.

This medium-sized theropod shares a suite of characters with the primarily Gondwanan, mostly Late Cretaceous abelisaurids, including *Carnotaurus sastrei*, *Aucasaurus garridoi*, and *Ilokelesia aguadagrandensis*. The virtually complete postcranial axial skeleton of one specimen (UA 8678), a rarity among dinosaurian taxa, has enabled a detailed examination of morphological transformations along the entire vertebral and costal series. Of particular interest is the presence of extensive pneumaticity throughout the entire postatlantal, precaudal vertebral, and cervical rib series. This study demonstrates that specific pneumatic features (e.g., number, size, and/or position of pneumatic features in cervical vertebrae) should be used cautiously in character analyses as they exhibit interregional, intraregional, and bilateral variability in their presentation.

Although pneumaticity of the postcranial skeleton is relatively extensive in *Majungasaurus*, and has been used to refine inferences related to pulmonary structure in theropods generally,

many other features of the skeleton indicate that this animal was relatively robust through its axial core. Enlarged areas of cervical muscle attachment (e.g., hypertrophied cervical epipophyses and a high, broad occiput), along with a tightly interlocking cervical vertebrae and rib series, suggest a specialized role for these structures. Such cervicocephalic specialization (i.e., the presence of a robust skull and neck), along with the concomitant reduction of the forelimbs, suggests a divergent foraging strategy for *Majungasaurus* (and abelisaurids generally) relative to most other theropods, perhaps one related to powerful 'rip-and-tear' processing of large-bodied prey items.

ACKNOWLEDGMENTS

This work was initiated as a component of a doctoral dissertation in the Department of Anatomical Sciences at Stony Brook University. I thank the following individuals for assistance: M. Carrano, C. Forster, D. Krause, M. Lamanna, S. Sampson, L. Witmer, and two anonymous reviewers for providing invaluable comments on earlier versions of this manuscript; N. Ravelomanantsoa and J. Ratsimbazafy for assistance with translation; R. Ridgely for skillfully executing Figure 1; L. Betti-Nash for line drawings in Figures 6–11; M. Stewart, T. Creamer, and J. Sattler for photographic assistance; L. Betti-Nash, J. Sattler, and J. Jacobberger for assistance with computer graphics; M. Loewen and M. Carrano for providing photographs used for comparative purposes.

I gratefully acknowledge the following individuals for assistance with excavating locality MAD96-21 over two field seasons: N. Stevens, E. Roberts, A. Rabarison, H. Rasolondalao, L. Rahantarisoa, C. Forster, D. Krause, S. Sampson, G. Buckley, M. Gottfried, and P. Dodson. V. Heisey (SBU) and the preparation staff of the FMNH skillfully prepared specimens used in this study.

I also thank A. Rasoamiaramanana, G. Ravololonarivo, and the late B. Rakotosamimanana (University of Antananarivo), P. Wright, B. Andriamihaja, and the staff of the Madagascar Institute pour la Conservation des Environnements Tropicaux (MICET), the villagers of Berivotra, and Mahajanga Basin Project field crews for logistical support. I am indebted to the following individuals, collections managers and curators for access to specimens in their care: B. Battail, M. Brett-Surman, G. Buckley, S. Chapman, M. Dawson, J. Flynn, W. Hammer, A. Henrici, P. Holroyd, X. Luo, A. Milner, M. Norell, K. Padian, R. Purdy, P. Sereno, W. Simpson, P. Taquet, and D. Unwin.

Finally, support for this research was provided to P.M.O. by the National Science Foundation Graduate Research Fellowship, the Society of Vertebrate Paleontology Estes Memorial Award, the Society for Integrative and Comparative Biology, the Paleontological Society, the Jurassic Foundation, the Stony Brook University Gabor Inke Graduate Research Fellowship, and the Ohio University College of Osteopathic Medicine and Department of Biomedical Sciences. Grants from the National Science Foundation (DEB-9224396, DEB-9904045, EAR-9418816, EAR-9706302, EAR-106477, EAR-116517, EAR-0446488), the Dinosaur Society (1995), and National Geographic Society (1999, 2001, 2004) were instrumental for the discovery and subsequent research on specimens used in this project.

LITERATURE CITED

Accarie, H., B. Beaudolin, J. Dejax, G. Friès, J.-G. Michard, and P. Taquet. 1995. Découverte d'un Dinosaure Théropode nouveau (*Genusaurus sisteronis* n. g., n. sp.) dans l'Albien marin de Sisteron (Alpes de Haute Provence, France) et extension ua Crétacé inférieur de la lignée cératosaurienne. Comptes Rendus de l'Academie des Sciences, Paris, Série IIa 320:327–334.

Alcober, O., P. C. Sereno, H. C. E. Larsson, R. Martinez, and D. J. Varricchio. 1998. A Late Cretaceous carcharodontosaurid (Theropoda: Allosauroidea) from Argentina. Journal of Vertebrate Paleontology 18 (3, Supplement): 23A.

Bonaparte, J. F. 1986. Les dinosaures (Carnosaures, Allosauridés, Sauropodes, Cétiosauridés) du Jurassique Moyen de Cerro Cóndor (Chubut, Argentine). Annales de Paléontologie (Vert.-Invert.) 72: 247–289.

Bonaparte, J. F., and F. E. Novas. 1985. *Abelisaurus comahuensis*, n. g., n. sp., Carnosauria del Crétacico Tardio de Patagonia. Ameghiniana 21:259–265.

Bonaparte, J. F., F. E. Novas, and R. A. Coria. 1990. *Carnotaurus sastrei* BONAPARTE, the horned, lightly built carnosaur from the Middle Cretaceous of Patagonia. Contributions in Science, Natural History Museum of Los Angeles County 416:1–41.

Britt, B. B. 1991.Theropods of Dry Mesa Quarry (Morrison Formation, Late Jurassic), Colorado, with emphasis on the osteology of *Torvosaurus tanneri*. Brigham Young University Geology Studies 37:1–72.

Britt, B. B. 1993. Pneumatic postcranial bones in dinosaurs and other archosaurs. Ph.D. dissertation, University of Calgary, Calgary, Alberta, 383 pp.

Britt, B. B. 1997. Postcranial pneumaticity; pp. 590–593 in P. J. Currie and K. Padian (eds.), Encyclopedia of Dinosaurs. Academic Press, San Diego.

Britt, B. B., P. J. Makovicky, J. Gauthier, and N. Bonde. 1998. Postcranial pneumatization in *Archaeopteryx*. Nature 395:374–376.

Brochu, C. A. 1996. Closure of neurocentral sutures during crocodilian ontogeny: implications for maturity assessment in fossil archosaurs. Journal of Vertebrate Paleontology 16:49–62.

Brochu, C. A. 2003. Osteology of *Tyrannosaurus rex*: insights from a nearly-complete skeleton and high-resolution computed tomographic analysis of the skull. Society of Vertebrate Paleontology Memoir 7:1–138.

Buffetaut, E., P. Mechin, and A. Mechin-Salessy. 1988. Un dinosaure théropode d'affinitiés gondwaniennes dans la Crétacé supérieur de Provence. Comptes Rendus de l'Academie des Sciences, Paris, Série II 306:153–158.

Carrano, M. T. 2007. The appendicular skeleton of *Majungasaurus crenatissimus* (Theropoda: Abelisauridae) from the Late Cretaceous of Madagascar; pp. 163–179 in S. D. Sampson and D. W. Krause (eds.), *Majungasaurus crenatissimus* from the Late Cretaceous of Madagascar. Society of Vertebrate Paleontology Memoir 8.

Carrano, M. T., and P. M. O'Connor. 2005. Bird's eye view. Natural History 114:42–47.

Carrano, M. T., S. D. Sampson, and C. A. Forster. 2002. The osteology of *Masiakasaurus knopfleri*, a small abelisauroid (Dinosauria: Theropoda) from the Late Cretaceous of Madagascar. Journal of Vertebrate Paleontology 22:510–534.

Coria, R. A., and L. Salgado. 1998 (2000). A basal Abelisauria NOVAS, 1992 (Theropoda–Ceratosauria) from the Cretaceous of Patagonia, Argentina. Gaia 15:89–102.

Coria, R. A., L. M. Chiappe, and L. Dingus. 2002. A new close relative of *Carnotaurus sastrei* BONAPARTE 1985 (Theropoda: Abelisauridae) from the Late Cretaceous of Patagonia. Journal of Vertebrate Paleontology 22:460–465.

Currie, P. J., and X.-J. Zhao. 1993. A new carnosaur (Dinosauria, Theropoda) from the Jurassic of Xinjiang, People's Republic of China. Canadian Journal of Earth Sciences 30:2037–2081.

Depéret, C. 1896. Sur l'existence de dinosauriens sauropodes et théropodes dans le Crétacé supérieur de Madagascar. Comptes Rendus de l'Academie des Sciences, Paris 122:483–485.

Farke, A. A., and P. M. O'Connor. 2007. Pathology in *Majungasaurus crenatissimus* (Theropoda: Abelisauridae) from the Late Cretaceous of Madagascar; pp. 180–184 in S. D. Sampson and D. W. Krause (eds.), *Majungasaurus crenatissimus* from the Late Cretaceous of Madagascar. Society of Vertebrate Paleontology Memoir 8.

Forster, C. A., and P. M. O'Connor. 2000. The avifauna of the Upper Cretaceous Maevarano Formation, Madagascar. Journal of Vertebrate Paleontology 20(3, Supplement.):41–42A.

Forster, C. A., L. M. Chiappe, D. W. Krause, and S. D. Sampson. 1996. The first Cretaceous bird from Madagascar. Nature 382:532–534.

Forster, C. A., S. D. Sampson, L. M. Chiappe, and D. W. Krause. 1998. The theropod ancestry of birds: new evidence from the Late Cretaceous of Madagascar. Science 279:1915–1919.

Gauthier, J. 1986. Saurischian monophyly and the origin of birds; pp. 1–55 in K. Padian (ed.), The Origin of Birds and the Evolution of Flight. Memoirs of the California Academy of Sciences, Number 8.

Gilmore, C. W. 1920. Osteology of the carnivorous Dinosauria in the United States National Museum, with special reference to the genera *Antrodemus* (*Allosaurus*) and *Ceratosaurus*. Bulletin of the United States National Museum (Smithsonian Miscellaneous Contributions) 110:1–159.

Gower, D. J. 2001. Possible postcranial pneumaticity in the last common ancestor of birds and crocodilians: evidence from *Erythrosuchus* and other Mesozoic archosaurs. Naturwissenschaften 88:119–122.

Groebbels, F. 1932. Der Vögel: Bau, Funktion, Lebenserscheinung, Einpassung. Borntraeger, Berlin. Two Volumes, 1465 pp.

Harris, J. D. 1998. A reanalysis of *Acrocanthosaurus atokensis*, its phylogenetic status, and paleobiogeographic implications, based on a new specimen from Texas. New Mexico Museum of Natural History and Science Bulletin 13:1–75.

Hwang, S. H., M. A. Norell, J. Qiang, and G. Keqin. 2002. New specimens of *Microraptor zhaoianus* (Theropoda: Dromaeosauridae) from northeastern China. American Museum Novitates 3381:1–44.

Janensch W. 1947. Pneumatizität bei wirbeln von Sauropoden und anderen Saurischiern. Palaeontographica Sup 7:1–125.

Krause, D. W., S. D. Sampson, M. T. Carrano, and P. M. O'Connor. 2007. Overview of the history of discovery, taxonomy, phylogeny, and biogeography of *Majungasaurus crenatissimus* (Theropoda: Abelisauridae) from the Late Cretaceous of Madagascar; pp. 1–20 in S. D. Sampson and D. W. Krause (eds.), *Majungasaurus crenatissimus* from the Late Cretaceous of Madagascar. Society of Vertebrate Paleontology Memoir 8.

Krause, D. W., P. M. O'Connor, K. Curry Rogers, S. D. Sampson, G. A. Buckley, and R. R. Rogers. 2006. Late Cretaceous terrestrial vertebrates from Madagascar: implications for Latin American Biogeography. Annals of the Missouri Botanical Garden 93:178–208.

Lamanna, M. C., R. D. Martinez, and J. B. Smith. 2002. A definitive abelisaurid theropod dinosaur from the Early Late Cretaceous of Patagonia. Journal of Vertebrate Paleontology 22:58–69.

Lavocat, R. 1955. Sur une portion de mandibule de théropode provenant du Crétacé supérieur de Madagascar. Bulletin du Muséum National d'Histoire Naturelle, Série 2, 27:3.

Madsen, J. H. 1976. *Allosaurus fragilis*: A revised osteology. Utah Geological Survey Bulletin 109:1–163.

Madsen, J. H., and S. P. Welles. 2000. *Ceratosaurus* (Dinosauria, Theropoda) a revised osteology. Miscellaneous Publications of the Utah Geological Survey 00–2:1–80.

Makovicky, P. J., S. Apesteguía, and F. L. Agnolín. 2005. The earliest dromaeosaurid theropod from South America. Nature 437: 1007–1011.

Marsh, O. C. 1881. Principle characters of American Jurassic dinosaurs. Part V. American Journal of Science 21:418–423.

Marsh, O. C. 1884. Principle characters of American Jurassic dinosaurs. Part VIII. The order theropoda. American Journal of Science 27: 329–340.

Novas, F. E., F. L. Agnolin, and S. Bandyopadhyay. 2004. Cretaceous theropods from India: a review of specimens described by Huene and Matley (1933). Revista del Museo Argentino de Ciencias Naturales, n.s. 6(1):67–103.

O'Connor, P. M. 2003. Pulmonary pneumaticity in extant birds and extinct archosaurs. Ph.D. dissertation, Stony Brook University, Stony Brook, New York, 304 pp.

O'Connor, P. M. 2004. Pulmonary pneumaticity in the postcranial skeleton of extant avians: a case study examining Anseriformes. Journal of Morphology 261:141–161.

O'Connor, P. M. 2006. Pulmonary pneumaticity: an evaluation of soft-tissue influences on the postcranial skeleton and the reconstruction of pulmonary anatomy in archosaurs. Journal of Morphology 267: 1199–1226.

O'Connor, P. M. and L. A. P. M. Claessens. 2005. Basic avian pulmonary design and flow through ventilation in non-avian theropod dinosaurs. Nature 436:253–256.

O'Connor, P. M. and S. D. Sampson. 1998. The vertebral column of *Majungatholus atopus* (Theropoda: Abelisauridae) from the Late Cretaceous of Madagascar. Journal of Vertebrate Paleontology 18(3, Supplement.):67A.

Owen, R. 1842. Report on British fossil reptiles, part II. Report of the British Association for the Advancement of Science 11:60–204.

Owen, R. 1856. Monograph on the fossil Reptilia of the Wealden and Purbeck Formations-Part III, Dinosauria (*Megalosaurus*). Palaeontographical Society Monographs 9:1–26.

Perry, S. F. and C. Reuter. 1999. Hypothetical lung structure of *Brachiosaurus* (Dinosauria: Sauropoda) based on functional constraints. Mitt Mus Natkd Berl Geowiss Reihe 2:75–79.

Perry, S. F. and M. Sander. 2004. Reconstructing the evolution of the respiratory apparatus in tetrapods. Respiration Physiology and Neurobiology 144:125–139.

Rauhut, O. W. M., G. Cladera, P. Vickers-Rich, and T. H. Rich. 2003. Dinosaur remains from the Lower Cretaceous of the Chubut Group, Argentina. Cretaceous Research 24:487–497.

Ravoavy, F. 1991. Identification et mise en catalogue des vertébrés fossiles récoltes dans le Crétacé supérieur continental de la région de Berivotra (Majunga) fouille 1987. Université d'Antananarivo Mémoire de Recherche, Part II:55–104.

Rieppel, O. 1992a. Studies on skeleton formation in reptiles. I. The postembryonic development of the skeleton in *Cyrtodactylus pubisulcus* (Reptilia: Gekkonidae). Journal of Zoology 227:87–100.

Rieppel, O. 1992b. Studies on skeleton formation in reptiles. III. Patterns of ossification in the skeleton of *Lacerta vivipara* Jacquin (Reptilia, Squamata). Fieldiana: Zoology 68:1–25.

Rieppel, O. 1993. Studies on skeleton formation in reptiles: patterns of ossification in the skeleton of *Chelydra serpentina* (Reptilia, Testudines). Journal of Zoology 231:487–509.

Rogers, R. R., J. H. Hartman, and D. W. Krause. 2000. Stratigraphic analysis of Upper Cretaceous rocks in the Mahajanga basin, northwestern Madagascar: implications for ancient and modern faunas. Journal of Geology 108:275–230.

Rogers, R. R., D. W. Krause, and K. Curry Rogers. 2003. Cannibalism in the Madagascan dinosaur *Majungatholus atopus*. Nature 422: 515–518.

Rogers, R. R., D. W. Krause, K. Curry Rogers, A. H. Rasoamiaramanana, and L. Rahantarisoa. 2007. Paleoenvironment and paleoecology of *Majungasaurus crenatissimus* (Theropoda: Abelisauridae) from the Late Cretaceous of Madagascar; pp. 21–31 in S. D. Sampson and D. W. Krause (eds.), *Majungasaurus crenatissimus* from the Late Cretaceous of Madagascar. Society of Vertebrate Paleontology Memoir 8.

Rowe, T. 1989. The early history of theropods; pp. 100–112 in K. Padian and D.J. Chure (eds.), The Age of Dinosaurs, 12th Annual Short Course of the Paleontological Society. University of Tennessee, Knoxville.

Rowe, T. and J. Gauthier. 1990. Ceratosauria; pp. 151–168 in D. B. Weishampel, P. Dodson, and H. Osmólska (eds.). The Dinosauria. University of California Press, Berkeley.

Sampson, S. D., and L. M. Witmer. 2007. Craniofacial Anatomy of *Majungasaurus crenatissimus* (Theropoda: Abelisauridae) from the Late Cretaceous of Madagascar; pp. 32–102 in S. D. Sampson and D. W. Krause (eds.), *Majungasaurus crenatissimus* from the Late Cretaceous of Madagascar. Society of Vertebrate Paleontology Memoir 8.

Sampson, S. D., M. T. Carrano, and C. A. Forster. 2001. A bizarre predatory dinosaur from the Late Cretaceous of Madagascar. Nature 409:504–506.

Sampson, S. D., D. W. Krause, P. Dodson, and C. A. Forster. 1996. The premaxilla of *Majungasaurus* (Dinosauria: Theropoda), with implications for Gondwanan paleobiogeography. Journal of Vertebrate Paleontology 16:601–605.

Sampson, S. D., L. M. Witmer, C. A. Forster, D. W. Krause, P. M. O'Connor, P. Dodson, and F. Ravoavy. 1998. Predatory dinosaur remains from Madagascar: implications for the Cretaceous biogeography of Gondwana. Science 280:1048–1051.

Schepelmann, K. 1990. Erythropoietic bone marrow in the pigeon: development of its distribution and volume during growth and pneumatization of bones. Journal of Morphology 203:21–34.

Seeley, H. G. 1888. On the classification of the fossil animals commonly named Dinosauria. Proceedings of the Royal Society of London 43:165–171.

Sereno, P. C. 1999. The evolution of dinosaurs. Science 284:2137–2147.

Sereno, P. C. and A. B. Arcucci. 1994. Dinosaur precursors from the Middle Triassic of Argentina: *Marasuchus lilloensis*, gen. nov. Journal of Vertebrate Paleontology 14:53–73.

Sereno, P. C. and F. E. Novas. 1993. The skull and neck of the basal theropod *Herrerasaurus ischigualastensis*. Journal of Vertebrate Paleontology 13:451–476.

Sereno, P. C., J. Conrad, and J. A. Wilson. 2004. New Dinosaurs link

southern landmasses the Mid-Cretaceous. Proceedings of the Royal Society of London B 271:1325–1330.
Tykoski, R. S., and T. Rowe. 2004. Ceratosauria; pp. 47–70 in D. B. Weishampel, P. Dodson, and H. Osmólska (eds.). The Dinosauria, 2nd Ed. University of California Press, Berkeley.
Wedel, M. J. 2003. Vertebral pneumaticity, air sacs, and the physiology of sauropod dinosaurs. Paleobiology 29:243–255.
Welles, S. P. 1984. *Dilophosaurus wetherilli* (Dinosauria, Theropoda) osteology and comparisons. Palaeontographica 185:85–180.
Wilson, J. A. 1999. A nomenclature for vertebral laminae in sauropods and other saurischian dinosaurs. Journal of Vertebrate Paleontology 19(4):639–653.
Wilson, J. A. , P. C. Sereno, S. Srivastava, D. K. Bhatt, A. Khosla, and A. Sahni. 2003. A new abelisaurid (Dinosauria, Theropoda) from the Lameta Formation (Cretaceous, Maastrichtian) of India. Contributions from the Museum of Paleontology, University of Michigan 31(1):1–42.
Xu, X., M. A. Norell, X. Kuang, X. Wang, Q. Zhao, and C. Jia. 2004. Basal tyrannosauroids from China and evidence of protofeathers in tyrannosauroids. Nature 431:680–684.
Zhao, X.-J., and P. J. Currie. 1993. A large crested theropod from the Jurassic of Xinjiang, People's Republic of China. Canadian Journal of Earth Sciences 30:2027–2036.

Submitted December 16, 2004; accepted January 5, 2007.

APPENDIX 1. List of anatomical abbreviations.

axi, axial intercentrum
bce, blunt costal end
ca, capitulum (costal)
caaf, caudal articular facet (chevron)
cacdl, caudal centrodiapophyseal lamina
capdl, caudal paradiapophyseal lamina
cf, chevron facet
cg, costal groove
chaf, single chevron articular facet (1st chevron only)
cir, cranial intercostal ridge
clp, craniolateral process
cmf, caudomedial flange
cprl, centroprezygapophyseal lamina
craf, cranial articular facet (chevron)
crcdl, cranial centrodiapophyseal lamina
crcpl, cranial centroparapophyseal lamina
crfl, cranial flange of chevron
crpr, cranial process of chevron
ctw, capitulotubercular web
de, dorsal expansion of neural spine
dex, distal expansion of chevron
dp, diapophysis
dlp, dorsolateral process
dpdl, dorsal paradiapophyseal lamina
ep, epipophyses
fs, region of fused neurocentral sutures
ha, hypantrum
hc, haemal canal
ho, hyposphene
ics, intracostal suture
idfs, infradiapophyseal fossa
ipofr, infrapostzygapophyseal foramen
ipofs, infrapostzygapophyseal fossa
iprfr, infraprezygapophyseal foramen
iprfs, infraprezygapophysesal fossa
isls, interspinous ligament scar
ivf, intervertebral foramen
lb, lateral blade of brevis fossa
lpfr, laminopeduncular foramen
mb, medial blade of brevis fossa
mce, midchevron expansion
mpr, medial process of atlantal neurapophysis
msr, muscle ridge
mv?, possible missing vertebra
nafs, nonspecific neural arch fossa
nc, neural canal
ncs, neurocentral suture
ns, neural spine
nsr, neural spine ridge
od, odontoid
ped, pedicle
pfr, pneumatic foramen
pfs, pneumatic fossa
pp, parapophysis
poai, postacetabular iliac blade
posf, postspinal fossa
poz, postzygapophysis
pozsh, postzygapophyseal shelf
prai, preacetabular iliac blade
prz, prezygapophysis
prdl, prezygodiapophyseal lamina
prel, prezygoepipophyseal lamina
prpl, prezygoparaphyseal lamina
prsf, prespinal fossa
sas, supraacetabular shelf
ser, serrations from denticle drag
spel, spinoepipophyseal lamina
spol, spinopostzygapophyseal lamina
sprl, spinoprezygapophyseal lamina
sr_3, third sacral rib
sr_4, fourth sacral rib
stp, styliform process
stpf, facet for styliform process
tm, tooth mark
tpol, intrapostzygapophyseal lamina
trc, transverse cleft
tu, tuberculum
tvp, transverse process
tvp_2, second sacral transverse process
tvp_3, third sacral transverse process
tvp_4, fourth sacral transverse process
unp, uncinate process of atlantal neurapophysis
vb, ventral buttress
vf/pfr?, vascular and/or pneumatic foramen

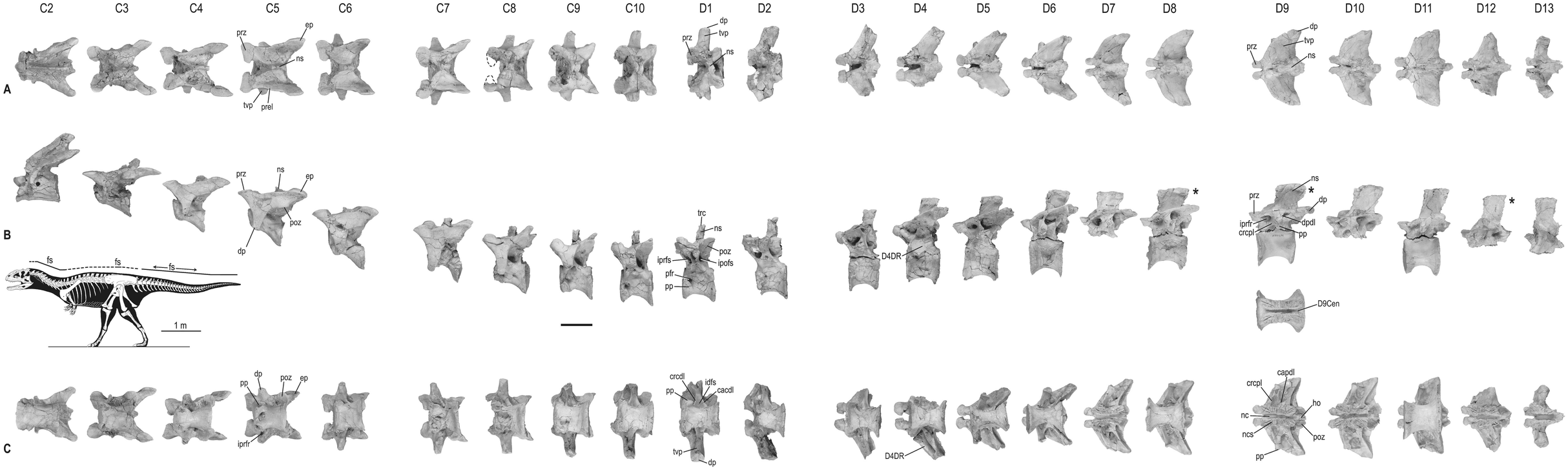

FIGURE 3. Presacral vertebral series of *Majungasaurus crenatissimus* (UA 8678) in dorsal (**A**), left lateral (**B**), and ventral (**C**) views (cranial to caudal progression in each row from left to right). Inset skeletal reconstruction to illustrate fusion status in different regions of the vertebral column; dashed line above reconstruction indicates unfused neurocentral sutures whereas solid line indicates fused sutures. For general context, only selected vertebrae are labeled; see Figs. 5–12 for additional morphological information pertaining to specific regions of the vertebral series. **Notation**: **C2-C10**, second to tenth cervical vertebrae; **D1-D13**, first to thirteenth dorsal vertebrae; **D4DR**, fourth left dorsal rib head articulated with D4 parapophysis; **D9Cen**, ninth dorsal vertebral centrum (dorsal view); asterisk (*) indicates reversed image. See Appendix 1 for list of anatomical abbreviations. Scale bar equals 5 cm.